International Scientific-Technical and Production Journal

The Paton WELDING JOURNAL

August 2012 # 8

English translation of the monthly «Avtomaticheskaya Svarka» (Automatic Welding) journal published in Russian since 1948

Founders: *E.O. Paton Electric Welding Institute of the NAS of Ukraine*
International Association «Welding»

Publisher: *International Association «Welding»*

Address:
E.O. Paton Electric Welding Institute,
International Association «Welding»,
11, Bozhenko str., 03680, Kyiv, Ukraine
Tel.: (38044) 200 82 77
Fax: (38044) 200 81 45
E-mail: journal@paton.kiev.ua
URL: www.rucont.ru

State Registration Certificate
KV 4790 of 09.01.2001

Subscriptions:
$324, 12 issues per year,
postage and packaging included.
Back issues available.

CONTENTS

GROWTH OF CORROSION CRACKS IN STRUCTURAL STEEL 10GN2MFA

V.I. MAKHNENKO[1], **L.I. MARKASHOVA**[1], **O.V. MAKHNENKO**[1], **E.N. BERDNIKOVA**[1], **V.M. SHEKERA**[1] and **A.S. ZUBCHENKO**[2]
[1]E.O. Paton Electric Welding Institute, NASU, Kiev, Ukraine
[2]«Hydropress», Podolsk, Russia

Relationship between corrosion crack growth rate and stress intensity factor, based on the static corrosion crack resistance diagram, is described. The main working hypothesis on the discrete nature of crack growth in structural steel is confirmed.

Keywords: *welded structures, NPP steam generator, static corrosion crack resistance diagram, structural steel, corrosion cracks, electron microscopy, stress intensity factor, hydrogen embrittlement*

Corrosion cracks are among the most dangerous defects formed in modern durable steel structures. In a number of cases the process of initiation and formation of such defects is hard to determine. Therefore, duration of this process of formation of corrosion cracks may substantially change with time, depending on rather small changes in specific factors.

Under these conditions, of high importance is to timely detect the formed corrosion crack and determine the kinetics of its growth with time during operation of a corresponding structure.

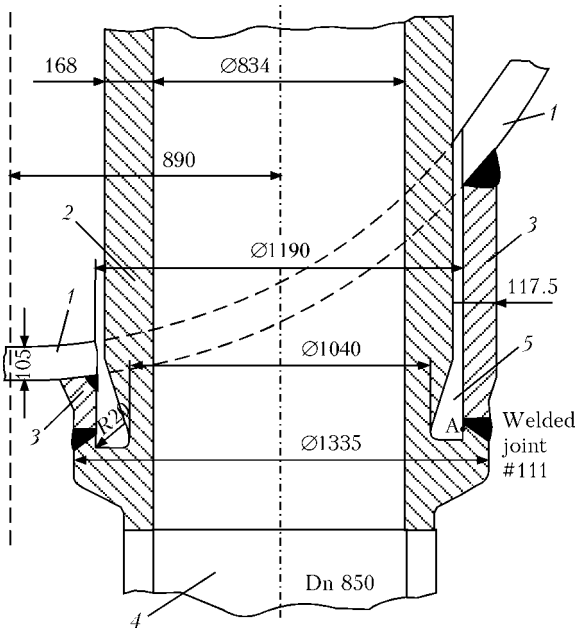

Figure 1. Schematic of the assembly of joining collector to steam generator casing by using branch pipe: *1* — steam generator casing; *2* — collector; *3* — branch pipe; *4* — main circulation piping; *5* — pocket

Very often the latter is crucial and requires accumulation and generalisation of the corresponding experimental data. So, the present study is dedicated particularly to this issue.

Welded joint 111 (Figure 1) in steam generators PG-1000 of modern power units of water-moderated water cooled reactor WWER-1000 considered in this study involves a problem in this respect, as each of units of this NPP comprises four steam generators. 13 such units at 4 NPPs with a service life of 8 to 28 years are in operation now in Ukraine.

The first defects in welded joints 111 were detected in Ukraine in 2003 at the South-Ukrainian NPP. Before that, such cracks in joints 111 were detected at the Novovoronezhskaya and Kalininskaya NPPs in Russia, whish had been in operation for about 20 years. The first detected cracks were mainly longitudinal, i.e. located along the weld, and of rather big sizes both on the circumference and in depth [1], which caused difficulties in detecting them by the non-destructive test methods. The special ultrasonic testing procedure was developed for these purposes [2], which allowed revealing such defects at the early stages of their formation. As the procedure for repair of these defects detected at the early stage of their formation is time-consuming and requires shutdown of the entire unit, the necessity arose for predictive estimates of safe service life of a steam generator with detected crack-like defects in welded joints 111 between both hot (joint 111-1) and cold (joint 111-2) collector and branch pipes of the steam generator casing (see Figure 1).

These predictions are based on the knowledge of the static corrosion crack resistance diagram (SCCRD) (Figure 2). Such diagrams are developed for specific materials (steels) and aggressive

environments depending on force factor K_I, i.e. the stress intensity factor for normal tear cracks. SCCRD (see Figure 2) consists of three zones [3]. In zone *I* ($0 < K_I < K_{ISCC}$), where corrosion growth is based on the mechanism of anodic dissolution, the role of the force factor is not high. In zone *II* ($K_{ISCC} < K_I < K_{IC}$), i.e. the zone of hydrogen embrittlement, the rate of growth of a corrosion crack is much higher. The upper bound of this zone, $K_I = K_{IC}$, corresponds to zone *III*, where the crack grows spontaneously.

So far, no sufficiently reliable SCCRD describing the $v = f(K_I)$ growth rate are available for welded joints 111 of high-strength low-alloy steel 10GN2MFA, as composition of the aggressive environment in pocket *5* on joints 111 depends on the service life of the steam generator. At the initial stage of operation, this is a feed water of the second loop at a temperature of about 300 °C and pressure of 6.4 MPa. In such an environment, steel 10G2NMFA used to make steam generator casing *1*, cold and hot collectors *2* and branch pipe *3* (see Figure 1) is almost insensitive to corrosion cracking. However, in long-time operation, owing to the stagnant phenomena taking place in pocket *5*, the composition of the environment in contact with the surface of one-sided welded joints changes. Conditions are created for pitting multicentric surface corrosion to occur along the circumferential weld, which then transforms to stage *I* of formation of a corrosion crack (see Figure 2). It is likely that the uncontrollable surface state in the pocket in a zone of the one-sided weld exerts a significant effect on the time of transition from pitting corrosion to formation of the corrosion crack. Moreover, it is highly probable that the intermediate state here is formation of a groove corrosion defect along the weld, from which the circumferential crack is then formed.

Improvement of thoroughness of control of the zone of welded joints 111 at NPPs in annual fixed-schedule maintenance (FSM) provides early detection of the defects under consideration. However, the predictive estimates of their behaviour turn out to be too conservative, this being associated with conservatism of the used approximate data on the rate of growth of crack sizes $v = f(K_I)$.

At the absence of appropriate SCCRDs, predictions were made by using literature data for similar casing steels and similar service conditions [4], which were in good agreement with calculated rates $v = f(K_I)$ obtained in solving the inverse problem by the results of measurements at the South-Ukrainian NPP in 2003, according to which [1]

$$v = 0 \text{ at } K_I < K_{ISCC},$$
$$v \cong 44 \text{ mm/year at } K_I > K_{ISCC},$$
$$K_{ISCC} \approx 10\text{–}20 \text{ MPa}\cdot\text{m}^{1/2}.$$

This approximation for SCCRD provides sufficiently good description of stage *II* (see Figure 2) at defect depths of over 30–40 mm, whereas at a depth of less than 25 mm it turns out to be rather conservative.

Substantial disagreement of the prediction data with the control measurement results obtained at further FSM, e.g. the results of growth of crack-like defects detected in 2009 in welded joints 111-2 at steam generators of unit 3 of the Rivnenska NPP, whose dimensions *a* and 2*c* remained almost unchanged in testing during further FSM in 2010 and 2011, cast doubt on applicability of the mechanism of growth of such defects (see Figure 2, stage *II*) for steel 10GN2MFA.

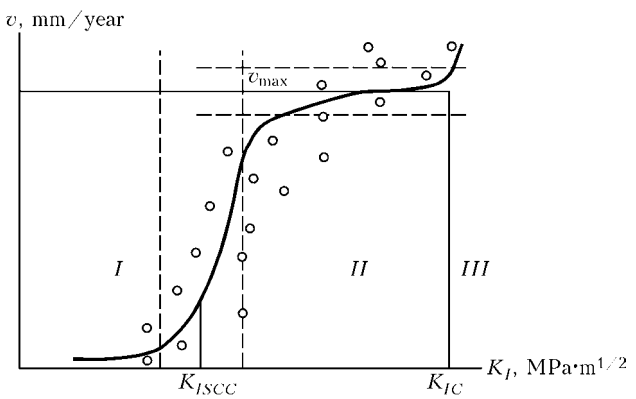

Figure 2. Static corrosion crack resistance diagram (see designations in the text)

Figure 3. Appearance of the testing machine for determination of SCCRD parameters

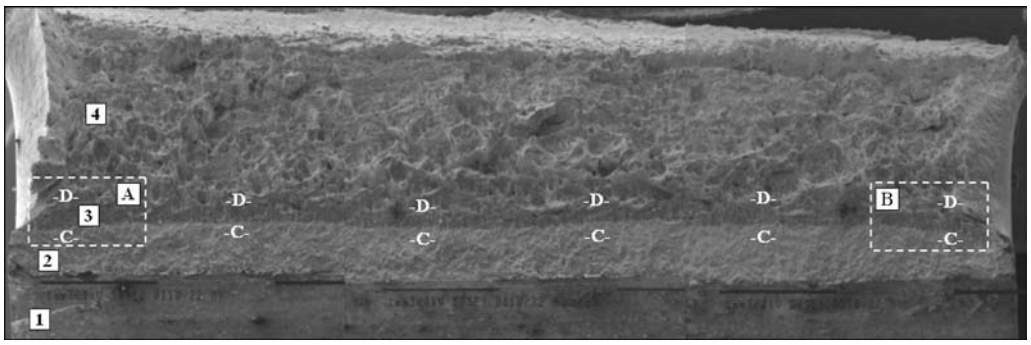

Figure 4. Panoramic view of fracture in specimen 1 (see designations in the text)

In this connection, the experimental study was carried out on specimens of steel 10GN2MFA of the following chemical composition, wt.%: 0.11 C, 0.28 Si, 0.89 Mn, 0.19 Cr, 2.1 Ni, 0.44 Mo, 0.04 V, 0.11 Cu.

The Charpy type specimens with a cross section of 10 × 10 mm, sharp notch and a preliminarily grown fatigue crack were loaded by three-point bending using the testing machine (Figure 3) described in studies [5–7]. The tests were carried out in 3 % solution of NaCl at a temperature of 35 °C and a load corresponding to K_I = = 25 MPa·m$^{1/2}$. The load was determined by dynamometer DOSM3-3. The machine was fitted with an acoustic emission sensor to fix the crack growth surges by using instrument AEC-USB-1.

Two specimens were tested for 778 (1) and 601 h (2). After the tests, the specimens were completely fractured and their surfaces were cleaned from the corrosion deposit, after which a panoramic view of the fracture surfaces was obtained (Figure 4) by using «Philips» scanning electron microscope SEM-515 equipped with the «Link» energy-dispersive spectrometers.

Four zones can be clearly seen in Figure 4. Zone 1 corresponds to the Charpy specimen notch 2 mm deep, zone 2 is a preliminarily grown fatigue crack, zone 3 is a corrosion crack between

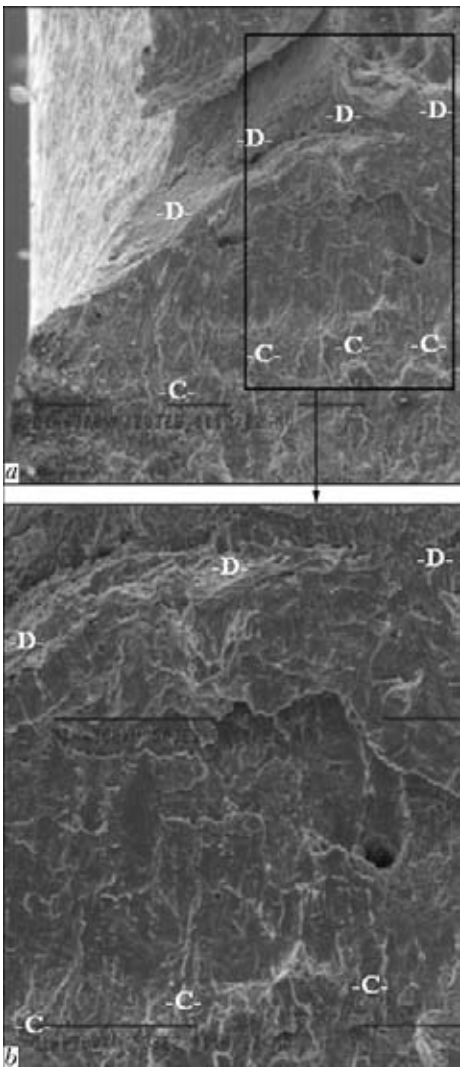

Figure 5. Fragments of fractographic pattern and zone A (see Figure 4): *a* — ×203; *b* — ×503

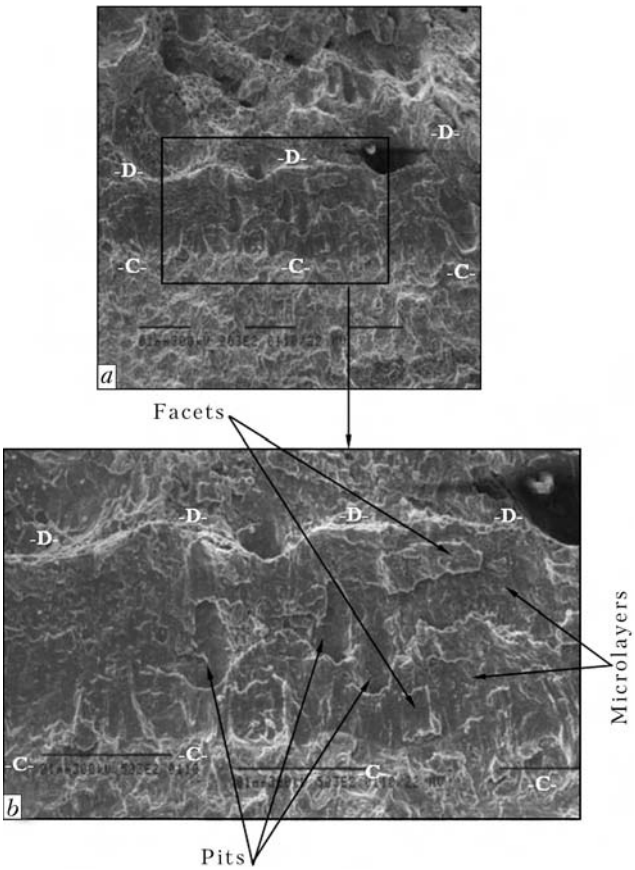

Figure 6. Fragments of fractographic pattern and zone B (see Figure 5): *a*, *b* — same as in Figure 5

lines C–C–C and D–D–D, and zone 4 is a complete fracture zone.

Width of the corrosion crack growth, i.e. the Δl value between lines C–C–C and D–D–D determined by using the scanning electron microscope in 16 regions with a pitch of 500–600 μm, was 200–350 μm. For specimen 1, Δl = 229 μm in region 1; 260 μm in region 2; 250 μm in region 3; 240 μm in region 4; 250 μm in regions 5 and 6, 280 μm in region 7; 300 μm in region 8; 270 μm in region 9; 230 μm in region 10; 240 μm in region 11; 260 μm in region 12; 300 μm in region 13; 350 μm in region 14, and 200 μm in regions 15 and 16.

In addition, the measurements were made on side surfaces of the specimens by using measurement microscope UIM-21 with an accuracy of not less than ±2 μm. In this case the width of the crack growth was 284 and 207 μm, this corresponding to a crack growth of 3.20 and 3.01 mm/year.

Further detailed studies of fractographic patterns of fracture were carried out in regions A and B (see Figure 4) close to side surfaces of the specimens. Corresponding data at different magnifications are shown in Figure 5, and those for region B — in Figure 6.

As shown by fractographic examinations, the corrosion crack in zone *II* of SCCRD of hydrogen embrittlement grows in jumps, the frequency of which corresponds to the fixed acoustic emission signals. However, it grows not simultaneously over the entire crack front, but in individual spots moving along the front in a chaotic manner, though forming the growth layers about 30–40 μm thick. An acoustic emission signal accompanies a jump of formation of the said crack spot, which can be regarded as a sign of stage II of hydrogen embrittlement in Figure 2.

CONCLUSIONS

1. Steel 10GN2MFA used to make the steam generator, collector and piping has a sufficiently high corrosion resistance in contact with the second loop environment, this being evidenced by an unptotected surface of the steam generator casing. However, under the high temperature and pressure conditions, which take place inside the collector and piping, the walls of the latter are protected by corrosion-resistant cladding of austenitic steel.

2. In pockets, where the joint between the collector and branch pipe Dn 1200 is situated, the stagnant phenomena result in formation of a very aggressive environment (at least compared to feed water inside the steam generator), this leading to the corrosion process occurring in the region of weld 111.

3. Depending on the aggressiveness of the environment in the pockets, as well as on the state of the contact surface, formation of the corrosion crack is preceded by the process of pitting corrosion of a differing duration and the probability of formation of a corrosion groove-like defect.

4. Conservatism of the predictive estimates of growth of a detected crack-like defect at the early stage is associated with multicentricity of the process, where formation of the crack along the length of the defect occurs non-simultaneously.

1. Makhnenko, V.I. (2006) *Safe service life of welded joints and assemblies of current structures*. Kiev: Naukova Dumka.
2. *MTsU-11–98p*: Procedure for ultrasonic testing of welded joint between collector and steam generator WWER-1000. Moscow: TsNIITMASh.
3. (2005) *Mechanics of fracture and material strength*: Refer. Book. Ed. by V.V. Panasyuk. Vol. 7: Reliability and life of structures of heat-power engineering equipment. Ed. by I.D. Dmitrakh. Kyiv: Akademperiodika.
4. Magdovski, R., Kraus, A., Speidel, O. (1995) Environmental degradation assessment and life prediction of nuclear pressure vessels and piping steels. In: *Proc. of Int. Symp. on Plant Aging and Life Prediction of Corrodable Structures*, 895–902.
5. (2001) *Fracture mechanics and strength of materials*: Refer. Book. Ed. by Z.T. Nazarchuk. Vol. 5: Nondestructive testing and technical diagnostics. Lviv: G.V. Karpenko FMI.
6. Makhnenko, V.I., Shekera, V.M., Onoprienko, E.M. (2008) Determination of parameters of simplified static corrosion crack resistance diagram for pipe steels in soil corrosion. *The Paton Welding J.*, **10**, 26–30.
7. Makhnenko, V.I., Markashova, L.I., Berdnikova, E.N. et al. (2010) Kinetics of corrosion crack growth in 17G1S pipe steel. *Ibid.*, **6**, 10–12.

STRUCTURE AND PROPERTIES OF WELDED JOINTS OF STEEL S390 (S355 J2)

V.D. POZNYAKOV, S.L. ZHDANOV and **A.A. MAKSIMENKO**
E.O. Paton Electric Welding Institute, NASU, Kiev, Ukraine

The influence of thermal cycles of welding on the change of structure and mechanical properties of HAZ metal of welded joints of steel S390 (S355 J2) was studied. The range of admissible rates of cooling of HAZ metal in the temperature range of 600–500 °C was established, and welding consumables were selected ensuring welded joint properties on the level of requirements to the base metal, as well as their resistance to cold cracking.

Keywords: *arc welding, high-strength steel, building metal structures, thermal welding cycle, structure, mechanical properties, cooling rate, cold cracks, diffusive hydrogen*

In the recent years the high-strength steel S390 (S355 J2) with yield strength of more than 390 MPa finds even more wider application in manufacture of construction welded metal structures. The domestic metallurgy industrial complexes mastered the production of rolled metal of this steel in the sheets of 16–100 mm thickness. According to the standard EN 10025-2:2004 it can be supplied both in as-normalized state as well as after controllable rolling. The steel has the following chemical composition, wt.%: 0.14–0.17 C; 1.42–1.45 Mn; 0.18–0.25 Si; 0.06–0.09 Cr; 0.22–0.24 Ni; ≤0.06 Cu; 0.003–0.005 S; 0.013–0.019 P. Mechanical properties of this steel are characterized by the following values: σ_y = 370–420 MPa; σ_t = 530–570 MPa; δ_5 = = 28–32 %; ψ = 52–68 %; KCV_{-20} = 110–210 J/cm^2.

In the domestic literature there are no information about formation of structure and properties of welded joints of steel S390 under conditions of arc welding that, therefore, became the object of investigations described in this paper.

The influence of welding thermal cycles (WTC) on the structure and properties of HAZ metal of welded joints of steel S390 was studied, the evaluation of their resistance to cold cracks formation depending on rigidity of fixation and content of diffusive hydrogen in deposited metal was performed, the mechanical properties of joints produced using arc manual and mechanized welding in shielding gas were determined.

To evaluate the WTC influence on change of microstructure and impact toughness of HAZ metal of welded joints, the method of bead-on-plate samples was used. The beads deposition on the plates of 600 × 400 × 20 mm size was carried out using automatic welding under the flux AN-60 and wire Sv-10NMA under conditions providing energy input Q_w = 16–54 kJ/cm. The cooling rate of HAZ metal in the temperature range of 600–500 °C ($w_{6/5}$) was changed from 3 to 50 °C/s. The specimens for structure analysis, measurement of hardness and tests on impact bending of HAZ metal with sharp (V-shaped) notch were cut out in the transverse direction relatively to the deposition axis. According to the GOST 13585–68 the notches were arranged in a way that their apexes were on the fusion boundary in the area of the HAZ metal overheating and at the distance of 1.5 mm from the fusion boundary (area of incomplete recrystallization).

The data on WTC influence on strength and ductility of HAZ metal of steel S390 were obtained from the results of mechanical tests on static tension of standard specimens (type II according to the GOST 6996–66). They were manufactured of model specimens of 150 × 13 × 13 mm sizes, which according to WTC were subjected to heating up to the temperature of 1250 °C (heating rate is 150 °C/s) and then cooling at different rates. The conditions of cooling of model specimens were selected in a way that in the temperature range of 600–500 °C the rate of their cooling in the range from 20 to 3 °C/s was provided.

In the course of metallographic examinations it was established that in the initial state the steel is characterized by fine-dispersed line ferrite-pearlite structure, where over the whole volume of austenite grain the precipitations of structure-free ferrite are uniformly distributed (Figure 1, *a*). The analysis of specimens manufactured of samples bead-on-plate showed that depending on the cooling rate of welded joints of steel S355 J2 the structure and hardness of HAZ metal can considerably change. The main com-

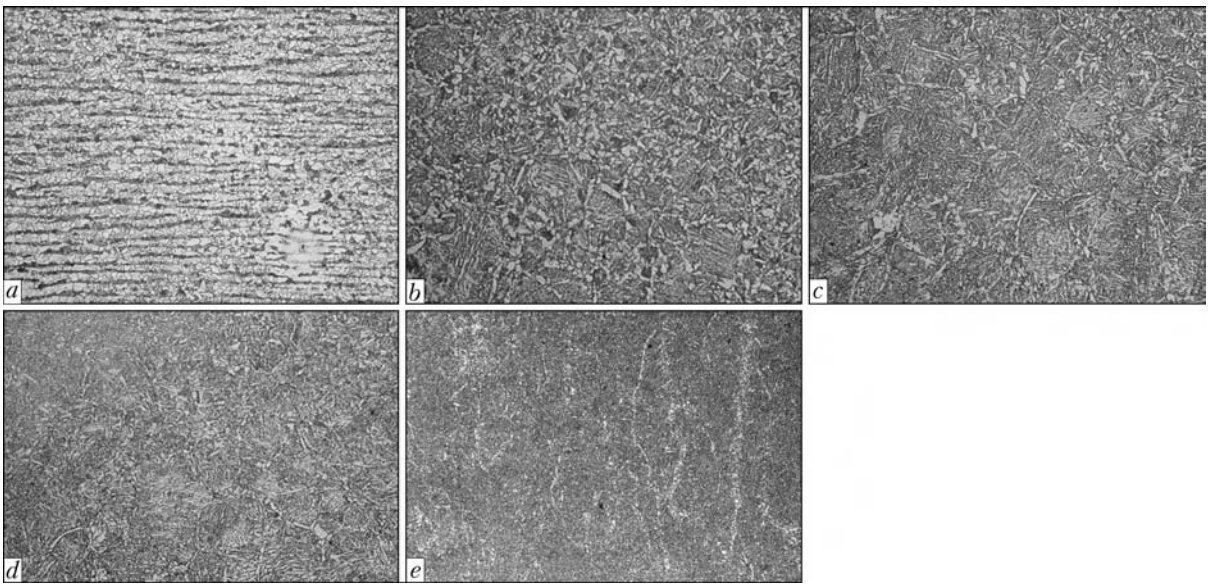

Figure 1. Microstructures (×320) of steel S390 (*a*) and area of overheating of HAZ metal of welded joints at the cooling rate $w_{6/5}$ = 3 (*b*), 10 (*c*), 20 (*d*) and 50 (*e*) °C/s

ponents of structure of metal at the area of overheating of the HAZ metal of joints, which were cooled at the rate of $w_{6/5}$ = 3 °C/s, are pre-eutectoid (along the grain boundaries) and non-equiaxial (inside the grains) ferrite, and also a small amount of bainite of lamellar and globular morphology (Figure 1, *b*). As the cooling rate of welded joints increases from 3 to 50 °C/s, the amount of pre-eutectoid and non-equiaxial ferrite in the structure decreases and fraction of bainite and dispersity of all structural components increases. It is predetermined by increase of hardness of HAZ metal from *HV* 150 to *HV* 220 (Figure 2).

As the results of static rupture tests of specimens showed, the structural changes in HAZ metal, occurred under the effect of WTCs, influence its strength and ductility (Figure 3). As the $w_{6/5}$ increases from 3 to 20 °C/s the yield strength of metal at the area of overheating of the HAZ metal increases as compared to the initial state from 410 to 550 MPa, however the tensile strength increases from 555 to 725 MPa. At the same time the values of its ductility (elongation and reduction in area) decrease from 30 to 24 and 75 to 62 %, respectively.

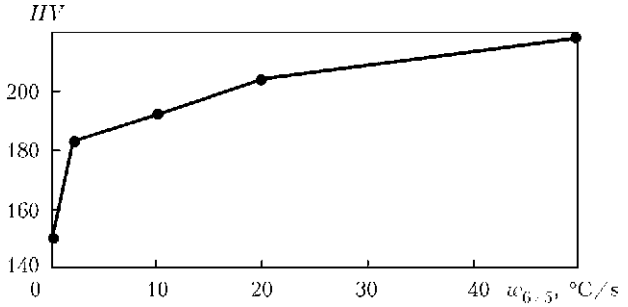

Figure 2. Dependence of HAZ metal hardness on cooling rate of welded joints

Under the influence of WTC the values of impact toughness of HAZ metal change (Figure 4). Their sharp decrease is observed at the area of overheating of the HAZ metal at the temperature of tests at −40 °C (independently of energy input of welding), and at the temperature of tests of 20 and −20 °C in case when cooling

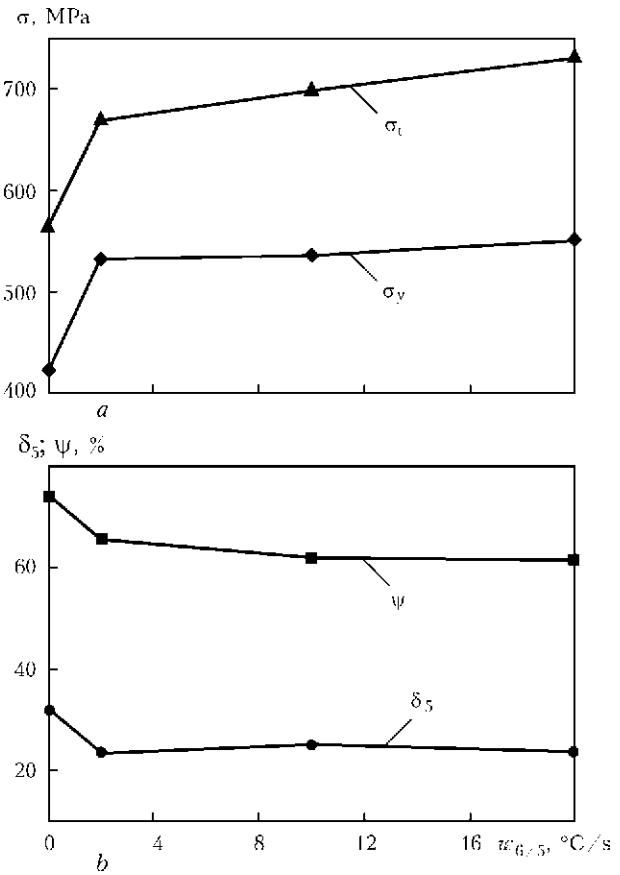

Figure 3. Dependence of values of strength (*a*) and ductility (*b*) at the area of overheating of HAZ metal on cooling rate of model specimens

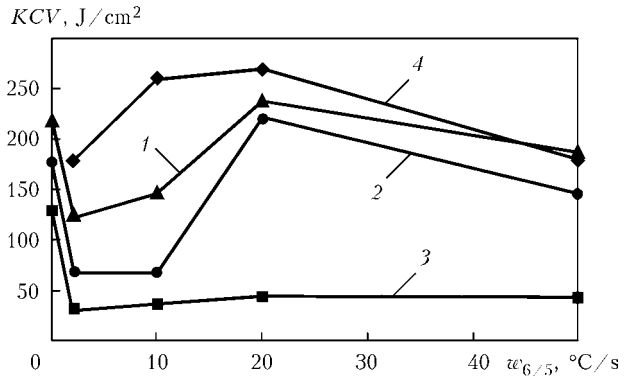

Figure 4. Influence of cooling rate on the impact rate of overheating area (*1–3*) and incomplete recrystallization (*4*) of HAZ metal at the test temperature 20 (*1*), -–20 (*2*, *4*) and –40 (*3*) °C

rate $w_{6/5}$ is below 20 °C/s. However in spite of that, the impact toughness of HAZ metal of welded joints of steel S390 remains at the level of requirements to the base metal ($KCV_{-20} \geq$ $\geq$ 34 J/cm^2). As the cooling rate increases to 20 °C/s the values of cold resistance of HAZ metal in the given area of welded joints increase and reach the values of impact toughness obtained at the tests of specimens manufactured of the base metal (Figure 4, $w_{6/5}$ = 0 °C/s).

The impact toughness of HAZ metal at the area of incomplete recrystallization independently of input energy of welding is preserved at the level of base metal, and in the range of 10–20 °C/s cooling rates it is even higher than those values (Figure 4, curve *4*).

The tendency of steel S390 to delayed fracture depending on diffusive hydrogen content in deposited metal was evaluated using the Implant method [1]. The resistance of welded joints to cold cracks formation was studied from the results of tests of butt joints of width of 100 and 200 mm [2] rigidly fixed on a massive plate and also technological samples «rigid T-joint» [3]. The diffusive hydrogen content $[H]_{diff}$ in deposited metal was determined by the method of pencil samples using mixture of glycerin with distilled water as the blocking liquid.

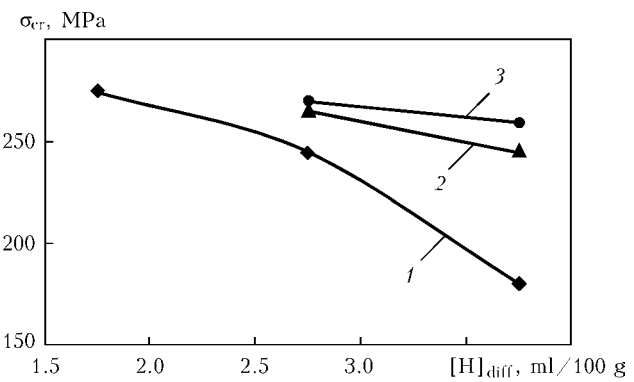

Figure 5. Influence of diffusive hydrogen in deposited metal and preliminary heating on resistance of steel S390 to delayed fracture: *1* — $T_{p.h}$ = 20; *2* — 60; *3* — 90 °C

During test using the Implant method the specimens-inserts of 6 mm diameter, manufactured of steel S390 of 100 mm thickness and cut out along the *Z*-axis with stress concentrator in a form of a screw-type notch, were used. The welding of specimens installed in the holes of basic plate of 20 mm thickness, fixed in test equipment, was performed using electrodes UONI-13/55 under the conditions of I_w = 160 A, U_a = 25 V, v_w = 9.5 m/h. The cooling rate of HAZ metal was varied by change of initial temperature of basic plate (the preliminary heating was used), and also by the adjustment of welding energy input. The concentration of diffusive hydrogen in deposited metal was changed using electrodes with different humidity of coating. The loading of specimens was started at reaching the post-weld temperature of 150–100 °C. As the resistance value of welded joints to formation of cold cracks the critical stress σ_{cr} was taken at which the specimen was not fractured during 24 h.

The technological samples of steel S390 of 20 mm thickness were performed by manual arc welding using electrodes UONI-13/55 of 4 mm diameter and also mechanized CO_2 welding using solid wire Sv-08G2S and flux-cored wire Megafil 821R of 1.2 mm diameter. The welding was performed under the conditions providing energy input of 11.0–12.5 (manual arc welding) and 14–17 kJ/cm (mechanized welding). The temperature of preliminary heating of samples $T_{p.h}$ was varied from 20 to 90 °C, and content of diffusive hydrogen in deposited metal — from 1.0 to 5.3 ml/100 g.

According to the results of tests of Implant specimens (Figure 5) it was established that at small concentrations of diffusive hydrogen ($[H]_{diff}$ = 1.7 ml/100 g) steel S390 has a low tendency to delayed fracture even in welding without preliminary heating ($\sigma_{cr} \approx$ 275 MPa $\approx$ $\approx 0.7\sigma_y$ of the steel). The increase of amount of diffusive hydrogen in the deposited metal up to 3.8 ml/100 g under the same welding conditions increases probability of cold cracks formation in HAZ metal of welded joints of the given steel (σ_{cr} of specimens does not exceed 180 MPa $\approx$ $\approx 0.45\sigma_y$ of the steel). To minimize the risk of cracks formation in the specimens at given concentration of hydrogen is possible due to their preliminary heating up to the temperature of 90 °C (Figure 5, curve *3*).

The data obtained from results of tests of the Implant specimens comply well with the results of investigations of technological samples. The

Table 1. Results of tests of technological samples

Joint type	Welding method	Welding material	Q_w, kJ/cm	$T_{p.h}$, °C	$[H]_{diff}$, ml/100 g	Presence of cracks
Rigid T-joint	MAG	Sv-08G2S	14.0	20	1.0	No
		Megafil 821R	17.0	20	3.0	Same
	MMA	UONI-13/55	12.5	20	3.0	»
				20	5.3	Present (100 %)
				60	5.3	No
Rigidly-fixed butt joint, b = 100 mm	MAG	Sv-08G2S	15.0	20	1.0	Same
		Megafil 821R	15.8	20	3.0	»
	MMA	UONI-13/55	14.0	20	3.0	»
				20	5.3	Present (100 %)
				60	5.3	No
Rigidly-fixed butt joint, b = 200 mm		UONI-13/55	11.0	20	5.3	Same

tests of the latter showed that in case when diffusive hydrogen content in deposited metal does not exceed 3 ml/100 g the cold cracks formation in technological tests comes to minimum even in welding without preliminary heating if it is performed at the environmental temperature higher than 10 °C (Table 1).

With the diffusive hydrogen content increase in deposited metal up to 5.3 ml/100 g, the welded joints of steel S390 become prone to cold cracks formation. In welding without preliminary heating the cracks in technological samples «rigid T-joint» are observed visually at the surface of welds after 2.5 h, and in rigidly-fixed butt joints of 100 mm width — in 4 h after formation of the joints. It was established that at given saturation of welds with diffusive hydrogen the increase of stability of welded joints to cold cracks formation is possible due to their preliminary heating to the temperature of 60 °C. Under these welding conditions the cracks were absent both in T-joints as well as in rigidly-fixed butt joints.

It is possible to minimize the risk of cold cracks formation in welded joints of steel S390 due to decrease of rigidity of their fixing which is proved

Table 2. Mechanical properties of weld metal and welded joints of steel S390

Welding method	Welding conditions	Q_w, kJ/cm	Weld metal						
			σ_y, MPa	σ_t, MPa	δ_5, %	ψ, %	KCV, J/cm^2, at T, °C		
							20	−40	−20
MAG	Sv-08G2S, Ar + CO_2, δ = 16 mm	14	–	–	–	–	240	90	–
	Sv-08G2S, Ar + CO_2, δ = 50 mm	14	–	–	–	–	–	60	–
MMA	UONI-13/55, δ = 20 mm	11	497	596	29.0	75.0	166	44	30
MAG	Sv-08G2S, δ = 20 mm	15	522	601	27.3	71.0	105	39	24
	Megafil 821R, Ar + CO_2, δ = 20 mm	16	491	605	27.1	62.6	135	61	35

Table 2 (cont.)

Welding method	Welding conditions	Welded joint						
		σ_t, MPa	α_b, deg	KCU		KCV		
				J/cm^2, at T, °C				
				20	−40	20	−20	−40
MAG	Sv-08G2S, Ar + CO_2, δ = 16 mm	543	81	205	197	208	197	–
	Sv-08G2S, Ar + CO_2, δ = 50 mm	569	65	–	101	–	70	–
MMA	UONI-13/55, δ = 20 mm	–	–	–	–	106	–	70
MAG	Sv-08G2S, δ = 20 mm	–	–	–	–	248	–	166
	Megafil 821R, Ar + CO_2, δ = 20 mm	–	–	–	–	219	–	140

by test results of butt joints of 100 and 200 mm width. They showed that increase of the base of fixing b, i.e. the width of joints, and decrease of level of residual stresses in them from 350 to 230 MPa allowed eliminating cold cracks formation in technological samples even in case when content of $[H]_{diff}$ in deposited metal amounted to 5.3 ml/100 g and welding was performed without preliminary heating.

Taking into account the selected welding conditions the butt joints of steel S390 16 and 20 mm thick with V-shaped edge preparation and those with 50 mm thickness and X-shaped edge preparation (S17 and S25 according to the GOST 14771–76) were made. The welding of joints was performed without preliminary heating by the electrodes UONI-13/55 of 4 mm diameter, conventionally applied for this grade of steels, and the wire Sv-08G2S of 1.2 mm diameter in CO_2 and mixture of gasses (Ar + 20 % CO_2) and also flux-cored wire Megafil 821R of 1.2 mm diameter in CO_2. The conditions of welding provided values of energy input given in Table 2. It presents also the results of mechanical tests of specimens of weld metal for static tension, of welded joints for static rupture and bending, and also impact bending. A round and sharp notch was made on the specimens for impact tests along the weld axis and fusion line, and the tests themselves were carried out at the temperatures from 20 to –40 °C.

The results of mechanical tests evidence that values of strength and ductility of weld metal of welded joints of steel S390, performed using mentioned materials, are compatible with similar characteristics of the base metal and correspond to the requirements specified to them. The impact toughness of weld metal of such joints is also at the high level and meets the requirements not only of domestic standards ($KCU_{-40} \geq 29$ J/cm^2), but also European standards ($KV_{-20} \geq 27$ J or $KCV_{-20} \geq$ ≥ 34 J/cm^2).

CONCLUSIONS

1. In the initial state steel S390 is characterized by fine-dispersed line ferrite-pearlite structure, thus providing the high ductility and impact toughness.

2. Under the influence of WTC at the area of HAZ metal overheating the ferrite-bainite structure is formed. As the cooling rate $w_{6/5}$ increases from 3 to 50 °C/s, the amount of ferrite in the structure decreases and amount of bainite and dispersity of all structural components increases.

3. The strength values of HAZ metal of welded joints of steel S390 increase relatively to the base metal and ductility, and impact toughness decrease but remain at the level of requirements to the rolled metal. The most remarkable decrease of impact toughness values is observed at $w_{6/5} <$ < 20 °C/s.

4. Welded joints of steel S390 are characterized by high resistance to cold cracks formation at the condition when diffusive hydrogen content in deposited metal does not exceed 3 ml/100 g.

5. The required mechanical properties of welded joints of steel S390 are achieved using materials, conventionally used for welding steels of this grade of strength: UONI-13/55 electrodes and Sv-08G2S wire.

1. Hrivnak, I. (1984) *Weldability of steels*. Ed. by E.L. Makarov. Moscow: Mashinostroenie.
2. Makhnenko, V.I., Poznyakov, V.D., Velikoivanenko, E.A. et al. (2009) Risk of cold cracking in welding of structural high-strength steels. *The Paton Welding J.*, **12**, 2–6.
3. Poznyakov, V.D. (2008) Mechanical properties of weld metal and cold cracking resistance of tee-joints on 13KhGMRB steel. *The Paton Welding J.*, **2**, 14–18.

MATHEMATICAL FORMULATION OF CARBON EQUIVALENT AS A CRITERION FOR EVALUATION OF STEEL WELDABILITY

V.A. KOSTIN
E.O. Paton Electric Welding Institute, NASU, Kiev, Ukraine

A new criterion is proposed for cold cracking susceptibility of HAZ metal of joints on hardenable steel, based on allowing for the kinetics of austenite decomposition and experimental determination of the incubation period of the start of martensite transformation. It is shown that this criterion can be mathematically reduced to the traditional parameter for assessment of such a weldability of hardenable steels — carbon equivalent. A mathematic dependence of the new criterion on value of carbon equivalent is proposed, which was verified experimentally.

Keywords: *modelling, carbon equivalent, weldability, criteria, cold cracks, diagram of austenite decomposition, martensite, technological tests*

Practice shows that not all of the steels have the same good weldability. One of them can be welded without any limitations. Welding of another requires special technological methods. «Weldability» concept [1–4] has significantly wide interpretation. It should include based on analysis of available works four interdependent factors, i.e. material type, structure type, necessary properties and reliability level [5]. One or another level of weldability is achieved depending on selection and combination of these factors.

Large work on systematization of «weldability» concept and methods of its evaluation was made by K.A. Yushchenko. Thus, he proposed [6, 7] a new understanding of this term based on analysis of existing approaches to evaluation of weldability and standards acting in different countries and organizations. He showed that in most cases the weldability evaluation is qualitative and subjective. This term is considered rather as a philosophical concept and its determination through material capability to form welded joint does not show how and using what it can be measured.

Weldability testing should determine steel appropriateness for welding, but in most cases it is substituted for tests determining susceptibility to formation of various type cracks. Such indices as hot cracking resistance, cold cracking resistance, lamellar cracking and tempering cracking resistance etc. are applied, for example, to carbon and alloyed-steel welded joints.

Results of various welding tests are frequently used for evaluation of weldability of different steels. Tekken, Implant, bead-on-plate, cruciform and Jominy tests are used for determination of cold cracking susceptibility in practice. Holdcroft («fishbone») test or test based on a method of the E.O. Paton Electric Welding Institute is used for evaluation of weld metal hot cracking resistance. «Cranfield» tests, «Window» type test, N-shape test, improved Implant test as well as cruciform test (GOST 28870–90) are applied for lamellar fracture. Circular tests of BWRA, Tekken, Lehigh University, CTS or MRT [5] are used for tempering cracks. Most of these tests are based on determination of external loading applied to the welded joint, which results in fracture or simple crack appearance.

Cold cracks often appear due to steel hardenability in quick cooling and hydrogen saturation of the weld metal and HAZ. They, as a rule, nucleate after welding and surfacing on the expiry of some time (delayed fracture) and propagate in a course of several hours or even days.

Concept of carbon equivalent is used for evaluation of metal tendency to cold cracking susceptibility. A series of indices [8–11] is assumed for application in present time. All of them are true for specific and, at that, sufficiently narrow concentration ranges and speeds of weld metal cooling. Systematization of the indices of carbon equivalent proposed by different authors (Table 1) is given in work [12].

Thus, analysis of works performed shows sufficiently wide range of applied coefficients that is caused by peculiarities of regression formulation of effect of the alloying elements on cold cracking resistance. Impossibility of a direct experimental determination of the carbon equivalent and its comparison with estimated values is a disadvantage of this approach.

Table 1. Coefficients (backward) in indices of carbon equivalent proposed by various authors [12]

No.	Author	Year	C	Mn	Si	Cu	Ni	Cr	Mo	Nb	V	B
1	IIW	1967	1	6	–	15	15	5	5	–	5	–
2	Ito, Bessyo	1968	1	20	30	20	60	20	15	–	10	1/5
3	Ito, Bessyo	1968	1	20	25	20	40	10	15	–	10	–
4	Stout	1976	1	6	–	40	20	10	10	–	–	–
5	Graville	1976	1	16	–	–	50	23	7	8	9	–
6	Harasawa	1977	1	6	–	15	15	5	5	–	5	–
7	Duren	1980	1	16	25	16	50	20	40	–	13	–
8	Yurioka	1982	1	6	24	13	40	6	4	5	5	1/10
9	Yurioka	1980	1	6	30	15	20	4	6	–	–	–
10	Yurioka	1981	1	6	24	15	20	5	5	5	5	1/5
11	Duren	1982	1	8	11	9	17	5	6	–	3	–
12	Terasaki	1984	1	3	–	4	8	10	3	–	–	1/5
13	Cottrell	1984	1	6	–	–	–	5	5	4×C	3	–
14	Suzuki	1985	1	6	24	15	15	5	5	–	3	1/15
15	Yurioka	1987	1	6	24	15	12	8	4	–	–	–
16	Yurioka	1987	1	5	24	10	18	5	2.5	3	3	–
17	Yurioka	1987	1	3.6	–	20	9	5	4	–	–	–

Aim of the present paper is correlation of the proposed mathematical formulation of criterion of steel weldability with the carbon equivalent and its experimental verification.

It is well known fact that cold cracks appear in HAZ metal under three conditions, i.e. formation of hardening microstructures, presence of diffusible hydrogen, and tensile stresses. Hypothesis that the weldability can be evaluated on index determining what minimum critical time of cooling is necessary for formation of 100 % of martensite in the weld metal makes a basis of mathematical approach for formulation of the carbon equivalent. Indices of 50 or 90 % of martensite formation are traditionally used for evaluation of the steel weldability. Index of critical time of formation 100 % of martensite is used in the present paper because of its sufficiently obvious position in a thermal-kinetics diagram of austenite decomposition (Figure 1).

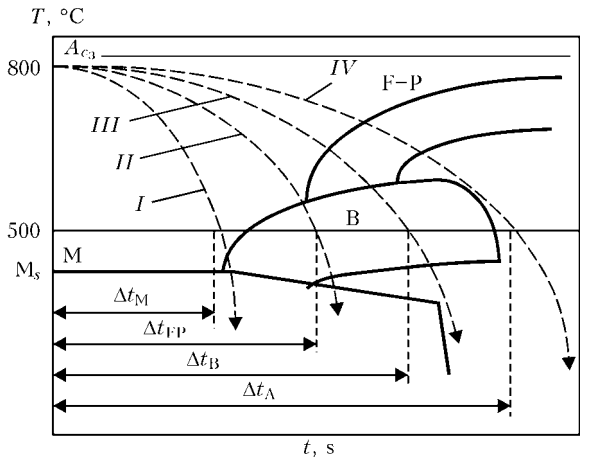

Figure 1. Determination of critical time of cooling in formation of martensite, bainite and ferrite-pearlite structures

Calculation of the carbon equivalent is based on additivity rule [13]. It is assumed that τ is some incubation (preparation) period depending on temperature and chemical composition of the material and showing that transformation has not yet started. Part of the incubation time in each step is expressed as dt/τ function if cooling curve in welding is divided on separate sections of dt duration. If transformation is completely finished then 1 will be obtained after integration of all these dt/τ parts. Besides, such an approach is sometimes used for transformation of TTT-diagram in CCT-diagram of austenite decomposition.

Criterion at which transformation does not take place is expressed in the following way:

$$\int_0^{t_e} \frac{dt}{\tau} \le 1. \qquad (1)$$

Thus, the transformation finishes when the left part of equation (1) equals not more than 1 and structure of steel makes 100 % martensite.

Critical time of cooling, at which value of the left part equals 1, in integration from $t = 0$, when the weld temperature achieves $T = A_{l_3}$ point, up to $t = t_e$ at $T = M_s$ at which martensite transfor-

mation start, can be determined using this equation.

Figure 1 shows the cooling curve *I* when equation (1) equals 1. Position of curve *I* in Figure 1 corresponds to the critical time of cooling, at which HAZ structure consists of 100 % martensite. This means that speed of cooling from 800 up to 500 °C along the curve *I* of austenite cooling determines the critical time of cooling Δt_{M}. If incubation time τ is set as a function of steel chemical composition then the carbon equivalent can be determined with the help of equation (1). Besides, if the formulae will include τ dependences on other factors (for example, size of austenite grain) then the level of their influence on carbon equivalent can be evaluated that is not considered in the most cases.

Perform modification of equation (1) in order to determine an effect of chemical composition on Δt_{M}:

$$\int_0^{t_e} \frac{dt}{\tau} = \int_{A_{e3}}^{\text{M}_\text{s}} \frac{1}{\tau}\left(\frac{dt}{dT}\right) dT = 1, \quad \frac{dt}{dT} \approx \frac{\Delta t_{\text{M}}}{300}, \tag{2}$$

$$\Delta t_{\text{M}} = 300 \Big/ \int_{A_{e3}}^{\text{M}_\text{s}} \frac{dT}{\tau}. \tag{3}$$

Equation below helps to evaluate HAZ metal hardenability:

$$\ln(\Delta t_{\text{M}}) = A \cdot CE_{\text{M}} + B, \tag{4}$$

where A, B are the constants, and M is the index relating to martensite. Considering expression (3) equation (4) will have the following form:

$$\ln(\Delta t_{\text{M}}) = \ln(300) - \ln\left(\int_{A_{e3}}^{\text{M}_\text{s}} \frac{dT}{\tau}\right). \tag{5}$$

It can be seen from matching of equations (4) and (5) that the carbon equivalent corresponds to linear term. The latter can be obtained if the second term of equation (5) is expanded in Taylor's series on each element:

$$A_X = \frac{\partial}{\partial X}\left[\ln\left(\int_{A_{e3}}^{\text{M}_\text{s}} \frac{dT}{\tau}\right)\right],$$

where X = (C, Si, Mn, Mo etc.).

Then the carbon equivalent can be expressed as

Table 2. Comparison of calculation coefficients (equation 11) of carbon equivalent with literature data

Element	A_X	A_X/A_c	IIW [9]	Ito [10]	Yurioka [17]
C	–3.02	1	1	1	1
Si	–0.08	1/38	1/24	1/25	1/24
Mn	–0.50	1/6	1/6	1/20	1/6
Ni	–0.25	1/12	1/15	1/40	1/12
Cr	–1.64	1/1.8	1/5	1/10	1/8
Mo	–1.30	1/2.3	1/5	1/15	1/4
Cu	–0.33	1/9.1	1/15	1/20	1/15
V	–	–	1/5	1/10	–

$$\ln(\Delta t_{\text{M}}) = \ln(300) - \{A_{\text{C}}(\text{C} - \text{C}_0) + A_{\text{Si}}(\text{Si} - \text{Si}_0) + A_{\text{Mn}}(\text{Mn} - \text{Mn}_0) + \ldots\} = \text{C}_0 - A_{\text{C}} CE_{\text{M}}. \tag{6}$$

Matching of the left and right sides of equation (6) gives

$$\text{C}_0 = \ln(300) A_{\text{C}} \text{C}_0 + A_{\text{Si}} \text{Si}_0 + A_{\text{Mn}} \text{Mn}_0 + \ldots,$$
$$CE_{\text{M}} = \text{C} + \frac{A_{\text{Si}}}{A_{\text{C}}} \text{Si} + \frac{A_{\text{Mn}}}{A_{\text{C}}} \text{Mn} + \ldots, \tag{7}$$

where C_0, M_0, Mn_0 etc. are the concentrations corresponding to concentrations at which Taylor's series is hold; CE_{M} is the expression for the carbon equivalent that can be calculated.

Expressions for τ, A_{e3} and M_s are to be known for determining CE_{M} using equation (7). Expressions proposed in works [14, 15] were taken for this:

$$\tau = \frac{\exp(83500/RT)}{2^{N/8}(A_{e3} - T)^3} \times (60\text{C} + 90\text{Si} + 160\text{Cr} + 200\text{Mo}), \tag{8}$$

$$A_{e3} = 1185 - 203\sqrt{\text{C}} = 15.2\text{Ni} + 44.7\text{Si} + 104\text{V} + 13.5\text{Mo} + 13.1\text{W} - 30\text{Mn} - 11\text{Cr} - 20\text{Cu} + 700\text{P} + 400\text{Al} + 120\text{As} + 400\text{Ti}, \tag{9}$$

$$\text{M}_\text{s} = 831 - 474\text{C} - 33\text{Mn} - 17\text{Ni} - 17\text{Cr} - 21\text{Mo}. \tag{10}$$

T is the temperature, °C; N is the grain number on ASTM; R = 8.31 J/(mole·K) is the gas constant in the equations given above.

The coefficients for a point about which Taylor's series expansion is carried out, i.e. C_0 = = 0.46; Si_0 = 0.23; Mn_0 = 0.78; Ni_0 = 0.27; Cr_0 = = 0.26; Mo_0 = 0.1; Cu_0 = 0.1, were obtained in works [14, 16].

As a result the equation for carbon equivalent is transformed in the following way:

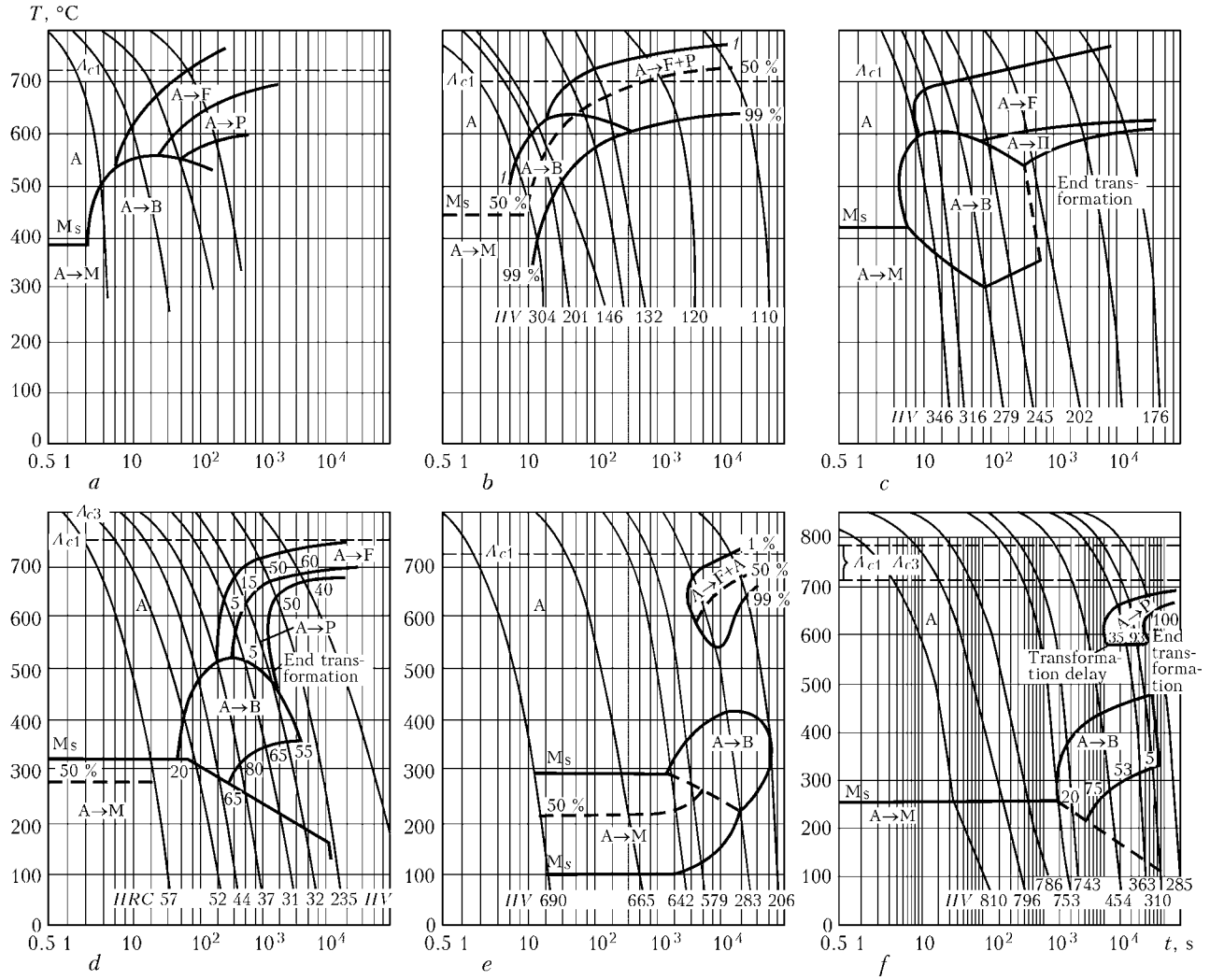

Figure 2. Thermal-kinetic diagrams of austenite decomposition of investigated steels [18]: *a* — 17G1S; *b* — 10G2S; *c* — 16G2AF; *d* — 35KhM; *e* — 35KhGSM; *f* — 50KhNM

Table 3. Chemical composition and temperatures of transformation points of investigated steels

Steel grade	Weldability	Chemical composition of steels, wt.%						
		C	Si	Mn	Cr	V	Mo	Ni/B
17G1S	Good	0.17	0.60	1.48	–	–	–	–
10G2S	Same	0.08	0.35	1.45	–	–	–	0.006
16G2AF	Satisfactory	0.17	0.36	1.44	–	0.11	–	–
35KhM	Limited	0.37	0.30	0.79	1.0	–	0.18	–
35KhGSM	Bad	0.39	1.49	1.41	0.74	–	0.51	–
50KhNM	Same	0.52	0.29	–	1.09	0.14	0.43	1.72

Table 3. (cont.)

Steel grade	Weldability	Temperature, °C				Δt_M, s	CE_M, % (IIW)
		A_{c1}	A_{c3}	M_s	T_s		
17G1S	Good	730	–	390	1130	2	0.44
10G2S	Same	700	850	440	880	4	0.37
16G2AF	Satisfactory	700	830	425	950	6	0.45
35KhM	Limited	750	–	320	850	60	0.75
35KhGSM	Bad	725	857	290	885	2000	0.94
50KhNM	Same	710	790	260	950	2000	0.98

$$CE_M = C + \frac{1}{38}Si + \frac{1}{6}Mn + \\ + \frac{1}{12}Ni + \frac{1}{1.8}Cr + \frac{1}{2.3}Mo + \frac{1}{9.1}Cu. \quad (11)$$

Table 2 shows the results of calculation of coefficients in the carbon equivalent equation and their correspondence to literature data. Analysis of the results shows good correspondence of the calculated coefficients to the coefficient proposed by IIW and Yurioka et al.

Thus, an approach proposed for the weldability evaluation on cold cracking susceptibility is verified mathematically, on the one side, and have understandable physical meaning, on the other side. It is based on evaluation of the critical time necessary for 100 % martensite transformation. It may sound strange, but the ideas is that the lower is the preparatory time necessary for 100 % martensite structure formation (i.e. the higher the critical speed of cooling) the better is weldability and higher is cold cracking resistance. This indicates that preparatory processes related with the cold crack formation have kinetic (diffusion) character and directly connected with redistribution of hydrogen in the weld metal. Hydrogen is quickly fixed in the weld metal in the case of short (1–10 s) incubation period of martensite formation, however, its local concentration appears to be not sufficient for initiation of cold cracking. If the incubation period of martensite formation is long (1000–2000 s) the time is found to be enough for hydrogen embrittlement of the metal being welded. Gradual redistribution of the hydrogen is possible at short incubation period and further long-term soaking depending on type of formed microstructure, that result in delayed fracture effect.

In conclusion assumed by us hypothesis (equitation (4)) will be checked experimentally. Steels proceeding from their weldability, i.e. steels 17G1S, 10G2S of good weldability, 16G2AF steel of satisfactory weldability, 35KhM steel of limited weldability and 35KhGSM, 50KhNM steels of bad weldability [19] were taken for this purpose. Figure 2 shows the thermal-kinetic diagrams of austenite decomposition of these steels. Chemical composition and character temperatures of the critical points are given in Table 3.

Analysis of results of Table 3 and Figure 3 showed that the dependence proposed in equation (4) is valid. Coefficients $A = 11.26$ and $B = -3.51$ of the equation (4) were determined experimentally. Present coefficients have good correspondence with the equation for numerical evaluation

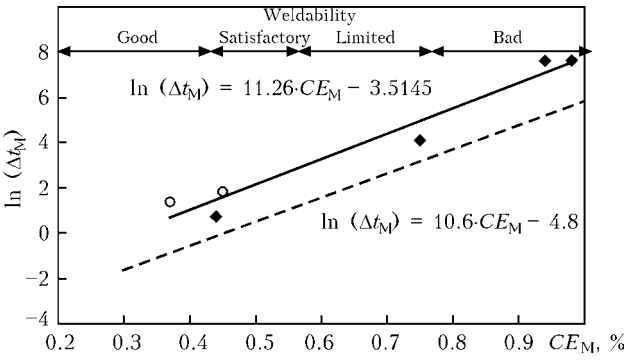

Figure 3. Influence of carbon equivalent of steels considered on function of time of martensite transformation start: points — experimental values; solid line — calculated; dashed — curve from work [20]

of weldability of low-alloyed steels assumed in work [20] and some variance is explained by difference in formulae, taken for the carbon equivalent calculation.

Advantage of the proposed criterion for evaluation of the steel weldability lies, on the one side, in the fact that it can be determined immediately during the experiment and, on the other side, technological peculiarities of welding (method and mode of welding) as well as its metallurgical parameters (chemical composition, influence of welding wire, flux or shielding gas, influence of additive and alloying elements, nonmetallic inclusions etc.) are already considered in the thermal-kinetic diagram of austenite decomposition.

Thus, proposed new criterion of the steel weldability evaluation can be mathematically reduced to the carbon equivalent which is a traditional parameter of steel weldability evaluation. Proposed mathematical dependence of new criterion on carbon equivalent was verified in experimental way.

1. *ISO 581:1980*: Weldability. Definition. General information.
2. *BS 499-1:2009*: Welding terms and symbols: Glossary for welding, brazing and thermal cutting.
3. *DIN 8528*: Pt 1: Weldability of metallic materials, concepts.
4. *GOST 29273–92 RF (ISO 581–80)*: Weldability. Definition.
5. Hrivnak, I. (1984) *Weldability of steels*. Moscow: Mashinostroenie.
6. Yushchenko, K.A., Derlomenko, V.V. (2007) Weldability of materials. Pt 1. *IIW Doc. VI-842–07*.
7. Yushchenko, K.A., Derlomenko, V.V. (2005) Analysis of modern views on weldability. *The Paton Welding J.*, **1**, 5–9.
8. Olson, G.B., Cohen, M. (1976) A general mechanism of martensitic nucleation. Pt I–III. *Metallurg. Transact. A*, **7**, 1897–1923.
9. (1967) The IIW formula for carbon equivalent. Techn. Rep. *IIW Doc. IX-535–67*.
10. Ito, I., Bessyo, K. (1968) Cracking parameter of high strength steels related to HAZ cracking. *J. JWES*, **9**(37), 983–991.

11. Yurioka, N., Oshita, S., Tamehiro, P. (1981) Pipeline welding in the 80s. In: *Proc. of AWRA Symp.* (March, 1981).
12. Lundin, C.D., Gill, T.P., Qiao, C.Y. (1991) Carbon equivalence and weldability of microalloyed steels. *SSC-357, AD-A234-850*.
13. Scheil, E. (1935) Nucleation period of austenite transformation. *Arch. Eisenhuettenwesen*, **12**, 565–567.
14. Kirkaldy, J.S., Thomson, B.A., Baganies, E.A. (1978) *Hardenability concept with application to steel*. Ed. by D.V. Doane, J.S. Kirkaldy. Warrendale: AIME.
15. Seyffarth, P. (1982) *Schweiss-ZTU-Schaubilder*. Berlin: Technik.
16. Tadashi, K., Yuji, H. (2007) Carbon equivalent to assess hardenability of steel and prediction of HAZ hardness distribution. *Nippon Steel Techn. Rep.*, **95**, 53–61.
17. Yurioka, N., Okumura, M., Kasuya, T. et al. (1987) Prediction of HAZ hardness of ferritic steels. *Metal Constr.*, **19**, 217–223.
18. Popova, L.E., Popov, A.A. (1991) *Diagrams of austenite transformation in steels and beta-solution in titanium alloys*: Refer. Book of heat-treater. Moscow: Metallurgiya.
19. (1974) *Reference book of welder*. Ed. by V.V. Stepanov. Moscow: Mashgiz.
20. Xavier, C.R., Delgado Junio H.G., de Castro, J.A. (2011) Numerical evaluation of the weldability of the low alloy ferritic steels T/P23 and T/P24. *Mat. Res.*, 14(**1**), 73–90.

INFLUENCE OF DEPOSITED METAL COMPOSITION ON STRUCTURE AND MECHANICAL PROPERTIES OF RECONDITIONED RAILWAY WHEELS

A.A. GAJVORONSKY, V.D. POZNYAKOV, L.I. MARKASHOVA, E.N. BERDNIKOVA, A.V. KLAPATYUK, T.A. ALEKSEENKO and **A.S. SHISHKEVICH**
E.O. Paton Electric Welding Institute, NASU, Kiev, Ukraine

Experimental data are given on the effect of composition of cladding consumables on formation of structure and mechanical properties of the deposited metal on wheels of steel 2. Strength properties, ductility and crack resistance of railway wheels repaired by cladding, were evaluated by analytical methods. It was found that to ensure the required combination of mechanical properties and high crack resistance of the base and deposited metals it is rational to apply cladding consumables of bainitic or bainitic-martensitic grade for repair of railway wheels of steel 2 by arc cladding.

Keywords: *arc welding, railway wheels, deposited metal, HAZ, structure, properties, crack resistance*

The problem of ensuring the reliability and fatigue life of rolling stock is becoming ever more urgent with increase of transportation volume and traffic intensity of railway transport. It is the most acute for basic parts and mechanisms of bogies of carriages and locomotives, the main part of which is the wheel, directly contacting the rail. Wheel tread wears in service. Flange inner surface is prone to considerable wear that is determined by service conditions of friction-rolling wheel–rail pair. Reconditioning of worn wheel tread is performed in specialized repair plants of railway transport by the method of mechanical turning, or by first performing repair cladding of flange surface.

Railway wheels of freight transport, locomotive wheel flanges, flanges of tram wheels of passenger transport are made of high-strength carbon steels, the composition and mechanical properties of which are given in Tables 1 and 2. As is seen, wheel steels feature high strength and hardness. Such metal properties ensure the required level of service strength of wheels. Flanges and all-rolled wheels from steel 2 are the most widely applied in railway transport of Ukraine and CIS countries. In keeping with GOST 10791–89, carbon content in wheel steel 2 is equal to 0.55–0.65 %. However, as shown by experience

Table 1. Composition of high-strength wheel steels, wt.%

Normative document	Steel grade	C	Mn	Si	V	S	P
						not more than	
GOST 10791–89	1	0.44–0.52	0.80–1.20	0.40–0.60	0.08–0.15	0.030	0.035
GOST 10791–89	2	0.55–0.65	0.50–0.90	0.22–0.45	≤0.10	0.030	0.035
TU U 35.2-23365425-600:2006	T	0.58–0.67	0.70–0.90	≤0.40	0.08–0.15	0.020	0.025

railway flanges and wheels are most often made from steel with not higher than 0.60 wt.% carbon content.

At present worn surfaces of railway wheels are repaired by cladding with application of several technologies, namely one- and two-wire submerged-arc cladding, and less often gas-shielded cladding. That is why cladding consumables used are solid welding wires of ferritic-pearlitic (Sv-08GS, Sv-08G2S), bainitic (Sv-10GSMT, Sv-08KhM) or bainitic-martensitic (Sv-10KhG23SMF) classes [1–3]. Worn flanges of all-rolled wheels of freight carriages are repaired by cladding with application of bainitic and bainitic-martensitic cladding consumables. Cladding is performed at controllable thermal cycle with application of preheating from 150 up to 250 °C and delayed cooling of wheels after cladding. These technologies ensure quality repair of worn metal of wheels and their performance during subsequent service. At the same time, at repair of the tread of tram wheel flanges 1960s technology is still used is some plants, when cladding was performed with Sv-08A wire without preheating or delayed cooling of items.

It is obvious that with such a diversity of technologies, the properties of deposited metal, fusion zone and HAZ metal regions of the joints differ essentially. This affects crack resistance of wheels repaired by cladding and their further serviceability. In terms of reliability and safety of railway traffic, during wheel repair by cladding it is necessary to ensure service properties of the deposited metal equivalent to those of wheel steel. For instance, at repair of flanges of all-rolled wheels of freight carriages, deposited metal hardness *HB* should be not lower than 2500 MPa, and ultimate strength — not lower than 700 MPa. It is necessary to ensure the homogeneity of the structure and minimum level of stress gradient in the zone of deposited-to-base metal transition, as item normalizing after cladding is not envisaged.

The objective of this work was performance of comparative evaluation of a set of deposited metal properties, depending on its composition, determination of peculiarities of structural changes in the deposits and their influence on mechanical properties of wheel steel joints. Wheel steel of grade 2 of the following composition (wt.%) was selected as the object of study: 0.58 C; 0.77 Mn; 0.44 Si.

Influence of thermodeformational cycle of welding on the structure and mechanical properties of wheel steel 2 is considered in [2], where it is shown that the cooling rate can have an essential influence on structural-phase composition and mechanical properties of HAZ metal. In the range of cooling rates $w_{6/5}$ = 1.15–32 °C/s ultimate strength of HAZ metal of wheel steel can change from 940 up to 1060 MPa, and yield point — from 600 up to 715 MPa. Its relative elongation δ_5 is in the range of 9.3–13.3 %, and reduction in area ψ — 24.9–33.3 %.

Table 2. Mechanical properties of high-strength wheel steels

Steel grade	σ_t, MPa	δ_5, %	ψ, %	KCU_{+20}, J/cm^2	*HB*, MPa
		not less than			
1	900–1100	12	21	30	2480
2	930–1130	8	14	20	2500
T	≥1100	8	14	18	3200

To determine deposited metal mechanical properties a method was selected, in which test specimens were cut out of upper layers of weld metal of multilayer welded joints with V-shaped groove of 350× 250×20 mm size, with 10 mm gap in the root. In such a variant of the joint mixing of base metal and weld in its central section is minimal, that can be equated to the conditions of multilayer cladding. Automatic submerged-arc welding of such joints was performed under a layer of AN-348 flux with solid wires of grades Sv-08G2S, Sv-08KhM and Sv-08KhMF of 2.0 mm diameter. Some joints were welded in CO_2 atmosphere with flux-cored wire PP-AN180MN (10KhGSMNFT alloying type) of 2.0 mm diameter. Welding of joints was performed with preheating up to the temperature of 150 °C. Welding modes were selected so as to ensure heat-input Q_w in the range of 11–13 kJ/cm. Furtheron special specimens for tensile (GOST 1497) and impact bend testing (GOST 9454) were cut out of upper layers of weld metal of the joints. Tables 3 and 4 give the composition and mechanical properties of weld metal. As shown by test results, except for Sv-08G2S wire, all cladding consumables allow producing deposited metal, the strength and hardness of which is on the level of requirements to reconditioned railway wheels of freight carriages.

As is known, deposited metal properties are determined by its structural-phase composition, which forms during welding and cooling of the joints. Therefore, the objective of further investigations was studying the influence of welding conditions on structural-phase composition of the metal of weld and HAZ of welded joints of wheel steel 2. Condition of metal structure was studied at various levels — from macro (grain) up to micro (dislocation) level.

Table 3. Weld metal composition, wt.%

Wire	C	Mn	Si	Cr	Ni	V	Mo
Sv-08G2S	0.10	2.10	0.95	–	–	–	–
Sv-08KhM	0.12	1.36	0.60	0.60	–	–	0.42
Sv-08KhMF	0.12	1.25	0.62	0.61	–	0.10	0.36
PP-AN180MN	0.12	1.00	0.35	0.67	0.80	0.10	0.40

Table 4. Mechanical properties of weld metal

Wire	$\sigma_{0.2}$, MPa	σ_t, MPa	δ_5, %	ψ, %	KCU_{+20}, J/cm^2	*HB*, MPa
Sv-08G2S	510	590	25.4	63.0	130	2100
Sv-08KhM	535	705	21.0	61.0	98	2500
Sv-08KhMF	610	730	17.2	56.3	86	2600
PP-AN180MN	700	790	12.7	57.6	97	2600

Allowing for these data and applying Archard equation, as well as well-known Hall–Petch, Orowan and other relationships, change of metal yield point $\sigma_{0.2}$ in different welded joint zones was determined by calculations:

$$\Sigma\sigma_y = \Delta\sigma_0 + \Delta\sigma_{s.s} + \Delta\sigma_{gr} + \Delta\sigma_s + \Delta\sigma_p + \Delta\sigma_d + \Delta\sigma_{d.s}, \quad (1)$$

where $\Delta\sigma_0$ is the metal lattice resistance to free dislocation motion; $\Delta\sigma_{s.s}$ is the solid solution strengthening by alloying elements or impurities; $\Delta\sigma_{gr}$, $\Delta\sigma_s$ is the strengthening due to a change of grain and subgrain size; $\Delta\sigma_p$ is the strengthening due to pearlite; $\Delta\sigma_d$ is the dislocation strengthening; $\Delta\sigma_{d.s}$ is the dispersion hardening.

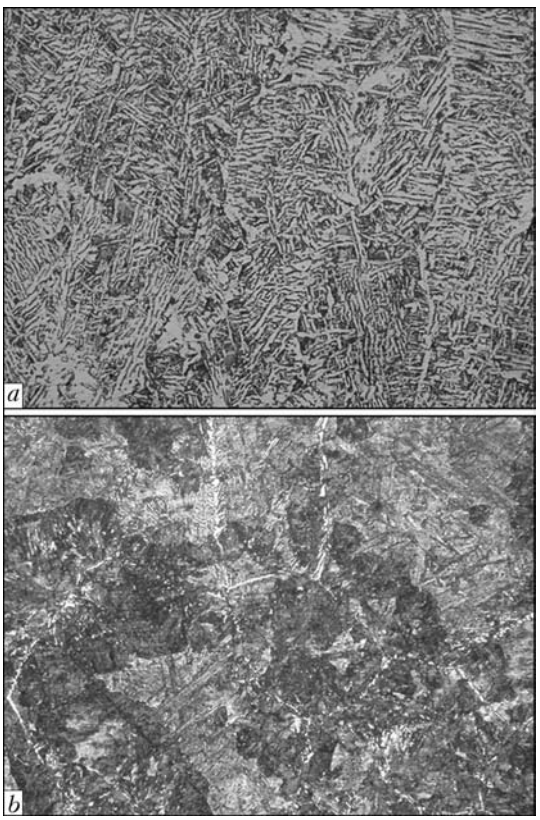

Figure 1. Microstructures (×500) of weld metal (*a*) and coarse-grain section of HAZ (*b*) of wheel steel 2 in welding with Sv-08G2S wire

Contribution of individual structural components, size of grain, subgrain, dislocation density into the change of total (integral) strength was assessed. Method of conducting analytical evaluation at performance of these investigations is similar to that described in [4, 5].

Critical stress intensity factor K_{1C} characterizing brittle fracture resistance of the metal, and local internal stresses $\tau_{in.s}$ in the structure, which are the potential sources of crack initiation and propagation, were found from the following formulas:

$$K^*_{1C} = (2E\sigma_y\delta_t)^{1/2}, \quad (2)$$

$$\tau_{in.s} = Gbh\rho/[\pi(1-\nu)], \quad (3)$$

where E is the Young's modulus; σ_y is the calculated value of yield point; δ_t is the value of critical crack opening displacement, equated to substructure parameters (subgrain size, lath width or fragment size); G is the shear modulus; b is the Burgers vector; $h = 2\cdot10^{-5}$ cm is the foil thickness; ν is the Poisson's ratio; ρ is the dislocation density.

All the above investigations were performed for cladding variants using solid wire Sv-08G2S and flux-cored wire PP-AN180MN, and their results are given in Figures 1–5.

As shown by metallographic investigations, weld metal of joints of wheel steel 2 made with Sv-08G2S wire has a coarse-grained structure, consisting of ferrite and pearlite (Figure 1, *a*).

Crystallite dimensions (h_{cr}×l_{cr}) are tentatively equal to (30–130)×(60–250) μm. Ferrite microhardness is HV(F) = 2010, that of pearlite HV(P) = 2210–2510 MPa. Metal structure in the overheated zone of the HAZ of such joints consists of martensite (M), and bainite (B), which have the following microhardness, respectively: HV(M) = 3660–4540, HV(B) = 2570–3570 MPa, and ferrite fringes F_{fr} of thickness $\delta(F_{fr})$ = 3–7 μm, located along grain boundaries (Figure 1, *b*). Grain size D_{gr} of M and B is equal to 115–215 and 40–155 μm, respectively, and their volume fraction is V_M = 30 and V_B = 65–68 %.

Weld metal of joints made with flux-cored wire PP-AN180MN is characterized by bainite-martensite (B–M) structure (Figure 2, *a*) with microhardness HV(B–M) = 2860–3290 MPa and crystallite dimensions h_{cr}×l_{cr} = (25–60)×(65–180) μm, as well as presence of ferrite fringes of thickness $\delta(F_{fr})$ = 3–5 μm along grain boundaries. Ratio of B and M volume fraction in the weld metal is equal to 70–30 %. A structure close as to its composition was also found in the metal of HAZ overheated zone of such joints (Figure 2, *b*). B and M volume fraction in this welded joint zone is equal to 75–80 and 25–20 %, respectively, while microhardness is in the range of HV(M) = 3660–4540 MPa and HV(B) = 2570–3570 MPa. Sizes of B and M grains are equal to 115–215 (M) and 40–155(B) μm. As in the previous cases, ferrite fringes of thickness $\delta(F_{fr})$ = 3–7 μm were found along grain boundaries.

Thus, optical metallography showed that a coarse-grained ferrite-pearlite structure with an abrupt gradient of grain size (it differs by 2 to 4 times) forms in weld metal of joints made with

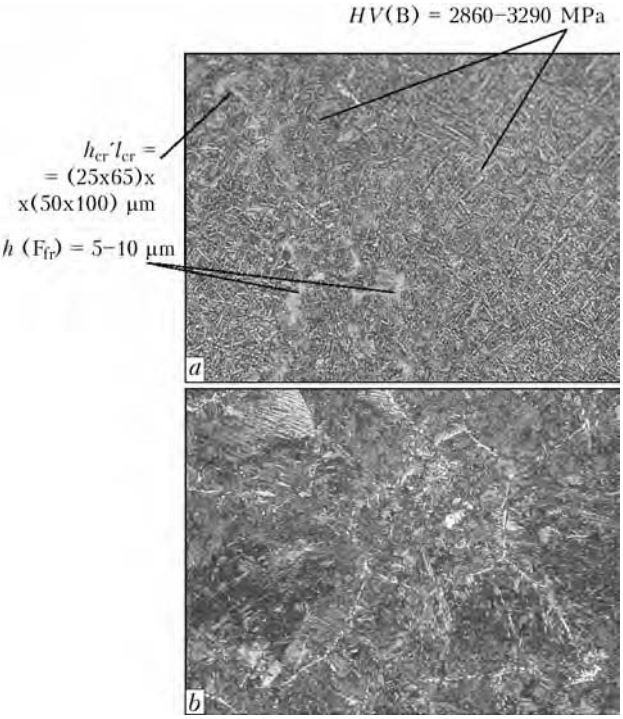

Figure 2. Microstructures (×500) of weld metal (*a*) and coarse-grain section of HAZ (*b*) of wheel steel 2 in welding with PP-AN180MN wire

Sv-08G2S wire, and a fine-grained bainite-martensite structure forms in the HAZ metal, its microhardness being practically 1.5 times higher than that of the deposited metal. In welded joints made with flux-cored wire PP-AN180MN, a bainite-martensite structure, quite close in its phase composition, and not having any abrupt gradients either by grain size, or by hardness, forms in the metal of weld and HAZ.

Features of variation of fine structure (lath width, substructure size and dislocation density) of the metal of weld and HAZ of wheel steel joints were studied by the methods of transmis-

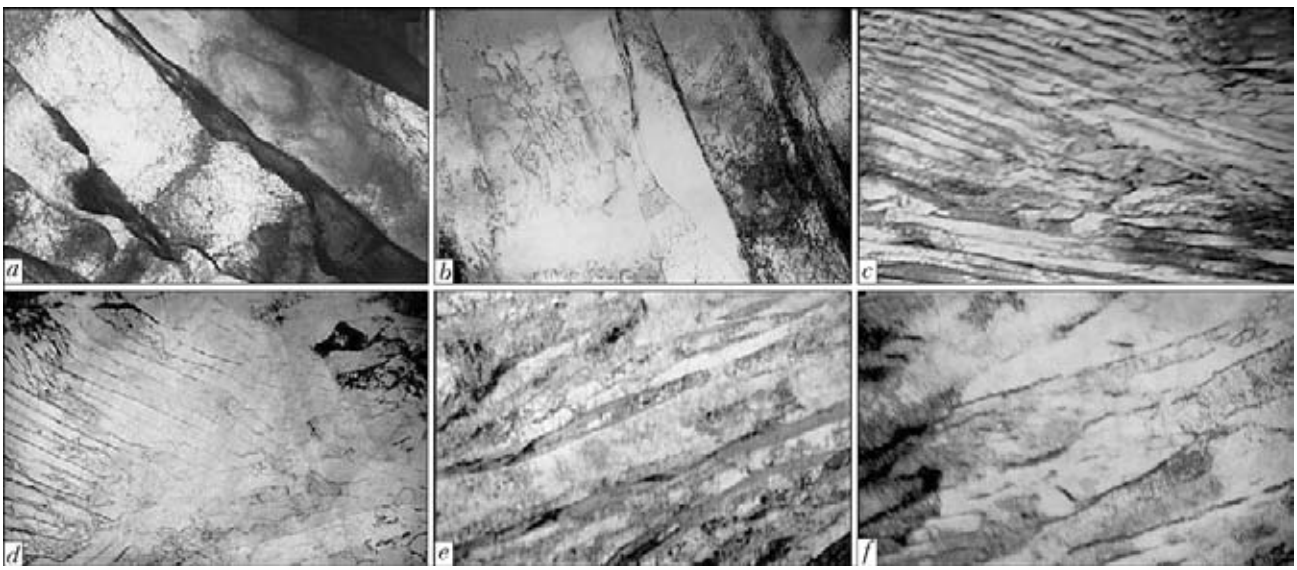

Figure 3. Fine structure of metal of weld (*a–d*) and coarse-grain section of HAZ (*e*, *f*) of joints of wheel steel 2 in welding with Sv-08G2S wire (*a*, *b*, *d*, *e* — ×20,000; *c*, *f* — ×30,000)

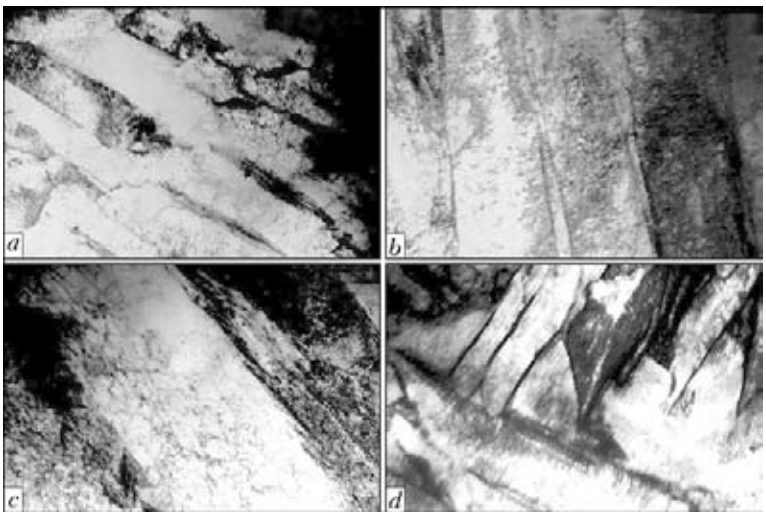

Figure 4. Fine structure of weld metal (*a*, *b*) and section of coarse-grain metal of HAZ (*c*, *d*) of joints of wheel steel 2 in welding with PP-AN180MN wire (*a* — ×15,000; *b* — ×20,000; *c*, *d* — ×30,000)

sion electron microscopy. They showed that in the main bulk of weld metal of joints made with Sv-08G2S wire, dimensions of cementite h_c and ferrite h_f plates in pearlite are equal to 0.1–0.4 and 0.7–1.5 μm, respectively, and dislocation density is $\rho = (4–6)\cdot10^9$ cm^{-2} (Figure 3, *a*, *b*). It is also established that in the weld section located in immediate proximity to the fusion line and at up to 500 μm distance from it, the structure is refined by an order of magnitude, and dislocation density rises up to $1\cdot10^{10}$ cm^{-2} (Figure 3, *c*, *d*). In the metal in HAZ overheated zone the width of upper bainite laths h_{Bup} is equal to 0.8–1.3 μm, that of lower bainite h_{Bl} is 0.3–0.8 μm, and of martensite h_M = 1.0–1.5 μm. Dimensions of fragments of lower bainite $d_{fr}(B_l)$ are in the range of 0.15–0.50 μm. Compared to weld metal, density of dislocations in this zone of welded joint rises up to $\rho = (5–8)\cdot10^{10}$ cm^{-2} (Figure 3, *e*, *f*).

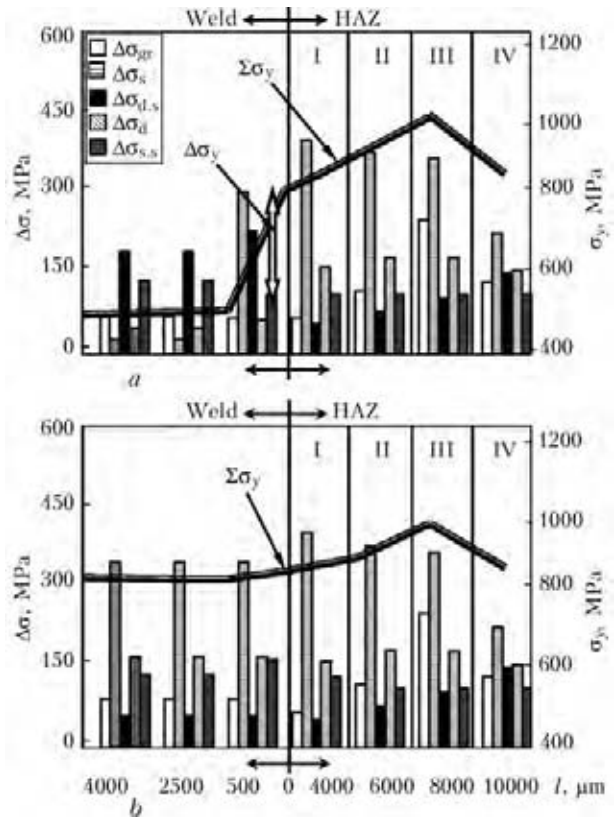

Figure 5. Contribution of structural components and strengthening of welded joint metal in welding with wires Sv-08G2S (*a*) and PP-AN180MN (*b*): I–IV — HAZ zones of overheating, normalizing, partial recrystallization and recrystallization, respectively

In welding with flux-cored wire PP-AN180MN a structure close as to its composition and element dimensions, consisting of upper and lower bainite, as well as martensite, forms in the metal of weld (Figure 4, *a*, *b*) and HAZ (Figure 4, *c*, *d*). Width of laths of upper bainite h_{Bup} is equal to 0.5–1.2 μm, that of lower bainite h_{Bl} = = 0.4–0.7 μm, and of martensite h_M = 1.0–1.5 μm. Distribution of dislocation density in such a joint is relatively uniform $\rho = 5\cdot(10^{10}–10^{11})$ cm^{-2}.

Figure 5 shows how metal yield point changes in different zones of welded joints, depending on deposited metal composition. It is established that strengthening of the bulk of weld metal of welded joints, made with Sv-08G2S wire, is due predominantly to the influence of carbide phases ($\Delta\sigma_{d.s}$ = 190–230 MPa) (Figure 5, *a*). Near the fusion line weld metal yield point rises practically 1.7 times, from 480 up to 800 MPa. This occurs mainly due to additional contribution of substructural ($\Delta\sigma_s$ = 300 MPa) and dislocation ($\Delta\sigma_d$ = 60 MPa) factors into metal strengthening.

Change of the values of metal yield point in different zones of welded joints, made with flux-cored wire PP-AN180MN, occurs smoothly (Figure 5, *b*). Strengthening of weld metal of such joints occurs mainly due to substructural ($\Delta\sigma_s$ = = 345 MPa) and dislocation ($\Delta\sigma_d$ = 140–

200 MPa) strengthening. Carbide phase particles have a weaker effect on this process ($\Delta\sigma_{part}$ = = 75 MPa). Strengthening due to refining (dispersion) of lower bainite substructure is equal to about 33 % ($\Delta\sigma_s$ = 280 MPa) of the total strengthening level.

Strengthening of HAZ metal of the above-mentioned joints proceeds in a similar fashion. This is related, primarily, to fragmentation of lower bainite substructure ($\Delta\sigma_s$ = 367 MPa) and increase of dislocation density ($\Delta\sigma_d$ up to 200 MPa), that is equal to 42–48 and 20–25 % of the total strengthening level, respectively. Yield point of HAZ metal is in the range of 820–1000 MPa.

Results of calculation-based evaluation of K_{1C} values of welded joints of wheel steel 2 made with Sv-08G2S and PP-AN180MN wires (Figure 6) showed the following. Despite higher strength characteristics, the bulk of the metal deposited with flux-cored wire PP-AN180MN has the same K_{1C} values as the joints made with Sv-08G2S wire, and in some regions it exceeds them practically 2 times. This is associated with the features of formation of favourable substructure in them, more uniform distribution of dislocations and grain refinement, whereas metal deposited with Sv-08G2S wire features a non-uniform distribution of dislocation density and presence of pearlite structures with extended cementite phase precipitates that is detrimental to K_{1C} values. On the whole, such investigations showed that in welding with PP-AN180MN wire the weld metal forms a structure combining the high strength with good brittle fracture resistance.

Results of calculation-based evaluation of local internal stresses $\tau_{in.s}$ at comparison of these values with theoretical strength of material (Figure 7) showed that the lower general level of local internal stresses, distributed in the weld, forms in welded joints made with Sv-08G2S wire (Figure 7, *a*). Their value is not higher than 400 MPa, that is equal to approximately 0.04 of metal theoretical strength τ_{theor}. Increase of dislocation density from $(4–6)\cdot10^9$ up to $(5–8)\cdot10^{10}$ cm^{-2} in the weld zone, which is in immediate vicinity to the fusion line (FL) and in the HAZ of such joints, leads to an abrupt increase of $\tau_{in.s}$ up to 2240–2430 MPa, that is equal to $(0.3–0.4)\tau_{theor}$, and to formation of considerable gradients of internal stresses ($\Delta\tau_{in.s}$ ~ 2000 MPa). Maximum $\tau_{in.s}$ values form on the mating boundary of F–P and B–M structures.

Total level of $\tau_{in.s}$ in weld metal in joints, made with flux-cored wire PP-AN180MN, is higher (1870–2240 MPa). They, however, are uniformly distributed in the weld metal and decrease relatively smoothly to 900–1100 MPa at transition to HAZ metal. Due to that no abrupt gradients of local stresses are observed in such joints that is favourable in terms of cracking prevention.

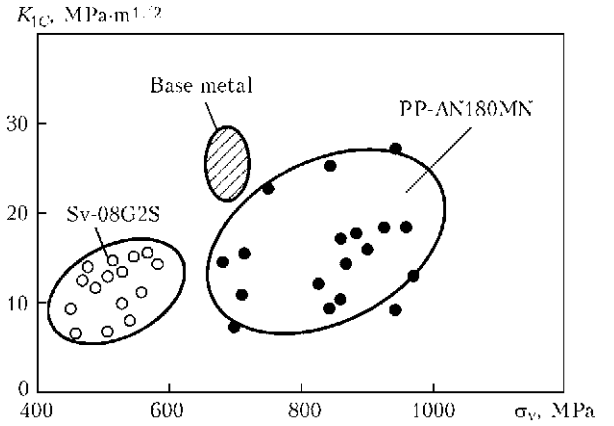

Figure 6. Diagram of the change of calculated mechanical properties ($\sigma_{0.2}$, K_{1C}) of weld metal of wheel steel welded joints depending on deposited metal composition

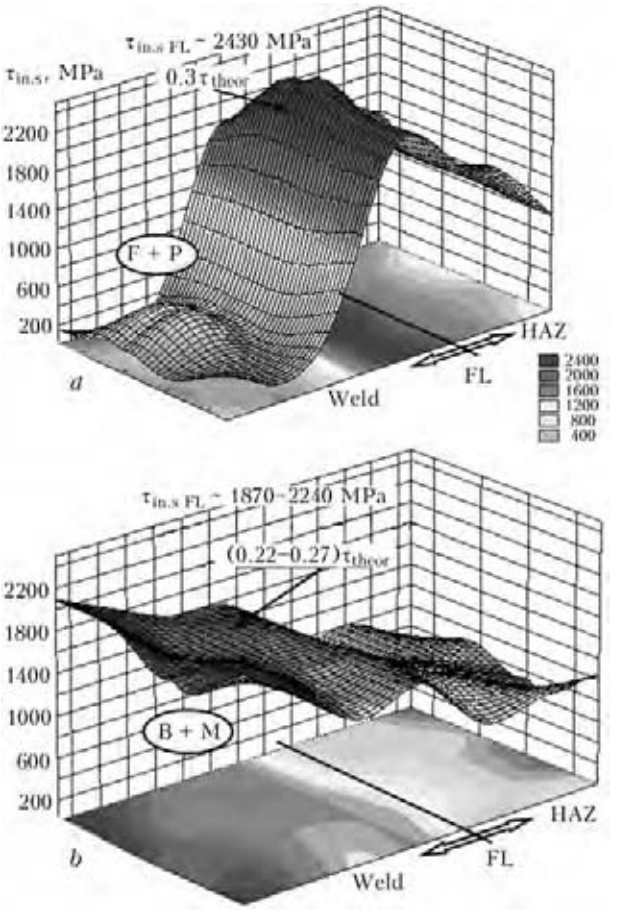

Figure 7. Level of local internal stresses $\tau_{in.s}$, forming in wheel steel welded joints, depending on deposited metal composition: *a* — Sv-08G2S; *b* — PP-AN180MN wire

CONCLUSIONS

1. Required set of mechanical properties of the deposited metal at reconditioning of worn surfaces of railway wheels (hardness $HB \geq 2500$, strength $\sigma_t \geq 700$ MPa) can be ensured by cladding consumables of bainite or bainite-martensite classes, namely solid wires Sv-08KhM, Sv-08KhMF and flux-cored wire PP-AN180MN.

2. Metal, deposited with flux-cored wire PP-AN180MN, combines high strength, hardness and crack resistance. All the regions of welded joints, made with this wire, have homogeneous finely-dispersed bainite-martensite structure with uniform distribution of local internal stresses.

1. Pavlov, N.V., Kozubenko, I.D., Byzova, N.E. et al. (1993) Cladding of flanges of railway wheel pairs. *ZhD Transport*, **7**, 37–40.
2. Sarzhevsky, V.A., Gajvoronsky, A.A., Gordonny, V.G. et al. (1996) Influence of technological factors on structure and properties of HAZ metal in repair-and-reconditioning cladding of flanges of all-rolled railway wheels. *Avtomatich. Svarka*, **3**, 22–27, 33.
3. Gudkov, A.V., Lozinsky, V.N. (2008) New technological and engineering solutions in the field of welding on railway transport. *Vestnik VNIIZhT*, **6**, 3–9.
4. Markashova, L.I., Poznyakov, V.D., Alekseenko, T.A. et al. (2011) Effect of alloying of the welds on structure and properties of welded joints on steel 17Kh2M. *The Paton Welding J.*, **4**, 5–13.
5. Markashova, L.I., Poznyakov, V.D., Gajvoronsky, A.A. et al. (2011) Evaluation of strength and crack resistance of railway wheels metal after long-term service. *Fizyko-Khimichna Mekhanika Materialiv*, **6**, 73–79.

NEW SYSTEM OF FILLER METALS FOR BRAZING OF TITANIUM ALLOYS

V.F. KHORUNOV and **V.V. VORONOV**
E.O. Paton Electric Welding Institute, NASU, Kiev, Ukraine

Based on the results of systematic studies of Ti–Zr–Co system alloys and allowing for published data, the liquidus surface of this system was plotted by using the simplex-lattice experimental design method. This system was found to have a region of alloys with decreased liquidus temperature, the most promising in terms of filler metal development. Spreading of experimental filler metals over titanium alloys of different classes (OT4, VT6 and VT22) was studied. The data on mechanical properties of the brazed joints are given.

Keywords: *brazing, titanium alloys, new system of brazing filler metals, liquidus surface, wetting, mechanical properties*

Titanium alloys play an important role in modern industry, especially in aircraft engineering, owing to their high characteristics, low density, high strength, high corrosion and fatigue resistance in particular, as well as high value of specific strength.

Meanwhile, the problem of current importance is fabrication of brazed structures of titanium alloys which cannot be manufactured by welding. Such structures include critical heat exchangers for cooling of compact nuclear reactors, as well as lamellar-ribbed and honeycomb structures used in aircraft engineering, ship building, etc. [1].

The modern brazing technology and filler metals should provide seams with the properties close to those of the base metal. This specifies important temperature-time bounds of the brazing cycles determined by the nature of titanium alloys. These bounds limit the probability of undesired changes in structure and properties of the alloys caused by polymorphism of titanium.

At a temperature below 882 °C titanium is in the α-state (hexagonal lattice), while above this temperature it is in the β-state (cubic lattice). This circumstance has a considerable effect on diffusion of depressant elements from the seam to a metal brazed and, as a consequence, on structure and properties of the brazed joints.

According to study [2], the need to limit the brazing temperature of titanium and its alloys is caused by a high rate of growth of its grain at temperatures above 1000 °C. Therefore, the melting point of a filler metal should not exceed 950–1000 °C.

In study [3] the upper bound of the brazing temperature was decreased to 900 °C for α- and pseudo-α-alloys, to 935 °C for α + β-alloys, to 870 °C for pseudo-β-alloys, and to 760–800 °C for β-alloys.

Limitation of the brazing temperature to a value of the $\alpha \rightarrow \beta$ transformation temperature is especially important for thin-walled structures

Commercial titanium-base filler metals

Filler metal	Composition, wt.%	Temperature, °C		
		Solidus	Liquidus	Brazing
VTi-1	Ti–15Cu–15Ni	902	950	980–1050
VTi-2	Ti–15Cu–25Ni	901	914	930–950
VTi-3	Ti–26Zr–14Cu–14Ni–0.5Mo			820–920
VTi-4	Ti–20Zr–20Cu–20Ni	848	856	
Ticuni 70	Ti–15Cu–15Ni	902	950	980–1050
MBF 5011	Ti–18.5Cu–27.5Ni	910	920	
MBF 5012	Ti–20Cu–20Ni	915	936	
VPr16	Ti–(8–16)Ni–(11–14)Zr–(21–24)Cu	880	900	920–970
STEMET1201	Ti–12Zr–12Ni–23Cu	830	955	900–1000
Ti–Zr–Be–Al	Ti–45Zr–4.7Be–5Al		910	
Ti–Zr–Be	Ti–48Zr–2Be		930	

usually applied in aircraft engineering, as active growth of grains and active diffusion of filler metal components to the base metal of a small thickness lead to embrittlement of the seam.

Today the most common filler metals for high-temperature brazing of titanium, which are successfully used for fabrication of different-purpose structures, are filler metals of the Ti–Cu–Ni and Ti–Zr–Cu–Ni systems (Table).

However, these filler metals have application limitations because of the copper and nickel content. So, it is necessary to investigate new alloy systems in which these elements are absent. The Ti–Zr–Fe [4–6] and Ti–Zr–Mn [5, 6] systems have been considered in literature as an alternative to the known systems of filler metals. Filler metals of the above systems have good operational properties and provide good strength of the brazed joints. However, melting temperature T_{melt} of these filler metals is within 960 (for the Ti–Zr–Fe system) and 1050 °C (for the Ti–Zr–Mn system) [5, 6]. Accordingly, the brazing temperatures for these filler metals exceed the upper bound of the permissible temperatures.

The purpose of this study was development of a new generation of filler metals for brazing of titanium alloys to widen the field of application of the brazed titanium structures. Such filler metals should not contain the above element and have a decreased melting point (below 900 °C).

Investigation of the constitutional diagrams showed that unlimited solid solutions with titanium are formed only by refractory metals (zirconium, vanadium, molybdenum, niobium). Among them, zirconium and vanadium form solid solutions with a minimum on the liquidus curve, this making it possible to use the Ti–Zr and Ti–V systems as a base for development of filler metals. In particular, in our opinion the promising system is Ti–Zr–Co.

To determine optimal proportions of elements in an alloy, it was necessary to plot the liquidus diagram for the Ti–Zr–Co ternary system. Plotting of such a surface by traditional experimental methods is difficult and time-consuming. Therefore, we used a combination of the calculation and experimental method, in particular the simplex-lattice experimental design method, the

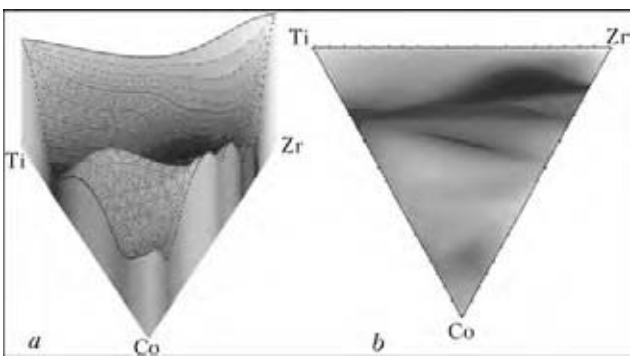

Figure 1. Results of calculation of liquidus surface for the Ti–Zr–Co system alloy in the 3D form (*a*) and on a plane (*b*)

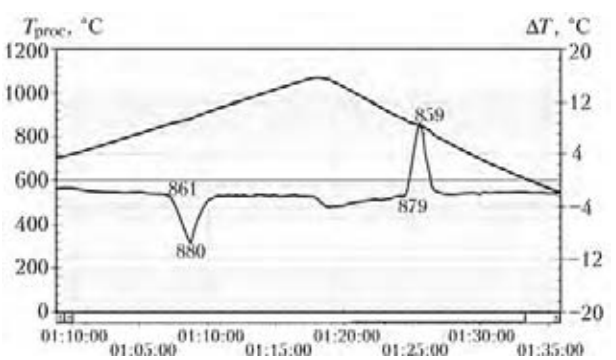

Figure 2. Results of high-temperature differential thermal analysis of experimental alloy of the Ti–Zr–Co system

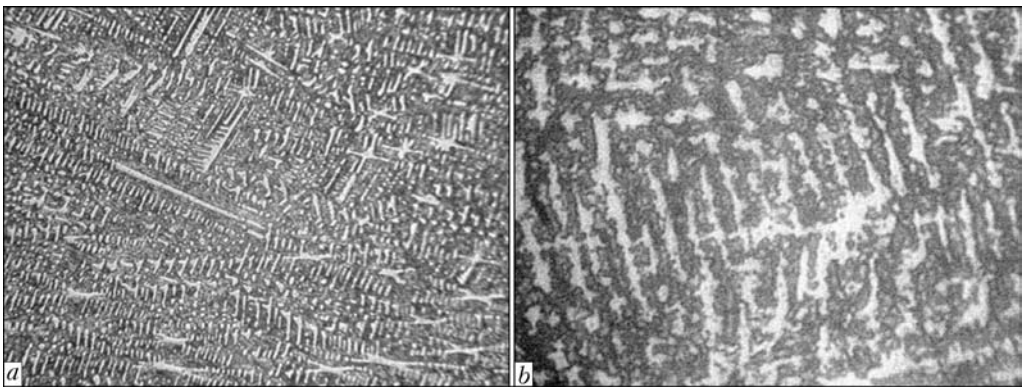

Figure 3. Microstructure of alloy Ti–Zr–Co in the cast state (*a* — ×500; *b* — ×1000)

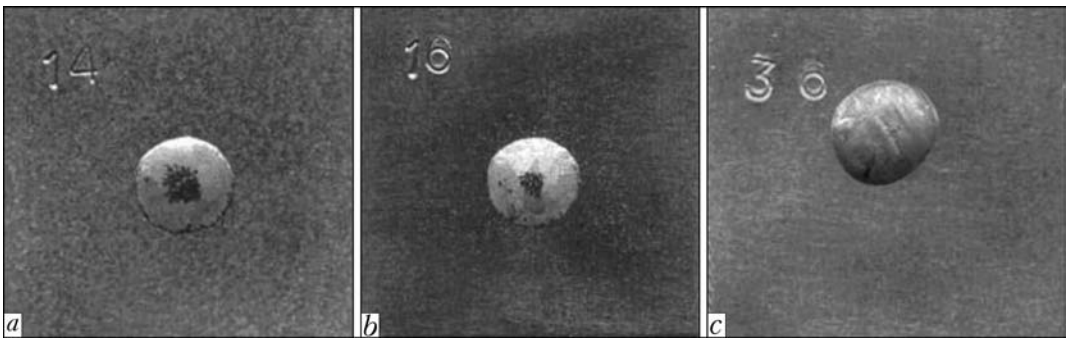

Figure 4. Appearances of specimens with filler metals spread over the substrate of alloy OT4: *a* — VPr16 (STEMET 1201) (T_{melt} = 990 °C, t = 10 min); *b* — Ti–Zr–Fe (T_{melt} = 1000 °C, t = 10 min); *c* — Ti–Zr–Co (T_{melt} = 920 °C, t = = 10 min)

mathematical tools for which are described in detail in studies [7, 8].

About 50 alloys melted on a cold substrate by electron beam heating were studied in the process of plotting the liquidus diagram for the Ti–Zr–Co system. The calculation results are shown in Figure 1.

It can be assumed on the basis of this diagram that the given system in a range of alloys with a low cobalt content (approximately along the line passing from alloy Ti–22Co to alloy Zr–15Co) has the line of monovariant eutectic, as well as the region with a decreased liquidus temperature (less that 900 °C), which in our opinion is most promising for development of filler metals.

Based on the calculation results and the plotted liquidus surface, several alloys of the Ti–Zr–Co system were chosen for further investigations.

After melting of experimental alloys, the differential thermal analysis and metallographic examinations of these alloys were carried out to check agreement of the calculation method results and experimental data.

Differential thermal analysis of the alloys was conducted by using instrument VDTA 8M-3 (heating and cooling rate was 30 °C/min).

One potentially promising alloy was chosen on the basis of the experimental results for further, more detailed investigations. As seen from the data in Figure 2, the chosen alloy has a temperature of the beginning of melting equal to 861 °C and that of complete melting — equal to 880 °C.

As seen from Figure 3, *a*, *b*, this alloy is a mixture of two phases — solid solution (white phase) and eutectic (dark phase). The fact that the differential curve in heating and cooling of the chosen alloy (see Figure 2) has only one peak can be explained so that these phases seem to have close melting temperatures.

To evaluate the level of wetting and spreading of the experimental filler metal over the substrate of titanium alloys of different classes, a series of

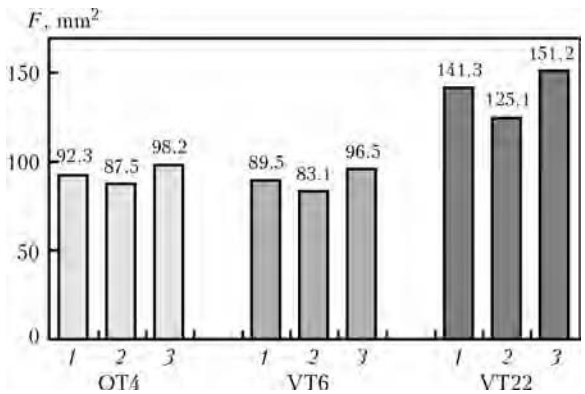

Figure 5. Area of spreading of cast filler metals over alloys OT4, VT6 and VT22 (heating in vacuum $5 \cdot 10^{-5}$ mm Hg): *1* — VPr16 (STEMET 1201) (T_{melt} = 990 °C, t = 10 min); *2* — Ti–Zr–Fe (T_{melt} = 1000 °C, t = 10 min); *3* — Ti–Zr–Co (T_{melt} = 920 °C, t = 10 min)

experiments was conducted to determine the areas of spreading of filler metals of the Ti–Zr–Co system over the substrate of alloys OT4 (low pseudo-α-alloy), VT6 (medium α + β-alloy) and VT22 (high α + β-alloy). Filler metal Ti–12Zr–12Ni–23Cu (STEMET 1201) in the cast state and a new experimental filler metal Ti–35Zr–25Fe developed by the E.O. Paton Electric Welding Institute were investigated for comparison.

The specimens were heated in vacuum furnace SGV 2.4–2/15I3 under the following conditions: environment of a work space of the furnace — vacuum $5 \cdot 10^{-5}$ mm Hg, heating rate ~30 °C/min, brazing temperature for filler metal Ti–Zr–Co — 920 °C, and for filler metals Ti–Zr–Fe and STEMET 1201 — 1000 °C.

The area of spreading of filler metals over the substrate was determined by using software AUTOCAD 2007. The experimental results are shown in Figures 4 and 5.

It can be seen from the given diagrams that the area of spreading of filler metal Ti–Zr–Co over titanium substrates of the three types is higher compared to filler metals of the other systems, which is probably related to an increased zirconium content in the experimental alloy.

Preliminary mechanical tests of the joints brazed with filler metal of the Ti–Zr–Co system (Figure 6) showed that strength of the joints of alloy VT6 brazed with the experimental filler metal is higher than that of the joints brazed with standard filler metals, despite a lower brazing temperature.

The results given demonstrate that the experimental filler metal of the Ti–Zr–Co system meet the requirements imposed on filler metals for fabrication of different-application structures of titanium alloys.

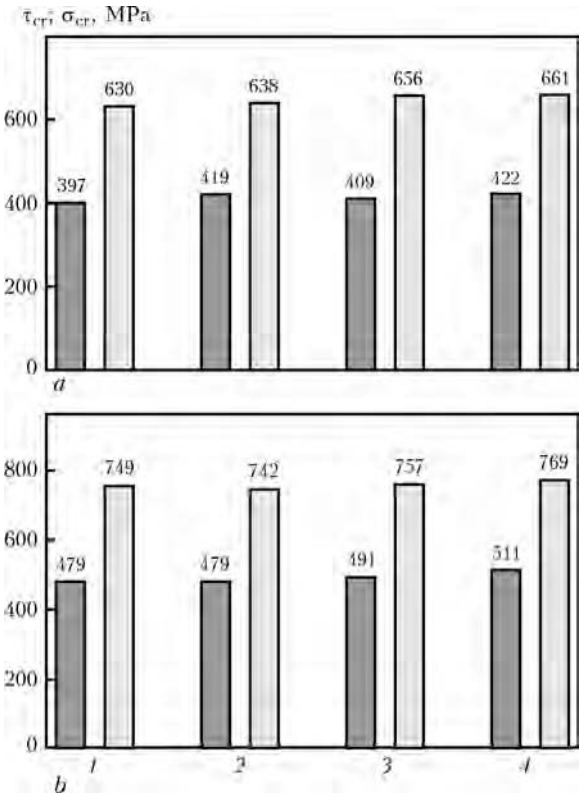

Figure 6. Mechanical properties of overlap (dark columns) and butt (light columns) joints of alloys OT4 (*a*) and VT6 (*b*) brazed by using different filler metals: *1*, *2* — VPr16, cast, and STEMET 1201, amorphous strip (T_{melt} = 990 °C, t = 10 min), respectively; *3* — Ti–Zr–Fe (T_{melt} = 1000 °C, t = 10 min); *4* — Ti–Zr–Co (T_{melt} = 920 °C, t = 10 min)

CONCLUSIONS

1. The promising filler metal was chosen for brazing of titanium alloys of different classes on the basis of the results of investigations of the Ti–Zr–Co system alloys, as well as the plotted liquidus surface for this system.

2. It was established that the area of spreading of the experimental alloy over the substrates of titanium alloys of different classes is higher than that of standard filler metals for brazing of titanium alloys.

3. The area of spreading of all investigated alloys increases with increase in the concentration of alloying elements in the brazed titanium alloys. For instance, in investigation of spreading the best results were obtained on high pseudo-β-alloy VT22.

4. Mechanical properties of the brazed joints on alloys OT4 and VT6 made with the experimental filler metal are in excess of strength of the joints brazed with known filler metals.

1. Shapiro, A., Rabinkin, A. (2003) State of the art and new potential aerospace applications of titanium-based brazing filler metals: Overview. In: *Proc. of 2nd Int. Brazing and Soldering Conf.* (San-Diego, Feb. 17–19, 2003).
2. Lashko, N.F., Lashko, S.V. (1977) *Brazing of metals*. Moscow: Mashinostroenie.
3. Shapiro, A.E., Flom, Y.A. Brazing of titanium at temperatures below 800 °C: Review and prospective applications. *http*:www.titanium-brazing.com/publications/DVS-Manuscript_1020-Copy2-19-07.pdf
4. Muller, H., Breme, J. (1999) Brazing of titanium with new biocompatible brazing filler alloys. In: *Proc. of 9th World Conf. on Titanium Science and Technology* (Saint-Petersburg, Russia, 7–11 June 1999), 1655–1758.
5. Khorunov, V.F., Maksymova, S.V., Ivanchenko, V.G. (2004) Development of filler metals for brazing heat-resistant nickel- and titanium-base alloys. *The Paton Welding J.*, **9**, 26–31.
6. Khorunov, V.F., Maksymova, S.V., Zelinskaya, G.M. (2010) Investigation of structure and phase composition of alloys based on the Ti–Zr–Fe system. *Ibid.*, **9**, 9–13.
7. Zedgenidze, I.G. (1976) *Experimental design for investigation of multi-component systems*. Moscow: Nauka.
8. Scheffe, H. (1958) Experiments with mixtures. *J. Roy. Stat. Soc. B*, 20(**2**), 344.

INTERVIEW WITH V.G. SUBBOTIN, DIRECTOR GENERAL OF OJSC TURBOATOM

Viktor Grigorievich, under your leadership TURBOATOM has substantially strengthened and promoted its positions in the world market of equipment for nuclear, heat and hydraulic power stations. What are the economic indices that characterise operation of your Company?

In 2012, the return from realisation of products was 1.4 Billion UAH at a growth rate by 2010 equal to 136.7 %. Specific weight of export in the volume of the realised products was 67 %. The total amount of money which TURBOATOM transferred to the state and local budgets in the form of taxes and other payments was 256.2 Million UAH. According to the results of work in the first quarter this year, the growth rate is about 45 % relative to that of the same period last year.

What is the average monthly salary of the operating personnel at TURBOATOM?

Increase of the output provided a big profit, which led to a corresponding growth of salaries. Compared to the same period last year it amounts to about 12 %. The average monthly salary of the operating personnel is 3447 UAH, and that of the main production workers is 4803 UAH. This is one of the highest salaries in the engineering industry of Ukraine. The operating personnel works at the main workshops in full three shifts. The mean age of workers at TURBOATOM during the last five years decreased from 51 to 44 years.

Viktor Grigorievich, how did the accident at NPP in Japan affect the volume of orders for nuclear power engineering?

The accident at NPP in Japan exerted almost no effect on development of nuclear power engineering and volume of orders which TURBOATOM performs. The stock of orders our Company receives consists of real contracts, their volume continuously grows and amounts today to 3 Billion UAH. In the nearest future we are expecting a number of the new paying orders.

What heat, nuclear and hydraulic power plant equipment has your Company manufactured and shipped this year?

• Three steam turbines with a total capacity of 748,000 kW for unit 6 of the Heat Power Plant in Aksu (Kazakhstan), unit 5 of the Starobeshevskaya HPP, and unit 8 of the Kurakhovskaya HPP (Ukraine);

• condenser and four rotors for unit 3 of the Rostov NPP (Russia);

• assemblies and components for upgrading of the condenser for HPP in Aksu (Kazakhstan);

• four sets of upgraded turbines K500-65/3000 for NPPs in Russia;

• power equipment for unit 1 of Zaporozhie HPP and unit 4 of Zuevskaya HPP (Ukraine);

• sets of power equipment for upgrading of the Nazarovskaya State Regional Power Plant, Rostov NPP, Balakovskaya NPP, Irkutsk HPP (Russia), and HPP in Habana (Kuba);

• three hydraulic turbines of a total capacity of 192,000 kW, including for DneproGES, unit 13; Dneprodzerzhinsk HPP, unit 2; and Kanevskaya HPP, unit 2 (Ukraine);

• propeller and parts for Kremenchug HPP 2 (Ukraine);

• embedded parts for Kamskaya HPP 15, Gotsatlinskaya HPP and Novosibirskaya HPP (Russia);

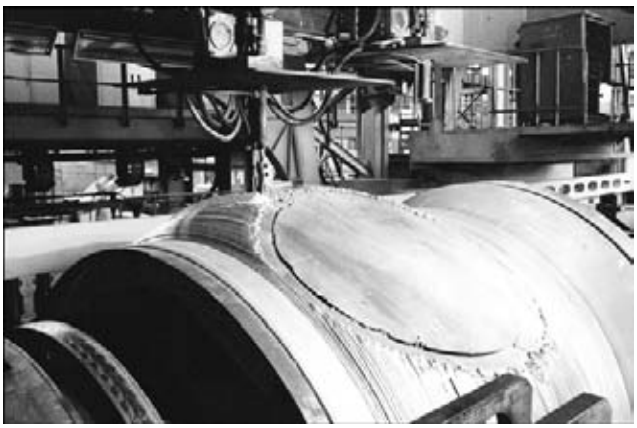

• sets of power equipment for upgrading of Kamskaya HPP and Nurekskaya HPP (Tajikistan).

Viktor Grigorievich, TURBOATOM has made the biggest contract in its history for manufacture of equipment for Rostov NPP. What this contract is about?

Our Company received an order for manufacture and delivery of the 1100 MW steam turbine with a condenser for unit 4 of Rostov NPP. The amount of the transaction is above 120 Million US Dollars. This is really the biggest contract in the entire history of TURBOATOM. The bidding conditions for this contract were very stringent. The fact that two power units with the TURBOATOM turbines are already operating to advantage at Rostov NPP, and that designs of the operating turbines are characterised by a high degree of reliability, also added to our success.

Substantial increase in the rates of development of TURBOATOM requires upgrading of the process equipment and application of the advanced technologies?

TURBOATOM systematically provides upgrading of its equipment. Our Company spent 35 Million UAH for re-equipment in 2010 and 57.4 Million UAH in 2011. For example, we purchased the latest metal cutting machine tools and welding equipment. This year we have planned to spend above 70 Million UAH for upgrading and R&D.

Which new welding processes is your Company mastering?

Recently we have applied several new technologies at TURBOATOM. For example, this is the technology for electric arc spraying of hydraulic turbine parts, and the orbital welding technology which we used to manufacture condensers with titanium and stainless steel tubes for Rostov, Balakovskaya, Kalininskaya and Novovoronezhskaya NPPs.

With the assistance rendered by specialists of the E.O. Paton Electric Welding Institute and National Technical University «Kharkov Polytechnic Institute» (R&D leaders — A.K. Tsaryuk and V.V. Dmitrik), we are introducing a new welding technology for manufacture of forged-welded medium-pressure rotors for turbines K-325. Design peculiarity of such rotors is that they consist of two parts joined by automatic welding. One part of the rotor is made from steel 20Kh3MVFA, and the other — from steel 25Kh2NMFA. Therefore, for the first time in turbine construction, to make rotors we used the technology of welding dissimilar steels, which differ in the level and heat resistance. Application of such rotors is stipulated by the fact that in the process of their operation one of the rotor

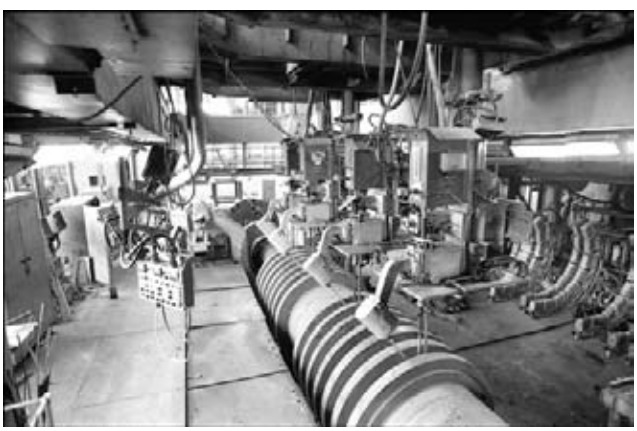

parts is heated to a temperature of 350 °C and the other part — to 560 °C. Design embodiment of the new rotors manufactured on the basis of the R&D results provides increase in their vibration resistance and reliability during operation.

As far as the equipment is concerned, we are upgrading the gas and plasma cutting lines. By now we have upgraded two gas cutting units of the «Messer Griesheim» Company, and we are holding a bid for upgrading the plasma cutting unit. For the auxiliary production, we have bought and applied the equipment for butt welding of tools.

The President of Ukraine posed a task for TURBOATOM to deliver equipment for upgrading of the Dnepropetrovsk cascade hydro-electric engineering facilities. How performing of this most important order for the economy of Ukraine is going on?

TURBOATOM is upgrading the entire Dnieper cascade, and it includes 100 hydraulic turbines. By today we have already reconstructed more than a half of them. In 2009 the first hydraulic unit of the Dnestrovskaya hydroelectric pumped storage power plant was commissioned, and today we are successfully upgrading the second hydraulic unit, the main strategic object of Ukraine. This is a considerable workload. After all, the weight of one hydraulic turbine is about 1500 t. And the substantial share of labour input is accounted for by performing welding operations.

I want to assure the President that the team of TURBOATOM will do its best to accomplish this task, which is very important for the economy of Ukraine, before the Power Engineer Day next year.

The interview was recorded by Doctor of Technical Sciences V.V. Dmitrik

The Kharkov Turbine Factory was built only for three and a half years, and was commissioned on the 21st of January 1934. This was the beginning of counting out of glorious victories of the Kharkov turbine constructors. As early as in 1935 the first steam turbine with a capacity of 50 MW was taken from the Factory rack, and the steam turbine with a capacity of 100 MW and the generator for it were manufactured in 1938, which were the highest power turbines at that time.

Today OJSC «TURBOATOM», being the head scientific organisation of the Ministry of Industrial Policy of Ukraine in power machine building, is among the leading turbine construction companies in the world.

The Company is specialising in production of turbines for heat and nuclear power stations, heat-electric generating plants, hydraulic turbines for hydroelectric power stations and hydroelectric pumped storage power plants, gas turbines and combined-cycle plants for heat power stations and other power equipment.

Manufacturing capabilities make it possible to produce annually steam and hydraulic turbines with a total designed capacity of 8 and 2 mln kW, respectively. Turbines are manufactured by the closed cycle: from development and research work to manufacture, assembly, testing of turbines and their shipment.

Internal audits by the Quality Management System at the Plant are performed annually, thus proving its effectiveness. The initial audit at TURBOATOM took place in 1996, and up to now, i.e. during 15 years, the Company has been confirming compliance of the Quality Management System with International Standard ISO 9001.

The sphere of certification includes: design, manufacture, supervision of erection and service of stationary steam turbines, combined-cycle plants, hydraulic turbines, pre-turbine gates, smoke exhaust ventilation heaters, steam turbine condensers and ejectors.

The fact that TURBOATOM has the Certificate of Conformance issued by the Independent Australian Company SAL GLOBAL allows it to compete on equal terms with the world-leading manufacturers of turbine construction equipment, take part in bids and win them.

COMBINED FUSION WELDING TECHNOLOGIES (Review)

G.I. LASHCHENKO
Scientific and Technical Complex «E.O. Paton Electric Welding Institute of the NAS of Ukraine», Kiev, Ukraine

Combined and hybrid welding technologies by using gas flame, electric arc, laser and electron beam as heat sources, as well as different shielding methods, are analysed. The expediency of commercial application of different methods for two- and three-arc welding with 1–2 mm diameter consumable electrodes is shown. It is suggested using the arc and gas flame, laser and electron beam as the combined heat sources.

Keywords: *combined and hybrid technologies, energy sources, electric arc, gas flame, laser, electron beam, shielding atmosphere*

Solving the problems of weldability of a specific material and assurance of the required quality of the welds and joints on welded structures at a sufficient productivity is the main task of the welding technology [1–4]. With different fusion welding technologies, this task is handled by choosing a type, power and distribution of heat sources between consumers, combining electrode and filler materials in terms of their shape and chemical composition, kind and composition of shielding of the welding zone, as well as other methods and approaches [1, 2, 5, 6]. In particular, in welding production the acceptance has been gained by the combined technological processes, which use simultaneously two or more similar or dissimilar energy sources [7, 8]. In case of utilisation of the dissimilar energy sources affecting one treatment zone (e.g. the weld pool), where the integrated result exceeds the sum of the results of each constituent energy source, the process is called the hybrid one. The growth of interest in the hybrid welding processes, where the use is made of the combined energy of the laser beam, plasma and electric arc, has been noted in the last years [9].

The purpose of this study is to analyse the existing fusion welding technologies and define the new possible areas of upgrading these technologies based on combining the energy input into the work zone and its shielding atmosphere.

Combining the energy sources and shielding atmospheres. In welding, the main energy sources are chemical reactions occurring with release of heat (exothermic), electric arc, low-temperature plasma, electron beam, laser radiation, resistance, electroslag and induction heating, heating in electrolytes, friction and ultrasonic heating [1, 3, 5, 6, 10, 11]. If necessary, the mechanical energy is fed to the welding zone by static, dynamic or pulse loading.

Table 1 gives the existing and possible combinations of welding methods based on the combinations of energy sources and kinds of mechanical loading for joining metallic materials.

Naturally, the quantity of the possible welding methods can be increased due to triple combinations of thermal energy sources and kinds of mechanical loading.

Different methods for metal shielding from air can be used within a specific fusion welding process (Table 2) [9, 12].

In case of using several heat sources, both identical shielding methods and methods differing in shielding composition and design can be used for each of the sources.

While performing its main function of shielding the molten metal from air, the shielding atmospheres exert a huge effect on physical, metallurgical and technological characteristics of the welding process.

Some known welding methods and methods suggested by the author, involving a combination of heat sources and shielding atmospheres, are considered below.

Consumable-electrode two- and three-arc welding. Mechanised consumable-electrode arc welding takes the leading position among other welding technologies. Single-arc welding has the widest application. Less widespread are two-, three-, four- and five-arc welding in the common pool [9]. The last two technologies are used mainly for manufacture of large-diameter pipes. Submerged two- and three-arc welding with 3–5 mm diameter wires is employed in ship and tank building, pipe production, for manufacture of different-purpose beam and sheet structures with extended welds.

As shown in study [13], two- and three-arc welding in shielding gases and by the submerged

Table 1. Combining of sources of thermal energy and kinds of mechanical loading in welding

Source of thermal energy and kind of mechanical loading	GF	TR	EA	LTP	EB	LB	RH	ESH	HE	IH	F	US	SL	DL	PL
Gas flame (GF)	+	+	+				+	+		+	+		+	+	
Thermit reaction (TR)	+	+	+					+		+		+	+	+	
Electric arc (EA)	+	+	+	+		+	+	+		+		+	+	+	
Low-temperature plasma (LTP)			+	+		+			+	+			+	+	
Electron beam (EB)			+		+	+				+		+	+	+	
Laser beam (LB)			+	+	+	+	+		+	+		+	+	+	
Resistance heating (RH)			+			+	+		+	+	+		+	+	+
Electroslag heating (ESH)		+	+	+				+		+		+	+		+
Heating in electrolytes (HE)				+		+	+			+		+	+	+	
Induction heating (IH)	+	+	+	+	+	+	+	+		+	+		+	+	
Friction (F)	+						+			+	+		+	+	
Ultrasound (US)			+	+	+	+		+	+	+	+		+	+	
Static loading (SL)	+		+		+	+	+	+	+	+	+	+	+	+	
Dynamic loading (DL)	+	+	+	+	+	+	+		+	+	+	+	+	+	
Pulse loading (PL)							+	+							+

Note. The «+» sign means that the process is applied or is possible.

arc method using 1–2 mm diameter electrode wires, considering their technological capabilities, is reasonable to apply more extensively instead of single-arc welding using 3–5 mm diameter wires, including for addressing such important problems as rise in labour productivity (2–3 times), decrease in heat input (1.7–2 times), reduction of residual strains, and providing of the required service characteristics of different metal structures.

Increased spattering and violation of stability of the process as a result of magnetic interaction of the arcs are considered to be the key drawbacks of gas-shielded two- and three-arc welding. At the same time, these and other problems can be successfully solved with the help of the existing

Table 2. Types of shielding of molten metal from air with different fusion welding methods

Shielding method	Welding method					
	Gas	Arc	Plasma	Laser	Electron beam	Electroslag
Gases:						–
inert	–	+	+	+	+	–
active	+	+	+	+	–	–
mixtures	+	+	+	+	–	–
vapours	–	+	–	–	–	–
continuous jet	+	+	+	+	+	–
annular jet	–	+	–	+	–	–
two-layer jets	–	+	+	+	–	–
two-velocity jets	–	+	+	–	–	–
pulsed jet	–	+	+	+	–	–
in chambers	–	+	+	+	–	–
Gases and slags	+	+	+	+	+	–
Slags (submerged arc)	–	+	–	–	–	+
Creation of vacuum	–	+	+	+	+	–

Note. The «+» sign means the possibility of using a shielding method, and the «–» sign — a shielding method is not used.

capabilities of electrical engineering, electronics and welding metallurgy (rational powering of the arcs, special current sources, control systems, shielding gas atmospheres, flux-cored wires, etc.).

One of the lines of further upgrading of two-arc welding with the open arcs can be the use of two-velocity gas shielding of one (first) or both arcs (Figure 1).

In the first variant shown in Figure 1, *a*, arc *1*, which is the first in the course of welding and powered by the direct current of reverse polarity, is additionally constricted by the shielding gas flow fed via nozzle *2* at a velocity that is much higher than that of the main shielding gas flow fed via nozzle *3*. The main shielding gas is used to shield molten metal and second arc *4*.

In the second variant (Figure 1, *b*), the high-velocity flow is also used for constriction of second arc *4*. In this case the concentration of heating is higher than in the previous case. The efficiency of using the additional high-velocity flow of argon gas was first investigated in consumable-electrode single-arc welding of aluminium [13, 14]. In this case the penetration depth and full thermal efficiency of the welding process under optimal conditions were increased approximately 2 times. In fact, this is consumable-electrode plasma-arc welding, and improvement of energy characteristics is related to the additional constriction of the arc and improvement of heat transfer to the base metal under the effect of the high-velocity gas flow.

It is shown in study [15] that raising the velocity of the additional flow of shielding gas to 40 m/s allows increasing the depth of penetration of steel 1.5–2 times, compared to the penetration depth achieved with the traditional welding method using 1.0–1.2 mm diameter electrode wire. In welding at a high velocity of the additional CO_2 jet, the resulting weld is narrow and characterised by a penetration coefficient of 0.71–0.33, as well as by a high reinforcement without smooth transition to the base metal.

In our opinion, formation of the welds can be improved due to using two arcs burning into one common pool and powered from separate sources.

In this case, both similar and dissimilar gases (gas mixtures) can be used for additional constriction of the arc (arcs) and shielding of the welding zone. Improvement of the weld formation and decrease of spattering can also be provided due to heteropolar burning of the first and second arcs (variant V_2), powering of the second arc by the alternating current (variant V_3) (see Figure 1, *a*) and using one or two flux-cored wires.

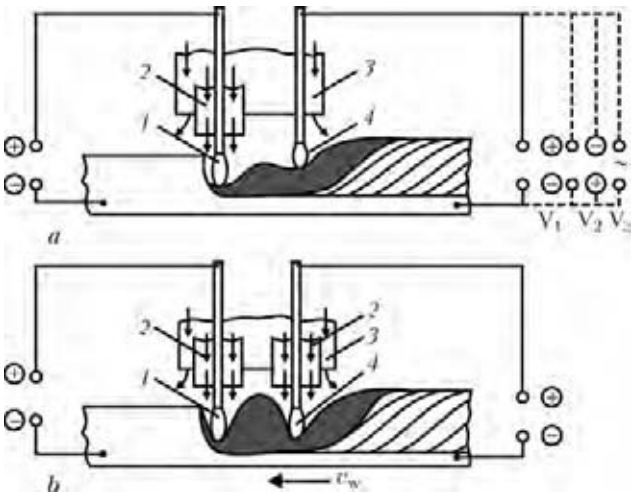

Figure 1. Schematic of two-arc welding with two-velocity gas shielding of one (*a*) and two (*b*) arcs: *1*, *4* — the first and second arc, respectively; *2* — nozzle for feeding the high-velocity gas flow; *3* — nozzle for feeding the shielding gas at normal velocity

The effect similar to the use of flux-cored wire can also be achieved by feeding a small amount of flux of a corresponding composition to the welding zone, including with the high-velocity gas jet. This process can be applied for welding of steels and other alloys, and aluminium alloys in particular.

Gas-shielded three-arc welding with 1–2 mm diameter consumable electrodes into the common pool is insufficiently studied so far. In case of three-arc welding, of high importance is the power circuit of the arcs that minimises their magnetic interaction. Three possible variants of connecting the arcs to independent current sources are shown in Figure 2. According to the variant shown in Figure 2, *a*, the first and third arcs in the course of welding are powered by the direct current of reverse polarity, while the second arc is powered by the direct current of straight polarity. As the direction of the current flowing through the first and third arcs does not coincide with that of the current flowing through the second arc, they will be repelled from it, and the welding process will be more stable than in powering of all the three arcs by the reverse polarity current.

With the arc connection variant shown in Figure 2, *b*, the first arc is powered by the direct current of reverse polarity, the third arc — by the direct current of straight polarity, and the second arc — by the alternating current. In this case the first and third arcs alternately, at a frequency of the alternating current, are attracted and repelled with respect to the second arc.

The arc powering variant shown in Figure 2, *c*, can have some advantages in welding of fer-

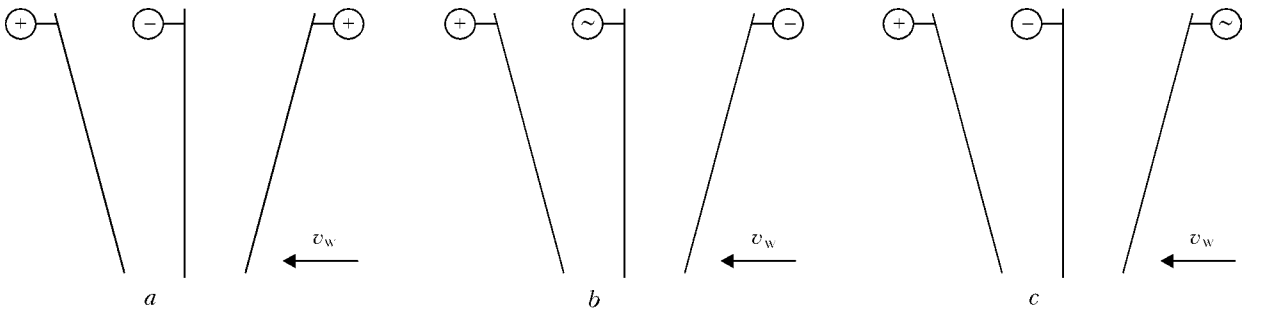

Figure 2. Schematics of electrode connections in gas-shielded three-arc welding at direct current (*a*) and at direct and alternating currents (*b*, *c*)

romagnetic materials, compared to the variant shown in Figure 2, *b*.

Increase of the process stability with all the variants considered can be achieved due to optimisation of the welding parameters, selection of a corresponding shielding gas (gas mixture) and using of two or three flux-cored electrode wires. In the case shown in Figure 2, *a*, the rational combination can be the one where a non-consumable tungsten electrode is connected to the DC source or powered by the modulated current.

Three-arc welding can provide an approximately three times increase in productivity and substantially widen the range of adjustment of heat input when joining different materials. In welding practice, often it is necessary to have a finer adjustment of heat input and local redistribution of heat within the forming weld pool. For this purpose, powering by the modulated current or oscillations of the electrode tip following different paths are used in gas-shielded and submerged single-arc welding [9].

Two- and multi-arc welding opens up extra possibilities for achieving the effect of current modulation and electrode oscillation. As an example, consider the welding method shown in Figure 3. Here it is suggested using two arcs, which differ substantially in their power, namely: power of the second arc in the course of welding is much lower than that of the first arc. In this case the basic characteristics of the process (heat input, productivity) are determined mainly by the power of the first arc, whereas the second arc having a relatively lower power serves for fine adjustment of thermal, hydrodynamic and metallurgical processes occurring in the weld pool. This effect of the second arc is increased due to the use of mechanical oscillations of the second electrode (Figure 4) or modulation of the current this arc is powered by.

The choice of this or that kind of oscillations and its parameters depends on the desired tech-

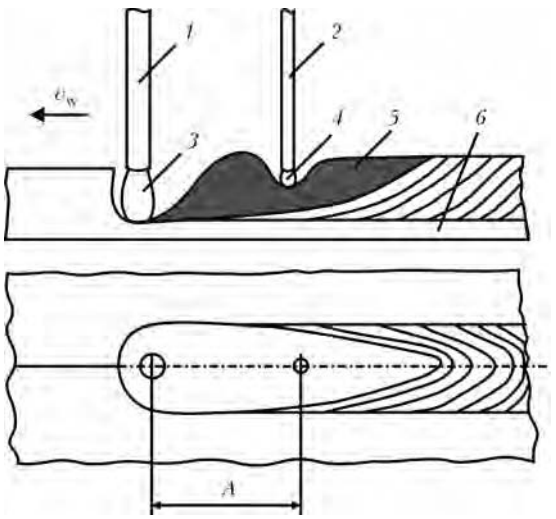

Figure 3. Schematic of two-arc welding method with two arcs having asymmetric power: *1*, *2* — first and second electrode, respectively; *3*, *4* — first and second arc, respectively; *5* — weld pool; *6* — workpiece; *A* — distance between electrodes

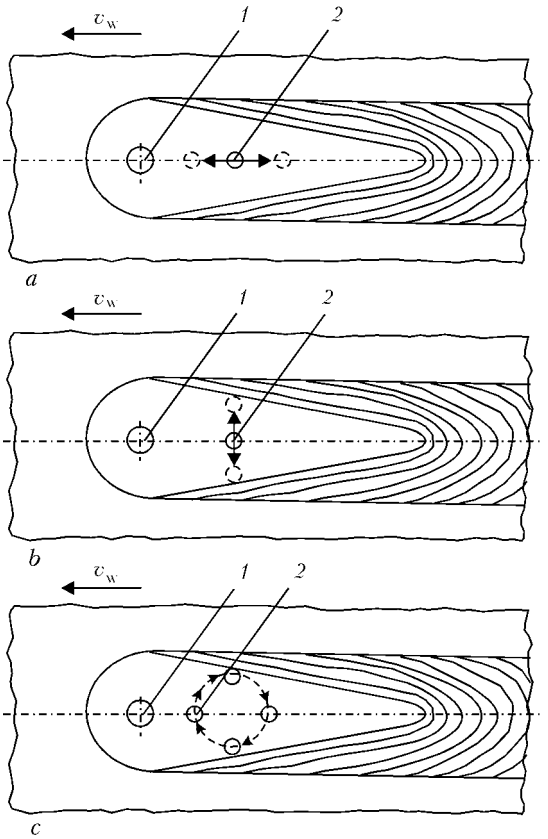

Figure 4. Schematic of two-arc welding with oscillations of the second electrode along (*a*) and across the weld (*b*) and on the circumference (*c*)

nological effect (improvement of the weld formation, increase of the welding speed, decrease of the content of harmful gases in the weld pool, increase of crack or porosity resistance, decrease in the amount of non-metallic inclusions, improvement of mechanical properties and service characteristics of the welded joints).

The variant of the two-arc process with the second arc powered by the modulated current, where the first arc is stationary, makes it possible, with no changes in basic parameters of the first arc and, hence, main conditions of formation of the weld (in particular, the penetration depth), to actively affect its solidification due to feeding the current pulses to the second arc located in the tailing, colder part of the weld pool. This creates more favourable conditions and widens the possibilities for adjustment of the weld formation and solidification process, compared to single-arc welding at the modulated current.

Implementation of the suggested method is possible also in a variant of the combined use of oscillations of the second, low-power arc and its powering by the modulated current. In this case the current pulses can be fed both constantly along the entire path of movement of the arc and at its separate points, including by using instantaneous stops of the electrode at these points. The latter case offers additional possibilities for thermal cycling treatment of different zones of a welded joint depending on the type and composition of the materials welded.

The said method can be implemented both in submerged arc and gas-shielded welding of different-application materials not only without any decrease in productivity, but with its 1.3–1.5 times increase.

Hybrid welding (arc + gas flame). Reaction of combustion of hydrocarbons is widely used for generation of heat in welding and related processes.

The low heat values in combustion of main fuel gases and temperatures of the flame in a mixture with oxygen are given in Table 3 [16]. The effective thermal power of the flame is adjustable over very wide ranges.

In standard flame equipment (welding and linear hardening torches and oxygen cutters) the velocity of outflow of the mixture is within 40–160 m/s, in rocket type units it is 800–1000 m/s, and in detonation spraying units — up to 3000 m/s [16, 17].

The maximal pressure of the gas jet to the weld pool at velocities of outflow of the fuel mixture 120–150 m/s can amount to 1 Pa, while the penetration depth at a high thermal power

Table 3. Low heat value in combustion and temperature of flame of fuel gases in a mixture with oxygen

Gas	Low heat value in combustion, mJ/m^3	Temperature of flame in mixture with oxygen, °C
Acetylene	100.8	3100–3200
N-butane	111.2	2700–2900
Hydrogen	19.2	2400–2600
Methane	32.0	2400–2700
Propane	83.2	2700–2850
MAPP gas	83.2	2800–2900

of the flame is 15 mm [17]. The pressure of the arc flow is known to be proportional to the square of the current intensity. In TIG welding in argon atmosphere at a current of 200 A the pressure on the arc flow axes is $5 \cdot 10^{-2}$ Pa [5]. As the current is increased to 500 A, the pressure grows approximately 2 times, remaining by an order of magnitude lower than in the above case of gas welding.

Although the gas flame is a less concentrated heat source (10^2–10^3 W/cm^2) than the electric arc (10^3–10^5 W/cm^2), it is characterised by a number of advantages:

- possibility of a very flexible adjustment of distribution of heat over the set surfaces of a workpiece, as well as between the base and filler metals in welding and surfacing;
- it is insensible to the effect of magnetic fields;
- gas dynamic effect on the molten metal surface can be varied over wide ranges and used for adjustment of the penetration depth, weld formation and holding of molten metal in the weld pool, including at different spatial positions of the weld.

As early as 1930, H. Muenter introduced the «arcogen» welding method, which combined heating by the acetylene-oxygen flame and by the electric arc. Because of complexity of the manual welding techniques available at that time, this method could not compete with the existing simpler methods using one heat source [18].

We can cite just one known example of commercial application of the combined electric arc and gas flame welding technology — it is arc welding with preliminary or concurrent heating by the gas flame. In this case the gas flame heat source acts outside the weld pool, whereas the hybrid welding method provides for the use of two dissimilar heat sources (in this case the arc and gas flame) affecting one treatment zone (weld pool). This effect can be realised by different ways (Figure 5).

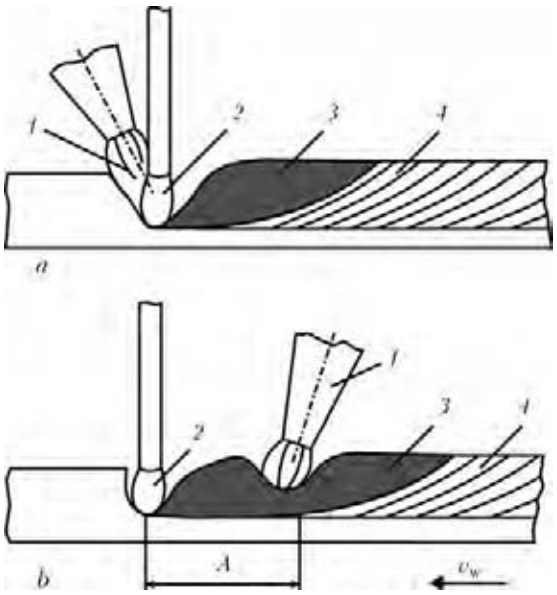

Figure 5. Schematic of hybrid arc + gas flame welding: *a* — gas flame is ahead of the arc; *b* — behind the arc; *1* — gas flame; *2* — electric arc; *3* — weld pool; *4* — weld

Figure 5, *a* shows a variant of hybrid welding using the electric arc and gas flame. Here the gas flame is located ahead of the electric arc in the immediate proximity to it. In this case the gas flame can promote increase in the penetration depth and electrode wire melting rate, as well as affect transfer of the molten metal through the arc gap.

In a variant of hybrid electric arc + gas flame welding shown in Figure 5, *b*, the gas flame heat source is located behind the arc, and by changing distance *A* between the heat sources it is possible to widely change the thermal cycle of welding and weld formation, including in making the multilayer and fillet welds.

Hybrid electric arc + gas flame welding can be implemented in a combination with gas and gas-slag shielding in a variant of the mechanised process. Considering specifics of the offered technology, it can be used for welding and repair of parts made from carbon steels, cast iron, copper and copper alloys.

Combined technologies of laser, electron beam and arc welding. In the last years more interest has been shown in laser welding, hybrid and combined welding methods [19].

Various approaches and methods, including the combination of laser heating with plasma arc or high-frequency one, are applied to increase the economic efficiency of laser welding (decrease in requirements to edge preparation, reduction of the risk of formation of thinning, porosity and undercuts, decrease in capital and other expenditures) [9, 11, 20–25].

It was established [20] that in one-pass hybrid welding of more than 5 mm thick steels the 1 kW power of the arc can be replaced by the 0.5 kW power of laser radiation. The case in point is using lower-power (less expensive) lasers for welding thick metal, which is economically attractive in a number of cases. However, it was found out that the use of the hybrid process at a fixed power of laser radiation makes sense only up to a certain thickness of the metal welded, above which the penetration depth does not grow independently of decrease in the welding speed. For further intensification of the penetration process it is necessary to increase the power of laser radiation.

It is considered [19] that capital expenditures for a fibre laser unit are about 0.1 Million Euro per 1 kW of the output power. Therefore, the economic efficiency of laser-arc welding will be determined primarily by the capital expenditures for purchase of a higher-power laser unit.

If we proceed from the requirement to increase the penetration depth in laser welding without increase in power of the laser unit, then this problem can also be solved by using vacuum shielding. On the one hand, this deprives the laser beam of certain advantages over the electron beam and, on the other hand, even a small degree of evacuation allows increasing the penetration depth from 3 to 5 times [26]. Moreover, specifics of the laser beam make it possible to transfer it through a transparent barrier or by using fibre optics, which can be utilised for manufacture of a number of parts in a vacuum chamber.

In laser welding in vacuum by using the about 5 kW beam, it is likely that the penetration depth on steel can be increased to 20 mm. This penetration in a case of conventional laser welding can be achieved at a laser power of about 20 kW, i.e. implementation of this technology will additionally require about 1.5 Million Euro of capital expenditures.

In vacuum laser welding, the additional capital expenditures will be required for a vacuum chamber and evacuation system. If these expenditures do not exceed 1.0–1.3 Million Euro, the variant of vacuum laser welding of 20 mm thick metals is economically justifiable.

The problem of vacuum laser welding can have a simpler solution, if a company already has an active electron beam welding unit. The vacuum system of this unit can be used for laser welding. Moreover, in this case the economic prerequisites are created for implementation of hybrid laser beam + electron beam welding. The technological effect and economical expediency of this process are hard to estimate today. The electron beam and laser have a different nature, but their com-

bination is quire acceptable, given that the laser beam is insensitive to the effect of magnetic fields and can be used with the electron beam in different variants. Experiments are required. As to combined electron beam and arc welding, such experiments were conducted [27].

It was established that in two-sided combined welding the arc discharge widens the keyhole in the root part of the weld. The forces caused by the effect of the electron beam and arc discharge on the molten metal have opposite directions, this resulting in stabilisation of hydrodynamic processes in the penetration channel, decrease in spattering and increase in resistance of the molten metal to flowing out over a wide range of the process parameters.

CONCLUSIONS

1. Two- and three-arc welding with 1–2 mm diameter consumable electrodes, using gas and gas-slag shielding of molten metal, additional constriction of the arc (arcs) by the gas flow, powering of one of the arcs by the modulated current, and displacement of the electrode tip along the preset paths, allows increasing the productivity, reducing the heat input, redistributing the heat flows in the weld pool, and improving the weld formation. These technologies are indicated for fabrication of metal structures of carbon, low-alloy and stainless steels and aluminium alloys, the weldability of which is insufficient for using traditional single-arc welding.

2. The conducted analysis showed a high potential of using in welding processes the combinations of such energy sources as the electric arc and gas flame, as well as the laser and electron beams, as these combinations allow increasing the penetration depth and improving the weld formation with simultaneous reduction of cost of the welding process (compared to achieving penetrations of the same depth by using one of the above sources).

1. (1974) *Technology of fusion electric welding of metals and alloys*. Ed. by B.E. Paton. Moscow: Mashinostroenie.
2. (1991) *Welding and weldable materials*. Vol. 1: Weldability of materials. Ed. by E.L. Makarov. Moscow: Metallurgiya.
3. (1988) *Theory of welding processes*. Ed. by V.F. Frolov. Moscow: Vysshaya Shkola.
4. Paton, B.E., Trufyakov, V.I. (1990) Means for improvement of reliability and decrease in metal intensity of welded structures. In: *Problems of welding and special metallurgy*: Transact. Kiev: Naukova Dumka.
5. Erokhin, A.A. (1973) *Fundamentals of fusion welding*. Moscow: Mashinostroenie.
6. (1978) *Welding in machine-building*: Refer. Book. Vol. 1. Ed. by N.A. Olshansky. Moscow: Mashinostroenie.
7. Litvinov, A.P. (2009) Trends in development of combined and hybrid welding and cladding technologies. *The Paton Welding J.*, **1**, 37–41.
8. Lashchenko, G.I. (2010) Application of combining principle in welding production. *Svarshchik*, **1**, 16–20.
9. Lashchenko, G.I. (2006) *Methods for consumable electrode arc welding*. Kiev: Ekotekhnologiya.
10. Popilov, L.Ya. (1971) *Fundamentals of electrotechnique and its new kinds*. Leningrad: Mashinostroenie.
11. Grigoriants, A.G. (1989) *Fundamentals of laser treatment of materials*. Moscow: Mashinostroenie.
12. Novozhilov, N.M. (1979) *Fundamentals of metallurgy of gas-shielded arc welding*. Moscow: Mashinostroenie.
13. Lashchenko, G.I. (2011) Technological possibilities of one-, two- and three-arc welding. *Svarshchik*, **2**, 14–19.
14. Alov, A.A., Shmakov, V.M. (1962) Argon-arc welding with auxiliary argon flow. *Svarochn. Proizvodstvo*, **3**, 13–15.
15. Kovalev, I.M., Akulov, A.I. (1967) Specifics of the gas-dynamic method for control of the penetrating power of the arc in consumable electrode CO_2 welding. *Ibid.*, **6**, 19–21.
16. Midlov, S.G. (2007) Thermal coatings in the technology for strengthening and repair of machine parts (Review). Pt 1: Flame and detonation spraying. *Ibid.*, **10**, 35–45.
17. Antonov, I.A. (1976) *Flame treatment of metals*. Moscow: Mashinostroenie.
18. Muenter, H. (1933) Der Einfluss von Schweiss- und Schutzgas Flammen auf die vorgange im Schweisslichtbogen. *Elektroschweissung*, **7**, 80–84.
19. Lashchenko, G.I. (2011) Trends in development of welding production technologies. *Svarshchik*, **6**, 6–11.
20. Shelyagin, V.D., Khaskin, V.Yu., Garashchuk, V.P. et al. (2002) Hybrid CO_2-laser and CO_2 consumable-arc welding. *The Paton Welding J.*, **10**, 35–37.
21. Shelyagin, V.D., Khaskin, V.Yu., Bernatsky, A.V. et al. (2010) Prospects of application of laser and hybrid technologies of welding steels to increase service life of pipelines. *Ibid.*, **10**, 29–32.
22. Reisgen, U., Olschok, S. (2009) Laser – submerged-arc hybrid welding. *Ibid.*, **4**, 38–43.
23. Middeldorf, K., von Hofe, D. (2008) Trends in joining technology. *Ibid.*, **11**, 33–39.
24. Dilthey, U., Stein, L., Woeste, K. et al. (2003) Latest developments and trends in high-efficient welding technologies. *Ibid.*, **10/11**, 146–152.
25. Kah, P., Salminen, A., Martikainen, J. (2010) Laser-arc hybrid welding processes (Review). *Ibid.*, **6**, 32–40.
26. Nazarenko, O.K., Morochko, V.P. (1988) Application of high-power CO_2 lasers in foreign welding production (Review). *Avtomatich. Svarka*, **4**, 43–46.
27. Ovechnikov, S.A., Dragunov, V.K. (2002) Double-sided simultaneous electron beam and arc discharge welding. In: *Abstr. of 8th Int. Sci.-Techn. Conf. of Students and Postgraduate Students on Radio Electronics, Electrical Engineering and Power Generation* (Moscow, 28 Febr.–1 March, 2002), Vol. 3. Moscow: MEI.

DEVELOPMENT OF FORGE-WELDED COMBINED MEDIUM-PRESSURE ROTOR FOR 325 MW STEAM TURBINE

A.K. TSARYUK[1], **S.I. MORAVETSKY**[1], **V.Yu. SKULSKY**[1], **N.N. GRISHIN**[2], **A.V. VAVILOV**[2], **A.G. KANTOR**[2] and **E.D. GRINCHENKO**[2]

[1]E.O. Paton Electric Welding Institute, NASU, Kiev, Ukraine

[2]OJSC «Turboatom», Kharkov, Ukraine

A forge-welded medium pressure rotor for 325 MW steam turbine is described, which is made from 20Kh3MVFA steel (high-temperature operation conditions) and 25Kh2NMFA steel (low-temperature conditions). Welding consumables were selected, and technology of mechanized submerged-arc welding of joints of 25Kh2NMFA + EI 415 steels was developed and certified. Physico-mechanical properties of welded joint metal in the condition after high-temperature tempering in the case of application of both local and imported welding consumables were assessed.

Keywords: *submerged-arc welding, low-alloyed steel, thermal power engineering, steam turbine, rotor, combined welded joint, welding consumables, mechanical properties of joints*

A tendency to design and manufacture powerful steam turbines with welded combined rotor operating in high- and low-temperature mode has emerged in turbine construction over the recent years [1, 2]. The rotors are made of dissimilar structural materials for cylinder operation at high pressure (HPC), medium pressure (MPC) and low pressure (LPC). A feature of making combined rotor joints is the possibility of development of the processes of carbon and alloying element diffusion in the fusion zone of dissimilar steels that essentially influences formation of the structure and service properties of welded joints. In addition, there is a rather complicated issue of postweld heat treatment of such combined joints, as it should be performed for each of the welded steels in different temperature ranges.

OJSC «Turboatom» designed a forge-welded combined MPC rotor for 325 MW steam turbine (Figure 1). Part of the rotor operating in high-temperature mode (stage *1–11*) should be made of EI 415 steel (20Kh3MVFA), and for stages *12–16* operating in the low-temperature mode application of 25Kh2NMFA steel is envisaged. Proposed design of combined MPC rotor also allows elimination of application of nozzle disks in low-pressure stages. Putting the developed design into production requires development of the technological process of manufacturing the forge-welded combined rotor. Therefore, the purpose of this work was selection of welding consumables and development of submerged-arc welding technology ensuring the quality and required service properties of welded joints of the developed combined rotor.

Standard technology of welding LPC rotor of 325 MW turbine, accepted in the plant, envisages welding 25Kh2NMFA steel with Sv-08KhN2GMYu wire (GOST 2246–70) using fused flux AN-17M (GOST 9087–81). Considering the critical shortage of applied wire in Ukraine (produced in RF by special order), as well as stopping fused flux production in the near future, «Turboatom» took a decision on application of imported welding consumables. Conducted marketing studies showed that it is the most rational to select instead of local welding consumables welding wire Union S 3 NiMoCr (ISO 26304) in combination with agglomerated flux UV420TT (EN 760), which are produced by Boehler-Thyssen (Austria, Germany). Selected wire composition, compared to Sv-08KhN2GMYu wire, is given in Table 1.

Fluoride-basic flux UV 420 TT contains the following components, wt.%: (SiO_2 + TiO_2) — 15; (CaO + MnO) — 35; (Al_2O_3 + MnO) — 21; CaF_2 — 25, with basicity of 2.5 to Bonishevskii [3]. During preliminary experiments it was established that concentration of diffusible hydrogen H_{dif} is not more than 1 $cm^3/100$ g of deposited metal at determination by alcohol test [4]. Content of residual gases in weld metal was determined by the method of sample melting in a flow of high purity carrier-gas (helium). It is established that application of Union S 3 NiMoCr wire in combination with UV 420 TT flux ensures

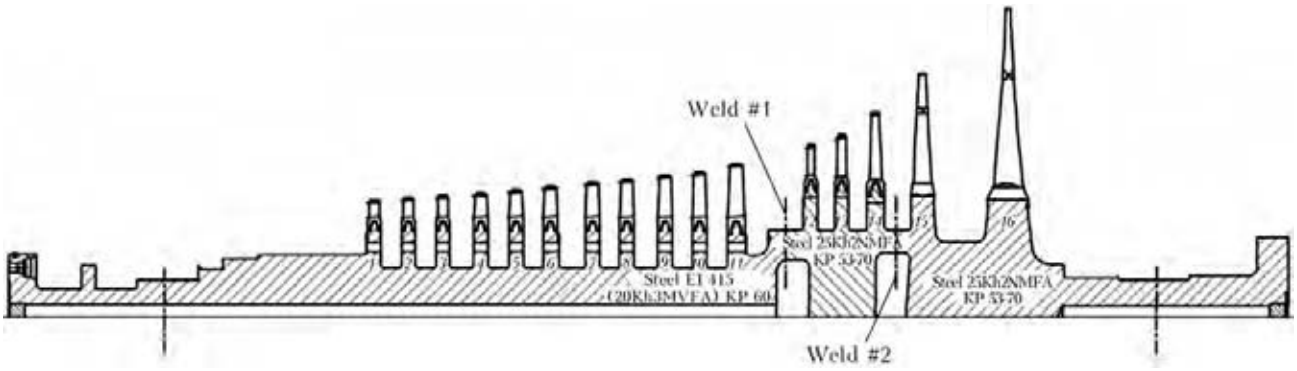

Figure 1. Sketch of longitudinal section of MPC welded rotor of 325 MW turbine.

0.0076–0.016 [N], 0.029–0.034 % [O] and 2.0–2.2 cm^3 [H] per 100 g of deposited metal in the weld. Considering positive results of preliminary studies, work on development and certification of the technology of welding, a combined joint of 25Kh2NMFA + EI 415 steels with application of both imported and local consumables was performed.

Certification of the technological process of welding combined joints of 25Kh2NMFA + EI 415 steels was conducted in keeping with DSTU 3951–2000 (ISO 9956:1995) that envisaged preparation and welding of a full-scale reference butt welded joint (outer diameter of 940 mm, base metal thickness of 95 mm) under the conditions of real production, according to preliminary welding procedure specification (pWPS) provided by the manufacturer.

As 25Kh2NMFA and EI 415 steels belong to the same structural class (Table 2), in order to make a reference combined welded joint of these steels, the same technological process was selected as that used for similar welded joints of 25Kh2NMFA steel. Combinations of local welding consumables, welding modes and postweld heat treatment parameters applied in the standard technology of welding similar joints of 25Kh2NMFA steel allow producing metal of the weld and welded joints with physico-mechanical characteristics satisfying the specification requirements (Table 3, lower line). These values were considered as specification requirements also to metal of combined welded joint of 25Kh2NMFA + EI 415 steels.

In keeping with the accepted technological process, welding of reference joint of 25Kh2NMFA + EI 415 steels was performed with U-shaped groove 26 mm wide with programmed control of bead arrangement with two beads in a layer at reverse polarity direct current. Pre-

Table 1. Content of chemical elements in wires for rotor steel welding and in weld metal of reference welded joint of 25Kh2NMFA + EI 415 steel, wt.%

Object of study	C	Si	Mn	Ni	Cr	Mo	Al	S	P
Sv-08KhN2GMYu wire (GOST 2246–70)	0.06–0.11	0.25–0.55	1.00–1.40	2.00–2.50	0.70–1.10	0.40–0.65	0.06–0.18	≤0.03	≤0.03
Sv-08KhN2GMYu wire[1]	0.08	0.32	1.09	2.15	0.87	0.47	0.11	0.012	0.015
Union S 3 NiMoCr wire (ISO 26304)	≤0.15	≤0.40	1.20–1.90	1.50–2.25	0.20–0.65	0.30–0.80	–	≤0.018	≤0.018
Union S 3 NiMoCr wire[1]	0.14	0.05	1.84	2.06	0.35	0.35	–	0.011	0.013
Weld metal when Sv-08KhN2GMYu wire is used	0.032	0.44	0.66	2.14	0.86	0.52	–	0.012	0.033
Weld metal when Union S 3 NiMoCr wire is used	0.088	0.319	1.61	2.31	0.44	0.60	–	0.009	0.022
Union S 3 NiMoCr wire[2]	0.09±0.01	0.3±0.1	1.3±0.1	2.0±0.1	0.60±0.05	0.5±0.1	–	min	min

[1]Wire actually used in the work.
[2]Requirement to chemical element composition in imported wire.

Table 2. Chemical element content in rotor steels, wt.%

Steel grade	C	Si	Mn	S	P	Cr
25Kh2NMFA (TU 108-995–81)	0.23–0.27	0.17–0.35	0.40–0.70	≤0.015	≤0.015	1.80–2.20
25Kh2NMFA[1]	0.27	0.28	0.50	0.010	0.014	2.10
20Kh3MVFA (TU 108-1029–81)	0.17–0.24	≤0.40	0.25–0.60	≤0.022	≤0.025	2.40–3.30
20Kh3MVFA[1]	0.22	0.27	0.32	0.010	0.012	3.14

Table 2 (cont)

Steel grade	Mo	V	W	Ni	Cu
25Kh2NMFA (TU 108-995–81)	0.40–0.60	≤0.05 acc. to calc.	–	1.30–1.60	≤0.25
25Kh2NMFA[1]	0.42	0.05	–	1.40	0.14
20Kh3MVFA (TU 108-1029–81)	0.35–0.55	0.45–0.70	0.30–0.50	≤0.50	≤0.25
20Kh3MVFA[1]	0.40	0.66	0.40	0.30	0.12

[1]Steel actually used in the work.

heating and concurrent heating of the reference welded joint up to the temperature of 350 °C was performed to prevent cold cracking.

In order to reduce material and labour content of investigations, it was planned to fill the groove of reference combined joint with local consumables to half of its height, and the second half — with imported consumables (Figure 2). Therefore, the weld lower part was made up to half of groove height with application of welding wire Sv-08KhN2GMYu of 2 mm diameter in combination with AN-17M flux. Filling of the weld upper part was conducted with application of Union S 3 NiMoCr wire of 2.5 mm diameter in combination with UV 420 TT flux. Welding was performed in the following mode using both the combinations of welding consumables: welding current 380–400 A; arc voltage 36–40 V; welding speed 19–22 m/h. Finished welded joint was subjected to high tempering at the temperature of 630 °C for 40 h. After that the welded joint was cut into templates for preparation of samples by certification testing program.

Templates, transverse relative to the weld, allowed making samples for testing welded joint metal, including all the possible combinations of base and weld metal, for tension, impact and static bending. In samples of type II to GOST 6996–66 for room temperature tensile testing and type 2k to GOST 9651–73 for tensile testing at the temperature of 350 °C the fusion line was in the middle of sample working part (Figure 3).

Table 3. Results of testing metal of combined welded joint of 25Kh2NMFA + EI 415 steels for static tension (by the results of three tests)*

Object of study	Mechanical characteristics at testing temperature, °C							
	20				350			
	σ_t, MPa	$\sigma_{0.2}$, MPa	δ_5, %	ψ, %	σ_t, MPa	$\sigma_{0.2}$, MPa	δ_5, %	ψ, %
Weld metal (Sv-08KhN2GMYu)	607.2	507	26.2	67.2	539.9	424	19.3	61.2
Weld metal (Union S 3 NiMoCr)	741	503.1	22.9	61.2	675.4	472.2	22.2	60.5
Welded joint metal:								
weld 1 — EI 415 steel	623.6	–	–	67.4	540.6	–	–	61.3
weld 1 — 25Kh2NMFA steel	614.1	–	–	65.3	537.9	–	–	62.5
weld 2 — EI 415 steel	739.1	–	–	61	617.2	–	–	56.3
weld 2 — 25Kh2NMFA steel	709.3	–	–	66.6	611.7	–	–	64.0

*Requirements to short-term mechanical properties of metal of rotor steel welded joints after high-temperature tempering: for 20 °C: σ_t > > 590 MPa, $\sigma_{0.2}$ > 470 MPa, δ_5 > 14 %, ψ > 40 %; for 350 °C: σ_t > 530 MPa, $\sigma_{0.2}$ > 400 MPa, δ_5 > 14 %, ψ > 40 %.

The following designations were used in Figure 3: *1* — zones of variable chemical composition; *2*, *3* — samples of type II and type 2k for testing at normal and increased temperature of metal of welded joint of weld (Union S 3 NiMoCr wire) — steel 25Kh2NMFA; *4*, *5* — weld (Sv-08KhN2GMYu wire) — 25Kh2NMFA steel; *6*, *7* — weld (Union S 3 NiMoCr wire) — EI 415 steel; *8*, *9* — weld (Sv-08KhN2GMYu wire) — EI 415 steel, respectively. In samples of type IX to GOST 6996–66 for impact bend testing the sharp notch was made in weld metal, along the fusion line and along HAZ metal on each of the steels at 1.0–1.5 mm distance from the fusion line (Figure 4). The following designations are used in Figure 4: *1*, *2* — weld zones not subjected to examination (location shown in Figure 3); *3*, *4* — samples for determination of *KCV* of metal of weld made with application of imported and local consumables; *5*, *6* — samples for determination of *KCV* of metal of welded joint with a weld made with imported consumable application; *7*, *8* — with application of local consumables, respectively; *9*, *10* — samples for determination of *KCV* of HAZ metal of welded joint with a weld made with application of imported consumables; *11*, *12* — with application of local consumables, respectively. In samples of type XXVII to GOST 6996–66 for static bend testing of welded joint metal, weld axis was located in sample mid-length. Samples of type II to GOST 6996–66 and type 2k to GOST 9651–73 for tensile testing of weld metal at the temperature of 20 and 350 °C, respectively, were made from templates longitudinal relative to the weld.

As is seen from tensile testing results given in Table 3, strength properties and ductility characteristics of the metal of weld and welded joint quite well satisfy the requirements made in welding with both local and imported welding consumables. Weld metal produced with application of imported consumables is stronger than weld metal produced using local welding consumables. At room temperature its ultimate strength is 22 % higher at the same yield point. At the temperature of 350 °C, σ_t value of weld made with imported welding consumables, rises by 25.1 %, and yield point becomes higher by 11.4 %.

It is established that at any testing temperature the joints welded with application of local welding consumables fail in the weld metal. Joints, welded with application of imported consumables, failed in the weld metal only at the temperature of 20 °C and just in samples including base metal — EI 415 steel (see Figure 3, *6* and *7*). In all the other cases joints, welded with application of imported welding consumables, fail in the base metal at 4 mm distance from the fusion line.

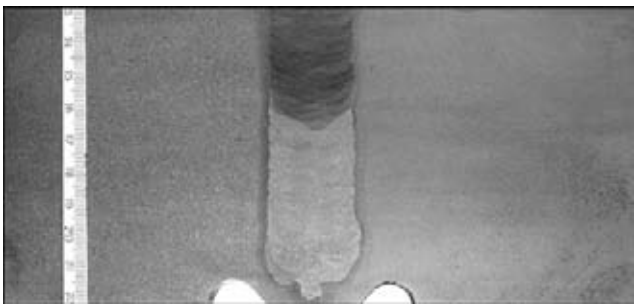

Figure 2. Macrostructure of metal of combined welded joint of EI 415 and 25Kh2NMFA steels (on the right)

Static bend testing showed that bend angle of combined welded joints of 25Kh2NMFA + EI 415 steels is not less than 150°, irrespective of welding consumable combination.

Results of impact bend testing were used to plot graphs of temperature dependence of metal impact toughness *KCV* (Figure 5). The impact toughness value accepted as the criterion for comparative evaluation was *KCV* = 59 J/cm^2, which, according to the current specifications, is the minimum admissible value for any region of similar welded joints of 25Kh2NMFA steel made by the standard technology. As is seen, cold resistance of 25Kh2NMFA + EI 415 welded joint is determined by cold resistance of fusion zone of the weld and EI 415 steel, irrespective of selected welding consumables. At graphic determination, critical brittleness temperature of fusion zone of weld with EI 415 steel is equal to 66 °C in the case of application of local welding consumables (notch in the fusion line). In the case of application of imported welding consumables critical temperature T_{cr} of the zone of weld fusion

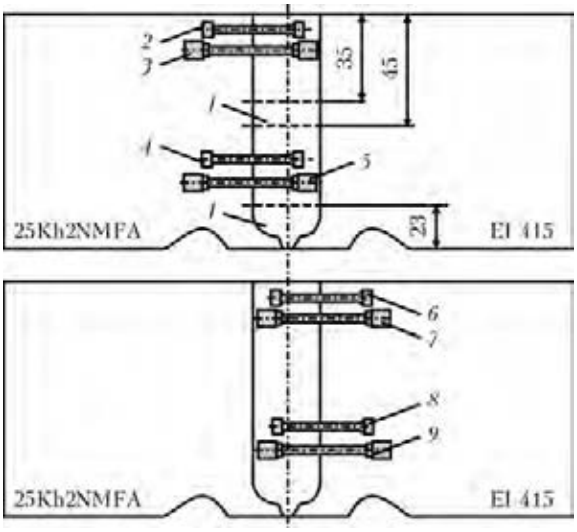

Figure 3. Location of weld zones by cross-sectional height of combined welded joint, and schematic of cutting out samples for tensile testing (for designations see the text)

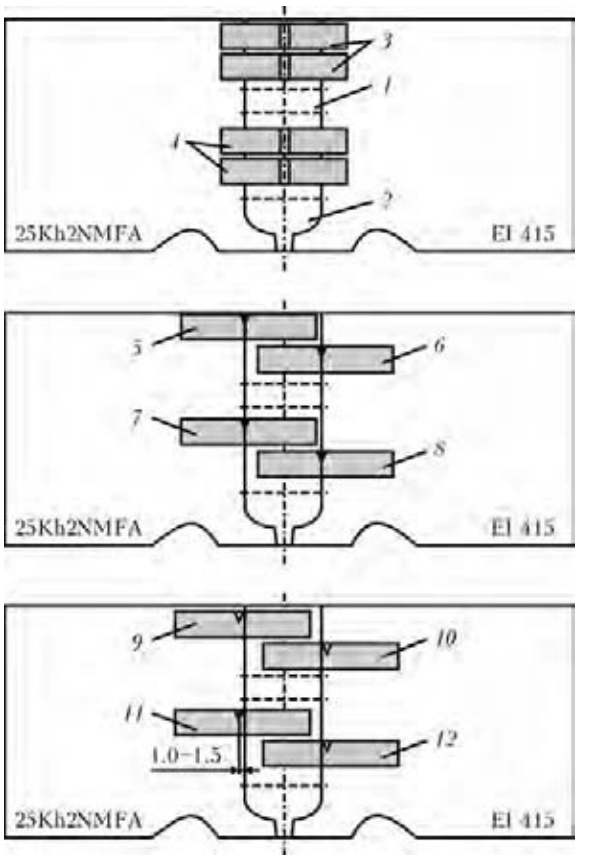

Figure 4. Schematic of cutting out samples of type IX to GOST 6996–66 for impact bend testing (for designations see the text)

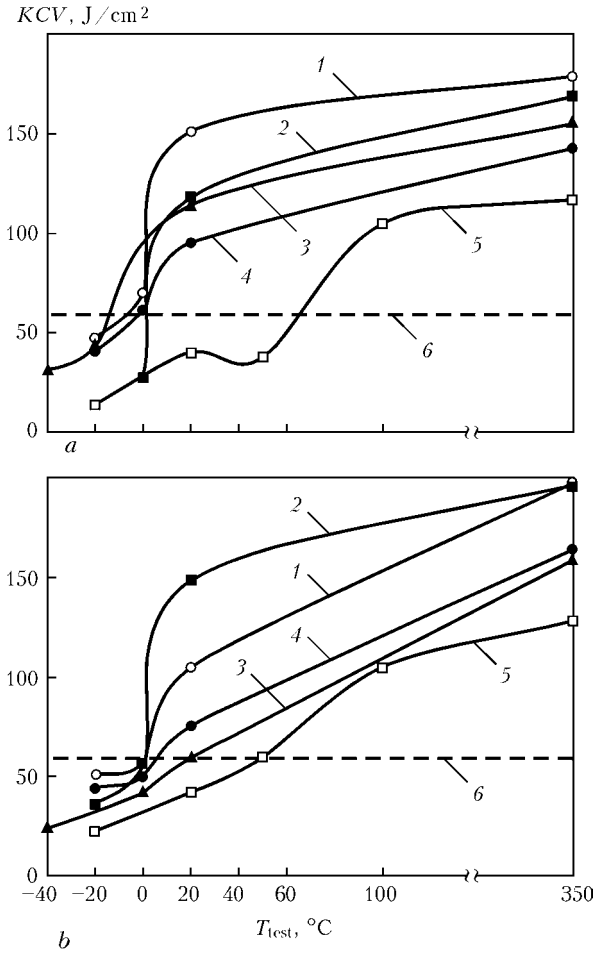

Figure 5. Temperature dependence of impact toughness of metal of combined welded joint of 25Kh2NMFA + EI 415 steels with weld made with local (*a*) and imported (*b*) welding consumables: *1*, *2* — notch in HAZ of 25Kh2NMFA + EI 415 steels, respectively; *3* — notch in Sv-08KhN2GMYu (*a*) and Union S 3 NiMoCr (*b*) weld; *4*, *5* — notch along the line of fusion with 25Kh2NMFA + EI 415 steels, respectively; *6* — RS requirement

with EI 415 steel is equal to 50 °C. For comparison: T_{cr} of the zone of weld fusion with steel 25Kh2NMFA is equal to –2 and 6 °C in the cases of application of local and imported welding consumables, respectively.

Distribution of metal hardness across the reference combined welded joint is shown in Figure 6. As is seen from the graph, the hardness of metal, deposited with application of imported welding consumables, is on average 30 units higher than that of weld metal made with local welding consumables. Average hardness of the zone of weld fusion with EI 415 steel is equal to 276, that is by 40 units higher than that of the zone of fusion with 25Kh2NMFA steel.

Obtained results show that the temperature of postweld tempering, optimum for the joint of weld with 25Kh2NMFA steel, is insufficient to reduce the hardness in the overheating zone of EI 415 steel. Increased hardness of the zone of fusion of the weld with EI 415 steel and HAZ on this steel is logically responsible for lower values of impact toughness of the metal of welded

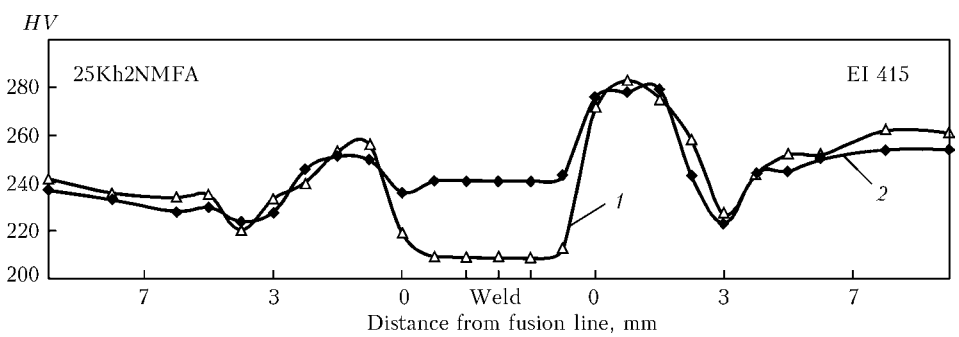

Figure 6. Hardness distribution of metal across the combined welded joint of 25Kh2NMFA + EI 415 steels: *1*, *2* — welded joint with weld made with Sv-08KhN2GMYu and Union S 3 NiMoCr wires, respectively

joint of the weld with EI 415 steel, irrespective of the selected welding consumables.

At impact bend testing it was also found that local welding consumables provide somewhat higher values of weld metal impact toughness at room and below zero temperatures, than imported welding consumables. At the temperature of 350 °C weld metal impact toughness values are quite close for both combinations of welding consumables. T_{cr} value of weld metal is equal to −14 and 20 °C at application of local and imported welding consumables, respectively.

Results of tensile and impact bend testing of weld metal at application of imported welding consumables, compared to the local consumables, are attributable to too high level of alloying of Union S 3 NiMoCr welding wire by carbon and particularly, manganese (see Table 1). In this connection for practical application of the above welding wire in rotor welding, the requirement of ensuring its composition within ISO 26304 specification, but in narrower ranges was coordinated with the supplier company (see Table 1, lower line).

Proceeding from the results of the performed work on certification of the technological process of welding combined MPC rotor of K-325 steam turbine, two imported welding consumables (Union S 3 NiMoCr wire in combination with UV 420 TT flux) can be selected instead of local consumables (Sv-08KhN2GMYu wire in combination with AN-17M fused flux) for mechanized welding of joints of 25Kh2NMFA + EI 415 steels. Imported welding consumables ensure good welding-technological properties, required composition and minimum content of impurities and gases in weld metal. To ensure high service properties of welded joints of MPC rotors, welding wire Union S 3 NiMoCr should be supplied to ISO 26304-A-S-55-4 requirements. Imported wire should have a more strictly specified composition within ISO 26304-A-S-55-4 specification that will allow bringing its composition closer to local wire composition and ensuring a high impact toughness of weld metal, respectively.

Technical council of OJSC «Turboatom» discussed the performed work on development of forge-welded MPC rotor of 325 MW turbine, and took a decision on suitability of the certified technology for manufacture of combined rotors of steam turbines from 25Kh2NMFA + EI 415 steels. Proceeding from the fact that the weld of the combined joint (see Figure 1, weld 1) will operate at the temperature of about 200 °C, when *KCV* value of metal of the zone of fusion of weld with EI 415 steel is higher than 100 J/cm^2 (see Figure 5), imported welding consumables, ensuring the required brittle fracture resistance of weld metal ($T_{cr} \le 20$ °C), were recognized to be acceptable for producing welded joint of 25Kh2NMFA + EI 415 steels.

CONCLUSIONS

1. Forge-welded combined rotor of MPC of 325 MW steam turbine was designed. Developed design allows elimination of nozzle discs in low pressure stages.

2. Technology of mechanized submerged-arc welding of a combined joint of MPC rotor from 25Kh2NMFA + EI 415 steels was developed and certified.

3. It is recommended to apply for mechanized welding imported welding wire Union S 3 NiMoCr (ISO 26304-A-S-55-4) in combination with agglomerated flux (UV 420 TT (EN 760) of Boehler-Thyssen (Austria, Germany).

4. Mechanized submerged-arc welding with application of the selected imported welding consumables can be applied to manufacture LPC and MPC rotors of powerful steam turbines.

1. Shige, T., Magoshi, R., Ito, S. et al. (2001) Development of large-capacity, highly-efficient welded rotor for steam turbines. *Mitsubishi Heavy Industries Techn. Rev.*, 38(**1**).
2. (2005) *Proc. of PWR ASME 50348* (April 5–7, Chicago).
3. (2005) *Welding filler metals*: Welding guide of Boehler Thyssen Schweisstechnik Deutschland GmbH. Sept.
4. Kozlov, R.A. (1986) *Welding of heat-resistant steels*. Leningrad: Mashinostroenie.

TECHNOLOGY OF PROJECTION WELDING OF PARTS OF LARGE THICKNESSES WITH T-SHAPED JOINTS

V.S. KUCHUK-YATSENKO, A.A. NAKONECHNY, V.S. GAVRISH and **S.V. CHERNOBAJ**
E.O. Paton Electric Welding Institute, NASU, Kiev, Ukraine

T-shaped joint projection welding of large-cross section low-carbon steels was studied. It is shown that the programmable change of compression force at the stage of melting and solidification of welded joint metal allows increasing heat input into welding zone, avoiding defects occurrence in joint formation and obtaining higher mechanical characteristics of welded joint. It was established that control of compression force yields the greatest effect in welding large cross-section products, when welding machines do not have required power factor for welding under rigid conditions.

Keywords: *projection welding, low-carbon steels, T-shaped joint, large sections, cast nugget*

The progress of modern machine building depends on implementation of resource-saving technological processes increasing labor efficiency and quality of products. The resistance projection welding process meets these requirements. However, nowadays the influence of technological parameters of welding conditions on the formation of welded joints of large area has not been yet studied sufficiently. The purpose of this work is to study influence of changes of welding force on heating in the contact zone, sizes of cast nugget and strength of T-shaped welded joint of section area of 1200 mm^2. The welded assembly of low-carbon steel represents a threaded nut of rectangular section of 26 × 47 mm and 28 mm height, welded-on to the plate of 20 mm thickness, and is a ledge of a frog.

In projection welding of T-joints in a form of rods, bolts, threaded nuts, welded-on to the plate, the cycle pattern with constant clamping force is mainly applied. It is predetermined by a small area of a welded joint and design of welding equipment, which does not provide the necessary quick response of a power drive of the welding machine.

To prevent crystallization cracks and pores in resistance spot welding and, as a result, to increase mechanical properties of welded joints, the recommendations exist on using forging force, however as for projection welding with T-joints, the rationality of its use has not been studied sufficiently. In practice the value of constant welding force is selected experimentally coming from the need to prevent initial and final splashes of molten metal at preset value of welding current. The required sizes of a cast nugget are provided by adjustment of welding current and time of welding. However, under the conditions of T-shaped joint projection welding of a rod with a plate, the formation of a joint is occurred under the conditions of solid-liquid state of metal in contact and significant plastic deformation, which restricts the influence of time of welding on heat input into the metal of a joint being formed. The basic factor influencing the formation of welded joint is temperature of plastic deformation front depending on density of current and welding pressure.

The threaded nut has a non-axial symmetric shape, which requires applying several projections to obtain the fusion zone over all the welding area with formation of a cast nugget. It provides stirring of metal of the surfaces being joined even at the presence of scale, rust and other contaminations, and guarantees obtaining high strength properties.

The variant with two deformable cones and limiting rim was designed, which maintains molten metal from splashes and during deformation it forms area of plastic deformation around the cast nugget. In the course of experiments it was established that optimal variant is the cone with the apex angle of 160°. Such projection provides the most quality welding without preliminary and final splashes, prevents deformation around the perimeter of the threaded nut and high mechanical properties of welded joints. The shape of projection allows performing welding even along the layer of a rust and scale without significant decrease of mechanical properties of metal and provides stable quality of welded joint.

Let us study the influence of cycle pattern of welding force on heating in the contact zone, sizes of cast nugget and strength of T-shaped welded joint. Figure 1 shows cycle pattern of

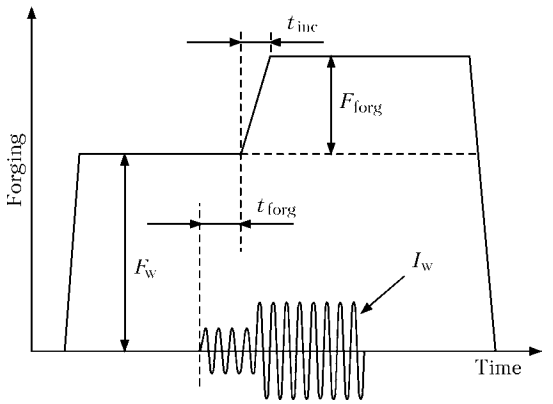

Figure 1. Cycle pattern of welding with forging force (see designations in the text)

welding with application of forging force. Welding force F_w, forging force F_{forg} and time of forging switch-on t_{forg} were the main parameters.

As is known the heat evolution in the contact is proportional to electric resistance of a contact and related to compression force in welding. This relation is non-linear and depends on temperature of a contact. In this connection, the comparative change of dynamic electric resistance of a contact at constant welding force and with applying of forging force was carried out. The dynamic resistance of a contact can be calculated knowing the drop of voltage, current during welding and resistance of welding circuit at open electrodes.

Figure 2 shows changes of contact resistance at optimal conditions with constant F_w = 3200 kN and conditions, at which the initial F_w = = 2000 kN and F_{forg} = 4000 kN. The welding current amounted to 34.5 kA, time of welding was 100 periods (2 s). The higher electric resistance in the zone of welding was obviously due to the higher temperature of deforming metal of projection and the whole zone of welded joint.

The measurement of temperature fields depending on F_w and F_{forg} is presented in Figure 3. The thermal effect and higher temperature of welding zone at the stage of formation of fusion zone at cycle patterns with increase of pressure per welding cycle are obvious. The record of temperature fields showed that temperature in near-contact zone in the spot of cut-in of thermocouple at the moment of formation of fusion zone increased by 140 °C, which proves the increase in thermal efficiency coefficient of the process.

The decrease of welding pressure F_w down to 1500 kN results both in more intensive heating, as well as in initial splashes of metal.

The optimal is the condition when F_w = = 2000 kN and increase of forging pressure during period of welding up to 4000 kN (Figure 4), current of 34.2 kA, time of welding of 120 mains

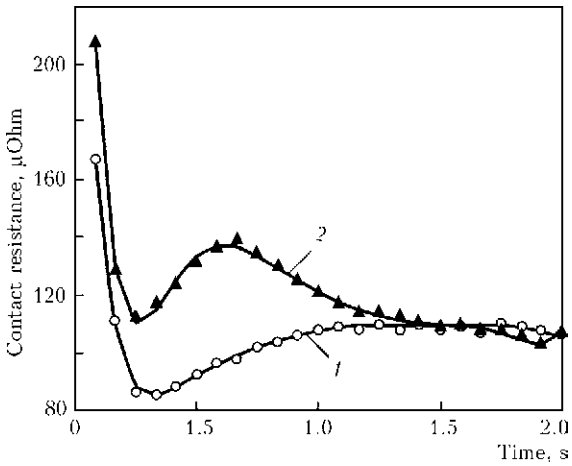

Figure 2. Change of contact resistance during welding: *1*, *2* — constant and increasing force, respectively

periods (modulation of increase of welding current from zero to nominal amounted to 10 mains periods).

The diameter of fusion zone and penetration depth amounted to 25 and 5 mm relatively, which is 12 and 25 % higher than in welding at a constant compression.

The experiments were also conducted under relatively mild and rigid conditions as to preset one providing the quality joint formation. Mild conditions have lower current and longer welding time, characterized by the more intensive heat removal into metal of a part and electrodes. Rigid conditions have higher current and shorter time

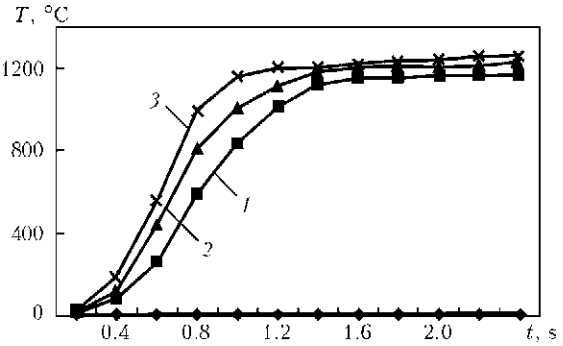

Figure 3. Heating of welding zone under different conditions of applying welding pressure: *1* — F_w = 3200 kN; *2*, *3* — F_{forg} = 4000 kN (*2* — F_w = 2000; *3* — 1500 kN)

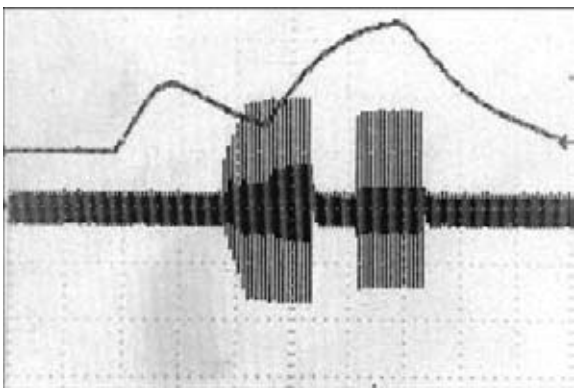

Figure 4. Oscillogram with increasing compression force

Figure 5. Macrosection (×4) of joint at increasing welding force

of welding, at rigid conditions such defects as initial and final splashes are possible. Three series of experiments, each consisted of three trials, were conducted. The results of mechanical shear P_{sh} and rupture P_r tests were carried out (Table).

Figure 5 represents macrosection of welded joint obtained with increasing welding force. The width of fusion zone is 25 mm, penetration depth is 7 mm, width of zone of thickening band (zone of solid-phase welding) is 2.5 mm.

In the zone of plastic deformation close to nugget zone the amount of bainite is larger, which allows supposing that metal of this zone was heated up to higher temperatures. In this zone of specimen the partial fusion of grains is observed, which evidences about deformation in a solid-liquid state.

The central zone has no clear features of cast dendrite structure, intercrystalline liquation and shrinkage defects. It evidences that formation of welded joints in T-shaped projection welding always occurs with plastic deformation of contact zone.

The metallographic analysis of zone of welded joint shows that in the specimen with changeable cycle pattern of pressure the metal of plastic deformation zone was heated up to higher temperature as a result of larger heat evolution and higher temperature of deformation front due to increase

Projection welding under mild (Nos. 1–3), optimal (Nos. 4–6) and rigid (Nos. 7–9) conditions

Condition No.	$U_{o.-c}$, V	I_w, kA	t_w, s	P_{sh}, kN	P_r, kN
1	8.5	30.5	2.7	28700	23100
2	8.5	30.5	2.7	29000	23900
3	8.5	30.5	2.7	27900	23300
4	9	34.2	2.4	31700	25500
5	9	34.2	2.4	32400	26100
6	9	34.2	2.4	31300	25200
7	9.5	37.1	2	29100	23900
8	9.5	37.1	2	29400	23000
9	9.5	37.1	2	29800	23500

of welding force proportionally to increase of area of deformation zone.

CONCLUSION

The projection welding of low-carbon steels of large sections with T-shaped joints was studied. It was shown that programming change of welding force at the stages of fusion and crystallization of metal of welded joint allows increasing heat input into welding zone, avoiding defects in formation and obtaining higher mechanical characteristics of welded joint.

The control of compression force gives the maximum effect in welding of products of large section, when welding machines do not have necessary reserve for welding under rigid conditions.

1. Gillevich, V.A. (1976) *Technology and equipment of projection welding*. Leningrad: Mashinostroenie.
2. Kozlovsky, S.N. (2003) *Principles of theory and technology of spot resistance welding*. Krasnoyarsk: SibGAU.
3. Zhang, H., Senkara, J. (2006) *Resistance welding fundamentals and applications*. Boca Raton.
4. Tang, H., Hou, W., Hu, S.J. (2002) Forging force in resistance spot welding. *J. Eng. Manufact.*, 216(**1**), 957–968.
5. Gillevich, V.A. (1970) *About choice of relationships between ordinary values of electrode force and welding current in projection welding machines*. Moscow: Mashinostroenie.

PORTABLE APPARATUS FOR CONSUMABLE-NOZZLE ELECTROSLAG WELDING

K.A. YUSHCHENKO[1], **I.I. LYCHKO**[1], **S.M. KOZULIN**[1], **A.A. FOMAKIN**[1], **V.A. DAKAL**[1] and **E.S. OGANISYAN**[2]
[1]E.O. Paton Electric Welding Institute, NASU, Kiev, Ukraine
[2]OJSC «Ukritarm», Kiev, Ukraine

Information is presented on a portable apparatus for consumable-nozzle electroslag welding and surfacing. Design peculiarities and technical advantages of the apparatus, as well as recommendations for its application, in particular in construction, are given.

Keywords: *portable welding apparatus, consumable-nozzle electroslag welding*

Workers of the welding production are offered a portable versatile apparatus AShP 113 M2 UKhL4 for consumable-nozzle electroslag welding of longitudinal and curvilinear butt, fillet and T-joints with a thickness of 40–120 mm (Figure 1). Welding is performed at the direct current with a vertical position of the joint (deviation ±15°). The apparatus can be used for fabrication of thick-walled large-size metal structures of carbon and alloyed steels and parts of complex configuration, as well as for surfacing and repair operations under factory and field conditions.

The apparatus (see Figure 1) consists of compact mechanism *1* for feeding two welding wires, both solid and flux-cored ones, which is fixed on bracket *3*. The latter also provides fixation of a consumable nozzle and supply of the welding current to nozzle *5*. Device *5* for correction of position of the consumable nozzle relative to the weld edges in a gap provides its smooth displacement with fixation in two mutually perpendicular planes. High reliability of guiding of the electroslag process is provided by using the electrode wire feed drive based on AC reduction gear motor *2* with frequency regulation of revolutions. The modular configuration allows an easy and promptly positioning of the apparatus over a joint, as well as its fast dismantling from a workpiece.

Electric part of the apparatus is made on a modern element base. Control cabinet *2* (Figure 2) can be located separately from power supply *1* or directly on the power supply, this substantially improving reliability of operation

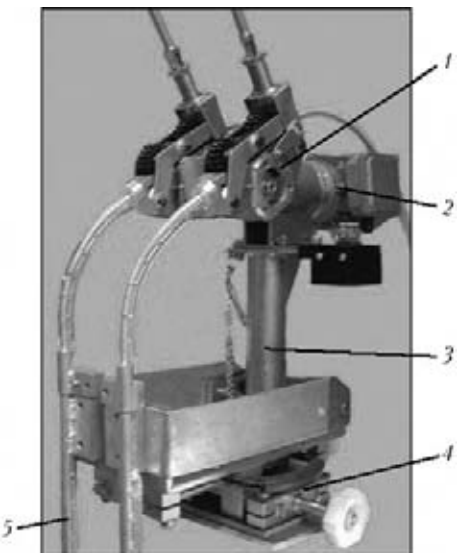

Figure 1. Appearance of apparatus AShP 113 M2 (see designations in the text)

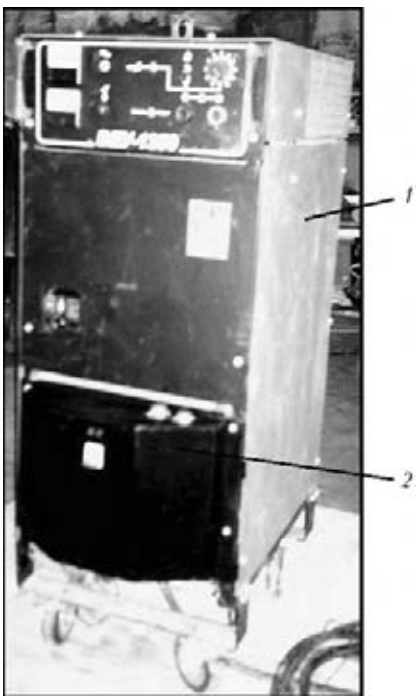

Figure 2. Power supply of apparatus AShP 113 M2 (see designations in the text)

Figure 3. Control panel of apparatus AShP 113 M2

of the electric part and facilitates re-arrangement of the welding equipment in welding of a large number of joints, especially in field operation. The welding process is performed by using a portable apparatus control panel (Figure 3), which meets all current requirements for information capability and ergonomics. The control panel provides digital indication of the main working parameters (slag pool voltage, welding current, electrode wire feed speed) and convenient control of the welding process. Indication elements and controls are protected from probable ingress of moisture and dust. The electric part of the apparatus provides for the possibility of connecting an extra unit comprising an information-recording system for monitoring of the welding process, and allows visualization and registering of the main parameters of the electroslag welding process, which can be used for certification of weldments.

Specifications of apparatus AShP 113 M2

Mains voltage, V	380
Mains frequency, Hz	50
Electrode wire diameter, mm	2.4–4.0
Quantity of electrode wires fed by welding module, pcs	2
Rated welding current per module (duty cycle 100 %), A	1000
Electrode wire feed speed, m/h	30–300

The apparatus can operate in the manual, automatic, or adjustment, 100 % duty cycle modes.

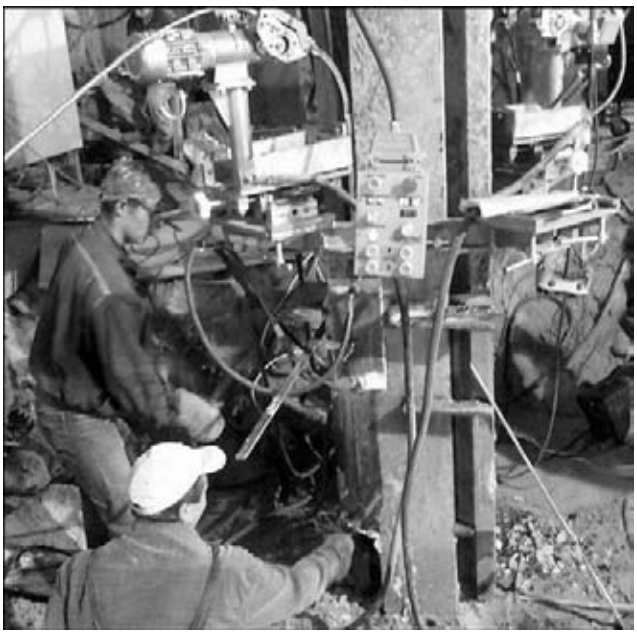

Figure 4. Electroslag welding of elements of reinforcement of building column flange openings by using apparatus AShP 113 M2

Main advantages of the apparatus:

• widening of technological possibilities of the consumable-nozzle electroslag welding process due to using both solid and flux-cored wires of different diameters;

• due to the modular configuration, it is possible to easily and promptly mount the apparatus over a joint, an dismantle it from a workpiece;

• high reliability of guiding of the electroslag process due to using the electrode wire feed drive based on the AC reduction gear motor with frequency regulation of revolutions;

• feed mechanisms are equipped with an increased-reliability electrode wire feed systems;

• for using the apparatus under field conditions, the indication elements and controls are protected from probable ingress of moisture and dust.

The new apparatuses are successfully applied for welding of openings of flanges of building columns of the cross wheel type (Figure 4). Up to now more than 1500 joints (about 1250 running metres of the welds) have been welded under field conditions.

The new apparatuses provide a substantial decrease in labour intensity of welding operations and increase in productivity due to reduction of time for mounting-assembly operations.

SPATIAL DISTRIBUTION OF MAGNETIC FIELD AND ITS MINIMIZATION IN RESISTANCE SPOT WELDING

O.G. LEVCHENKO, V.K. LEVCHUK and **O.N. GONCHAROVA**
E.O. Paton Electric Welding Institute, NASU, Kiev, Ukraine

Spatial distribution of magnetic field (MF) generated by resistance spot welding machine in the work zone was determined with allowance for its spectral composition. Results of experimental studies of the effect of welding process parameters and distance from current-conducting elements of the welding circuit on the index of exceeding the MF level, according to the current medical requirements, are presented. Recommendations on protection of welders from MF are suggested, which are intended for designers of resistance welding machines, technologists and users of these machines.

Keywords: *resistance spot welding, electromagnetic radiation, index of exceeding magnetic field level, methods of welder protection, shielding magnetic materials, alloy with amorphous structure*

At present resistance welding has become widely accepted in some industries of Ukraine, and it is one of the leading technologies in modern production. There is a large fleet of electrical equipment and machines of various types and purpose with power from several up to hundreds kilovolts per ampere. These are mainly 50 Hz AC machines.

During operation of these machines magnetic fields (MF) of considerable intensity are generated, which is several times higher than the value specified by sanitary codes [1]. MF of such intensity can affect service personnel health, causing certain negative functional changes in the body, because of the effect on cardio-vascular, nervous, urogenital, endocrinal and other systems. In this connection, the need arose to monitor the electromagnetic situation in welder workplaces and to ensure safe labour conditions for them. This problem became more acute with introduction of new norms in Ukraine [2], which specify safety conditions in operation with sources of electromagnetic noise, and take into account modern medical investigations.

At resistance welding pulsed MF are generated in the working zone. In welder work places the main source of these fields is the welding transformer, not completely shielded by the machine case and, as a rule, unshielded high-current elements of the welding circuit (electrodes, plugs, consoles, buses), as well as current-conducting cables and complex-shaped welded items. MF formed at resistance welding in different frequency ranges and general procedure of determination of their levels are described in [3].

The purpose of this work is establishing MF spatial distribution near resistance spot welding machine and determination of the possibilities of minimization of its intensity.

During experiment performance possible resistance spot welding modes were modeled in batch-produced spot welding machine MT-2202 of medium power, taking into account the following considerations.

First, welding modes are determined by welding equipment design and capability of their regulation. For modern resistance spot welding equipment, they are rather wide and envisage the following adjustments of heat input into the welded joint: switching of power stages of welding transformer with thyristor contactor; variation of the duration of pulses of sinusoidal full-phase 50 Hz current in one packet; welding (and heat treatment of welded joint in welding machine electrodes) by several (up to 3) packets of sinusoidal full-phase pulses with regulation of pulse number in packets and pause duration between packets; phase regulation of heating (welding current) in each packet (α_{ph} = 20–180°); modulation of leading and trailing edges of pulse packets, i.e. amplitudes of a certain pulse number from zero up to maximum values.

Secondly, as the instrumentation of welding cycle control supports (permits) these adjustments, welding technologists do not always use them in their work with discretion, and ignore sanitary norm requirements [2].

Investigations conducted at PWI show that for resistance welding radiation in 50–1000 Hz frequency range is the determinant sanitary-hygienic factor at evaluation of MF levels. The least hazardous welding mode, where MF spectrum contains the smallest number of essentially significant harmonic components higher than first harmonic of 50 Hz frequency, mainly determining

MF energy load, is the mode of welding with one packet of sinusoidal full-phase pulses of welding current, having the longest possible duration and the smallest possible amplitude (so-called soft welding mode). It is also established that for this welding mode, considering the sanitary aspect, the number of sinusoidal pulses (periods) of not less than 15 can be taken, i.e. the time of welding one spot should equal to $t_w \geq 15 \cdot 0.02 \geq$ ≥ 0.3 s. It would be convenient to take this welding mode as the reference one, with which other possible modes obtained as a result of hygienic evaluation, could be compared, and comparative analysis could be performed. In real application in production more stringent conditions are preferred. Therefore, stringent mode of welding (1.5 + 1.5) mm samples from carbon steel by 1 packet of 10 sinusoidal full-phase pulses of welding current (I_2 = 12 kA, U = 0.69 V) of 50 Hz frequency in the first (minimum) stage of transformer power regulation of the 4 available, was taken as the reference mode. At transition from the soft to rigid mode MF intensity in the above frequency range rises approximately 2 times.

For objective evaluation of MF levels in all the available frequency ranges a new generalized index is proposed — the index of the exceeding level of the magnetic field (MF IEL)

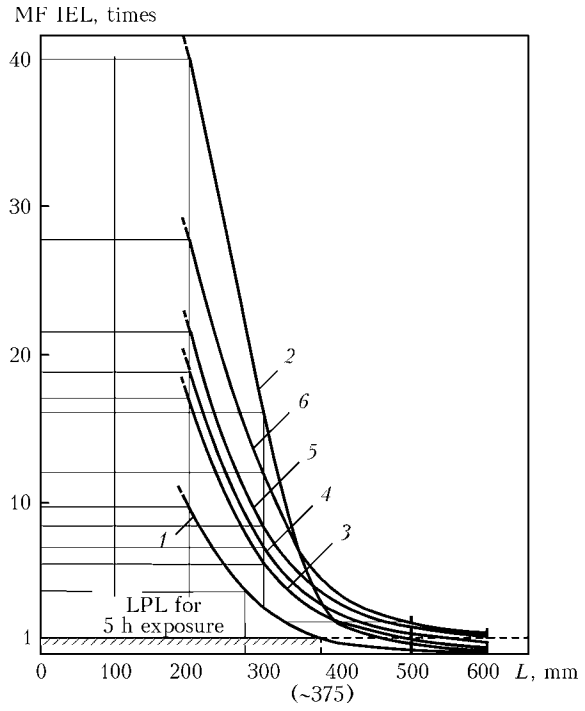

Figure 1. Dependence of MF IEL on distance to electrodes for spot welding machine MT-2202 and welding mode parameters in welder's work zone (in front of the machine) at height h = 1000 mm (in welded joint plane) from floor level (for designations see the text)

$$\text{MF IEL} = \sum_n \frac{H_n^2}{H_{n\,\text{LPL}}}, \qquad (1)$$

where H_n is the actual MF intensity by frequency ranges n, A/m; $H_{n\,\text{LPL}}$ is the intensity of limit permissible MF levels by frequency ranges n, A/m.

Figure 1 shows as an illustration the characteristic experimentally derived dependencies of IEL of MF for 5 h exposure in front of spot welding machine of medium power on distance to its electrodes for different kinds of MF signals, where *1* — for 1 packet of 10 sinusoidal full-phase pulses of 50 Hz welding current with modulation of the leading and trailing edges (one half-period each) in the transformer minimum stage; *2* — same, but in the maximum stage; *3* — for angle of phase regulation of heating α_{ph} = 45° (pulse corresponds to curve *1*); *4* — for 1 packet of 10 pulses with 50 % modulation of packet leading edge; i.e. 5 first pulses from zero to amplitude value; *5* — for 2 packets of 5 pulses each with 2 period pause between pulses; *6* — for 2 packets of 5 pulses each with 100 % modulation of packet leading edges with 2 period pause between pulses.

Figure 2 shows a tentative spatial distribution of MF IEL in front of the welding machine in welding in the stringent mode of one packet of 10 sinusoidal full-phase pulses of 50 Hz welding current with leading and trailing edge modulation (one half-period each) in the transformer first stage. Obtained data are indicative of a considerable exceeding of magnetic radiation levels in the frontal and even more so in the profile area of welder work space.

As is seen from the data in Figure 1, any regulation of welding mode parameters (differing from the reference mode), enabled by the instrumentation, leads to increase of MF IEL in the working zone. MF IEL largest value is observed in front of the welding machine in horizontal plane xOy, passing through the welded spot and in this case — at 1 m height from the non-ferromagnetic floor. Having approximated the data of graphs in Figure 2 on the area of welder's head and feet, it was established that MF IEL in these regions is tentatively 4–6 times lower than at waist level. Calculation of MF IEL on the side of welding circuit in vertical plane zOy shows (Figure 2, *b*) that its spatial distribution in this region is similar to distribution in front of the machine, but in the horizontal plane it is 2–2.5 times higher, while remaining approximately the same in the area of welder's head and feet.

Analysis of the derived data shows that reliable provision of maximum effectiveness of

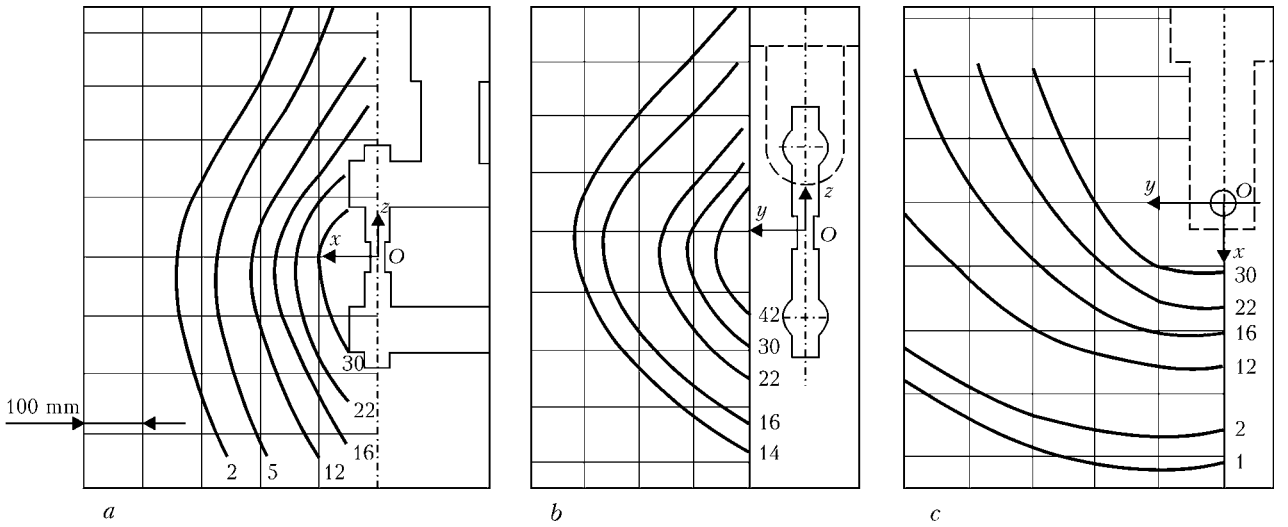

Figure 2. MF IEL distribution (for 5 h exposure) in plane xOz (*a*), yOz (*b*) and xOy (*c*)

welder's protection can be achieved by increasing the distance to radiation source or application of complete automation and moving the welder out of MF impact zone to not less than 1 m distance that is hardly feasible under the actual production conditions. Therefore, to resolve this situation and enable welder's operation of resistance spot welding machines in the frontal area, in the so-called manual mode, at distance $L \geq 150$–200 mm, the required effectiveness of protection E_{pr} from magnetic radiation should be not less than 60 to 40 times (see Figure 1). Required effectiveness of protection is determined by the following expression:

$$E_{pr} = H_{max}/H_l, \quad (2)$$

where H_{max} is the maximum value of MF intensity in the work place; H_l is the limit permissible value of MF intensity.

H_{max} value measured in welder's work place is used in E_{pr} calculation.

Development of protective gear for welders against electromagnetic radiation at operation of resistance spot welding machines in the manual mode, providing E_{pr} of the order of 100 times, should, apparently, envisage application of all the possible methods to lower magnetic radiation to the specified level [2], namely:

- protection by distance (up to $L_{min} \geq 250$–300 mm);
- protection by time;
- protection by optimization of welding modes, application of new welding processes with more acceptable physical parameters of electric current in sanitary terms and new principles of heat input regulation, when making the welded joint;
- shielding the current-carrying elements of welding circuit with preservation of maximum possible work space;
- application of individual protective gear;
- monitoring the magnetic situation in the work place by the welder himself using MF level detector.

Let us consider the capabilities of these methods.

Protection by distance. At operation of stationary spot welding machines in semi-automatic mode body parts the most loaded by MF are hands and arms, i.e. local body parts. Unlike the European sanitary norms, Ukrainian norms [2] do not specify application of local step-up factor for permissible level of MF intensity, equal to 2.5 at operation in pulsed MF, so that keeping hands at distance $L \leq 300$ mm from machine electrodes in the frontal area and especially in the profile area relative to machine welding circuit is inadmissible. Admissible distance to hands at operation should be the same as to the trunk. In this case application of such devices, as special technological fixtures, rotary tables, etc., as well as control panels with two interconnected buttons of welding switching on, ensuring minimum permissible distance, is a vital need.

Particularly negative consequences of MF impact on the welder are possible in operation with hand tools for resistance welding (tongs, spot welding guns and guns for impact capacitor-type stud welding) [3]. At 5 h exposure in this case MF IEL is higher than the norm approximately 400 times for hands and 100 times for head and trunk of the welder. Therefore, in hand tool design it is necessary to envisage not less than 250–300 mm distance from current-conducting parts of guns to their handles, and in case this leads to generation of considerable moments of inertia, it is necessary to fit the tool with a balancing device. Design and technological documentation should include the ergonomic component, i.e.

drawings, schematics of tool movement in space during operation, tool position in welding of each spot of the item, and its location relative to the body (head and trunk).

One can see, however, that at operation in the manual mode protection just by distance is insufficient.

Protection by time. Worker protection from electromagnetic radiation in different kinds of resistance welding is achieved through limitation of total time of the impact of MF, allowing for its spectral composition [2], on the welder during the work day by transferring him to other operations, not involving MF impact. Considering the real possible shortening of welder operation time (exposure time) to 2 h per shift, protection effectiveness with this method can be up to 2.5 times.

Protection by optimization of welding modes and welding process selection. Graphs shown in Figure 1 can provide some illustration of the method to improve the magnetic situation at the work places by mode optimization. Modes of spot (projection, seam, capacitor) welding can be regarded as quite diverse as to the obtained MF spectra, which is what determines the value of energy load on welder's body. Developers and manufacturers of new batch-produced equipment should take into account its application conditions and the acting sanitary norms, as application of this equipment in industry will be limited by levels of electromagnetic radiation in the working zone at its testing in the maximum power stage of welding transformer with different combinations of welding cycle regulator settings (see Figure 1). In the case of exceeding the specified levels of electromagnetic radiation and insufficient engineering capability for their lowering, production managers and welding equipment designers should apply additional measures for worker protection. For instance, the following engineering solutions can be applied in order to improve the magnetic situation around the hand tool:

- maximum limitation of welding modes by current (up to I_2 = 8 kA);
- welding performance in soft modes as far as possible, with one packet of full-phase sinusoidal current pulses with packet edge modulation (by one half-period);
- performance of heating power adjustment only by switching transformer power stages;
- connection of tools (tongs, guns, etc.) to a detached welding transformer by low-inductance (bifilar) cables.

The problem could also be solved by wider application of the technology of welding with gripper guns with remote control, when all the limitations on used welding cycle regulators, value and curve shape of welding current, and welding cycle pattern are eliminated, and high quality of welded joints is ensured. Research conducted at PWI shows that welding processes performed with rectified or pulsed rectified current of sufficient duration (several hundred milliseconds) have the best sanitary-hygienic characteristics. Therefore, it is recommended for welding technologists and welding equipment designers to thoroughly examine the possibility of application of resistance welding by rectified current, particularly in spot welding with hand tools.

Tentative lowering of MF energy load in the work places due to optimization of welding modes can be from 2 up to 10 times.

Shielding welding equipment and welder. At operation in the manual mode stationary shields, in addition to their functional purpose, should also meet two most important requirements: not to distort the nature of technological process, and not to lower significantly the labour efficiency.

It is important to satisfy the first requirement — not change the electric parameters of transformer secondary circuit, welding circuit, by introducing an additional resistance, that will lead to limitation of maximum welding current in it, and change of welding mode, respectively.

High labour efficiency can be actually ensured by free access to the welding site, preservation of the required dimensions of the work space for technological process performance, i.e. part mounting and removal, and prevention of additional operations with moving of the shield.

In terms of design and technico-economic characteristics, ferromagnetic materials (electric steel, carbon steel) are the most suitable material for manufacturing the shields for welding equipment. Specifics of welding equipment operation and design features of working electrodes and current-conducting buses do not allow application of the most efficient closed electromagnetic shields, but there is a possibility to install semi-closed shields, which are less effective.

Lowering of intensity of MF, generated by working elements and current-conducting buses of stationary spot welding machines, can be achieved using shielding devices (cylinder, closed shield, magnetic shunt), the effectiveness of which is from 2 up to 30 times. Shielding efficiency is understood to be the ratio of intensity (maximum value) in the work place H_{max} in the absence of the shield to intensity in the same

point of the work place in the presence of the shield $H_{\max\ sh}$:

$$E_{pr} = H_{max} / H_{max\ sh}. \quad (3)$$

E_{pr} is calculated using parameter H_{max}, measured in welder's work place at continuous operation of the transformer and permissible current:

$$I_{2\ ad} = I_{2r} \sqrt{\frac{DC}{100}}, \quad (4)$$

where I_{2r} is the rated welding current, A; DC is the duty cycle, %.

E_{pr} assessment by expression (3) is quite acceptable, although integral effectiveness of shielding pulsed MF by analogy with expression (2) and in keeping with the requirements of [2], is expressed as

$$E_{pr} = \sum H_n^2 / H_{n\ LPL}^2. \quad (5)$$

Final check of shielding effectiveness is performed experimentally taking into account MF spectral composition by expression (5).

Dependence of MF IEL on distance to electrodes of spot welding machine MT-2202 (same current characteristic as in Figure 1) at shielding of welder body by an elastic shield in the form of an apron [4] is shown in Figure 3, where *1*, *3* — for 1 packet of welding current pulses at minimum and maximum power, respectively; *2* — with elastic shield of 2 continuous non-closed layers in welding at minimum power; *4* — behind elastic single-layer non-closed shield in welding at maximum power; *5* — behind elastic single-layer shield in welding at minimum power for 1 packet of welding current with phase regulation of heating α_{ph} = 45°; *6* — same, as in *5*, but without a shield.

In terms of design, shields mounted on working electrodes and current-conducting buses can have the shape of a parallelepiped or cylinder, made of carbon steel 2–3 mm thick.

Application of individual protection gear (hooded cloaks, aprons, capes, coats with trousers, etc.) developed for super high frequencies, becomes practically senseless in the low-frequency range, as the effect of reflection of electromagnetic waves for the material with net or cellular structure is lost.

Individual protective gear, for instance, continuous elastic magnetic shield with high magnetic permeability of magnetically-soft cobalt alloy of Co–Fe–Cr–Si–B alloying system with an amorphous structure in the form of welder's apron [4], complete with oversleeves, can be useful in certain situations at trunk shielding in local MF of medium intensity (up to 1500 A/m by the first harmonic) and should be regarded as the last resort for ensuring magnetic safety, as their effective operation requires preliminary lowering of MF levels to 1500 A/m; shortening of the time of MF establishment in a thin shield of limit thickness (0.015 mm) by increasing the steepness of rising edge of welding current pulses, that leads to increase of MF energy load in the area of welder's hands and head (in the region of welder's abdomen and chest shielding effectiveness can be from 2 up to 5 times (see Figure 3)); ensuring conditions eliminating contact with open current-conducting parts of welding equipment [2], as the elastic shield has a metal base.

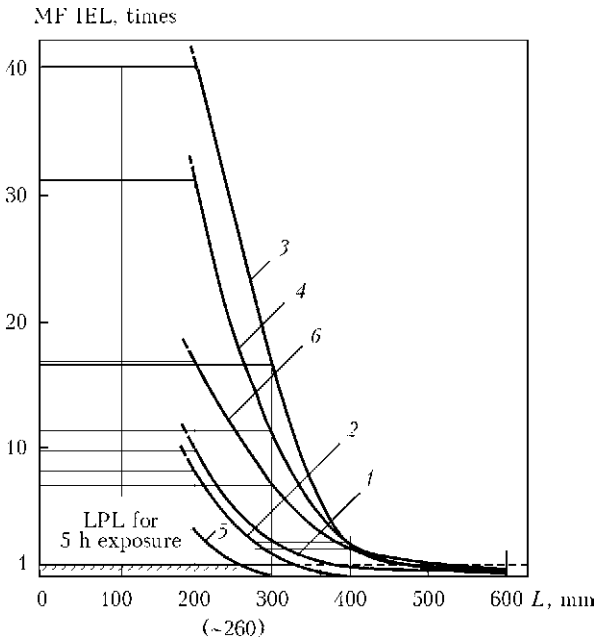

Figure 3. Dependence of MF IEL on distance to electrodes of spot welding machine MT-2202 at shielding of welder's trunk with an elastic shield in the form of an apron [4] (for designations see the text)

1. (1986) *Limit permissible levels of magnetic fields of 50 Hz frequency*. No. 3206–85. Moscow.
2. (2002) *DSN 3.3.6.096–2002*: National sanitary code and rules of operation of electromagnetic field sources. Kyiv: MOZ Ukrainy.
3. Levchenko, O.G., Levchuk, V.K. (2008) Safe level of electromagnetic field intensity in resistance welding. *The Paton Welding J.*, **5**, 38–46.
4. Lobanov, L.M., Levchenko, O.G., Levchuk, V.K. et al. *Welder's apron*. Pat. UA50293 Ukraine. Int. Cl. G 12B 17/00. Publ. 25.05.2010.

11th International Conference-Exhibition on Problems of Corrosion and Anticorrosive Protection of Structural Materials «Corrosion-2012»

The 11th International Conference-Exhibition on Problems of Corrosion and Anticorrosive Protection of Structural Materials CORROSION-2012 took place in Lvov in June 4–6, 2012.

Influence of the factors determining environmental safety and corrosion activity of man-caused media forms the conditions of human vital activity and functioning of industrial objects in the developed countries. Problem of corrosion protection is especially relevant in Ukraine, in particular, under the modern economic conditions of shortage of metals and energy resources and in a period of Ukrainian efforts to integrate in unique European system of the suppliers of energy carriers. These conditions determine a rise of safety requirements to pipeline systems. Problem of the corrosion protection takes the second place after the environmental protection problem. Damages caused by corrosion make approximately around one tenth of national income in the developed countries considering indirect damages. Therefore, efficiency of anticorrosive protection substantially determines the secure and long-term operation of metallic structures and their welded joints.

The international conference-exhibitions, holding in Lvov and dedicated to problems of corrosion and anticorrosive protection of structural materials, allow a wide range of specialists familiarizing with the new theoretical and practical developments in this scientific field, changing the experience on new methods of increase of corrosion resistance of metal structures of various designation as well as setting more tight scientific-and-production contacts between the Ukrainian and foreign specialists in this sphere.

Prof. V.I. Pokhmursky, Corresponding Member of the NASU, making a welcoming speech to the participants of the Conference-Exhibition

Ukrainian Association of Corrosion Specialists headed by its president V.I. Pokhmursky, Dr. of Tech. Sci., Corresponding Member of the NAS of Ukraine, is the organizer of the conference-exhibitions. The Ukrainian Association of Corrosion Specialists was founded in 1992 and being a voluntary union of organizations and separate specialists working in the field of corrosion protection. Today it joints around 50 scientific-and-technical enterprises, organizations and institutions and more than 100 individual members. The Ukrainian Association of Corrosion Specialists promotes collaboration with specialists of the international non-governmental organizations in the issues of corrosion and anticorrosive protection.

European Corrosion Federation, National Academy of Sciences of Ukraine, Ministry of Education, Science, Youth and Sports of Ukraine, Ukrainian Association of Corrosion Specialists, H.V. Karpenko Physico-Mechanical Institute of the NASU, Ivano-Frankovsk National Technical University of Oil and Gas, T. Shevchenko Scientific Association represented the Program Committee of the Conference.

Representatives of science and industrial enterprises from Germany, Russia, Ukraine, Poland, Kazakhstan, Turkey, Italy and other countries participated in the Conference work. Their number increases every year that indicates the Conference relevance.

«Fiziko-Khimicheskaya Mekhanika Materialov (Physico-chemical mechanics of materials), «Metally» (Metals) journals, «Metally. Tekhnologii. Oborudovanie» (Metals. Technologies. Equipment) all-Ukrainian branch newspaper and internet-portal: http://www.corrosion2012.ipm.lviv.ua/ supported the Conference.

The 11th International Conference-Exhibition CORROSION-2012 was opened by Prof. V.I. Pokhmursky, and Prof. V.V. Panasyuk, Director of H.V. Karpenko Physico-Mechanical Institute. Prof. B.E. Paton, President of the National Academy of Sciences of Ukraine, sent a welcoming letter in the Conference address.

Meeting of the section «Anticorrosive protection of equipment for oil-and-gas industry»

Corrosion specialists of the E.O. Paton Electric Welding Institute

Fundamental aspects of corrosion and corrosion-mechanical fracture; hydrogen and gas corrosion; inhibitor and biocide protection; methods of investigation and corrosion testing; electrochemical protection; new corrosion resistance materials and coatings; application of gas-thermal and other coatings for anticorrosive protection of structures; anticorrosive protection of equipment of oil-and-gas industry; anticorrosive protection of power and chemical equipment; corrosion and environmental problems were the main and traditional questions discussed on the Conference.

Plenary presentations, dedicated to theoretical studies in area of hydrogen corrosion, effect of inhibitor properties on carbon steel corrosion, application of electro-chemical and quantum-chemical methods for study of metal corrosion, investigation of properties of modified nanostructured polymers (speakers G. Gese, Technical University, Bursa, Turkey; S. Beloglazov, I. Kant Baltic Federal University, Russia; M. Khoma, H.V. Karpenko PhMI et al.) were listened during the Conference work. Participants were familiarized with the poster presentations dedicated to problems of metal stock preservation.

Representatives of enterprises of oil-and-gas branch were interested in works of applied character, in which questions of monitoring of metallic constructions, including gas- and oil pipelines, electrochemical protection and protective coatings were covered (speakers R. Dzhala, V. Chervatyuk, G. Nikiforchin, H.V. Karpenko PhMi et al.).

Round-table discussion on application of gas-thermal and other coatings for anticorrosive protection of structures; anticorrosive protection of equipment for oil-and-gas industry; anticorrosive protection of power and chemical equipment became a peculiarity of the Conference.

E.O. Paton Electric Welding Institute was represented by a delegation of young scientist-corrosion specialists headed by L. Nyrkova, Senior Staff Scientist, Cand. of Chem. Sci. The PWI representatives made oral and poster presentations on the following subjects: relevant applied developments in area of monitoring of man-caused media, including atmosphere corrosion, study of effect of polymer coating destruction products on corrosion properties of pipe steel in neutral solution using electro-chemical and corrosion-mechanical methods of investigations. Presentation about amendments in fundamental standard DSTU 4219 «Steel main pipelines. General requirement to corrosion protection» related with indices of protective coatings for main pipelines had a significant importance for representatives of oil-and-gas branch. Presentation of Junior Staff Scientist A. Klimenko dedicated to methods and means of monitoring of stress-corrosion fracture of main pipelines provoked an active discussion. The Ukrainian Association of Corrosion Specialists awarded the diploma for the best section presentation among the young scientists to the author.

The best works were marked during the closing meeting of the Conference and a proposal was made to pay greater attention to electrochemical protection of pipelines and other metal structures as well as normative documents in the field of corrosion protection in the next conferences.

Dr. L.I. Nyrkova,
Eng. S.A. Osadchuk, PWI

INTERNATIONAL SCIENTIFIC-AND-TECHNICAL CONFERENCE «SURFACE ENGINEERING AND RENOVATION OF PARTS»

The 12th International Scientific-and-Technical Conference «Surface Engineering and Renovation of Parts», organized by Association of Machine-Building Technologist of Ukraine, took place in village Gaspra, Yalta, in June 4–8, 2012. Proceedings including 132 presentations dedicated to issues of development of functional coatings and surfaces, technological control for quality of surfaces of machine parts and renovation of parts made by the scientists from R&DI, institutions of higher education, and representatives of industrial enterprise was published on the Conference results.

Realization of new high-end technologies and scientific-and-technical directions can only provide achievement of high quality and service reliability of machines as well as their lower cost, which are the condition for ensuring of high and stable level of market competitiveness. Surface engineering is one of such complex directions for task solving. It gains increasing importance as an effective mean of economy of materials and energy allowing simultaneously improving technical-economical characteristics of machines and developing fundamentally new parts.

International Scientific-and-Technical Conference was organized by All-Ukrainian Public Organization, Association of Machine-Building Technologist of Ukraine. Scientists from R&DI and institutions of higher education, specialists of industrial enterprises of Ukraine (Gorlovka, Dneprodzerzhinsk, Dnepropetrovsk, Zhitomir, Zaporozhie, Kiev, Kirovograd, Krivoj Rog, Lugansk, Mariupol, Odessa, Kharkov, Cherkassy), Russia (Belgorod, Blagoveshchensk, Bryansk, Izhevsk, Moscow, Nizhny Tagil, Novotroitsk, Omsk, Perm, Tomsk, Saint-Petersburg, Seversk, Stary Oskol, Ufa, Khabarovsk, Yurga), Belarus (Minsk), Uzbekistan (Almalyk, Tashkent, Fergana), Taiwan (Chi-Yi, Kaohsiung), Japan (Tokyo) participated in the Conference.

Prof. S.A. Klimenko, Director General of Association of Machine-Building Technologist of Ukraine, Deputy Director of V.N. Bakul Institute for Superhard Materials of the NAS of Ukraine, Academician of Academy of Technological Sciences of Ukraine, made a welcoming speech during the Conference opening. He indicated in his presentation a particular importance of surface engineering in development of modern technique and marked significant role of the Association of Machine-Building Technologist of Ukraine in informative joining of specialists and scientist-technologists of various countries.

Issues of transfer of professional activity in the field of welding from governmental regulation to self-regulation (A.V. Kondor, SRO NPP «National Agency of Welding Production»; Dr. of Tech. Sci. M.G. Sharapov, Central Research Institute of Structural Materials «Prometey», Saint-Petersburg), management of investments directed on modernization of machine-building manufacturing technologies (Cand. of Tech. Sci. S.V. Kovalev, V.A. Trapeznikov Institute of Management Problems, RAS, Moscow), industrial renovation of technical parts (Cand. of Tech. Sci. B.V. Namakonov, Gorlovka Auto Road Institute of Don NTU), mechanical treatment of parts with deposited and sprayed coatings (Prof. S.A. Klimenko), relation of condition of surface layer of the parts with their wear resistance (Prof. Yu.M. Luzhnov, Association of Tribology Engineers, Moscow) were considered during the plenary meeting.

M.G. Sharapov presented a new Russian Scientific-Manufacturing Self-Regulating Organization «National Agency of Welding Production». This organization proposed a series of programs and projects for development of welding

field in Russia. «Technical support of welding productions», «Interbranch integration», «Training of staff and special personnel», «Occupational safety of welding professionals» are the main programs having direct influence on regular, stable and effective development of welding branch in hole. Works on development of relationships with foreign welding societies, providing of possibility of participation for enterprise-members of SRO in realization of large international industrial projects, harmonization of standards to world normative documents were also announced.

Results of wide area of investigations, covering the most important concepts of surface engineering, were generalized and modern achievements in development and improvement of technology for control of service properties of machine parts and cutting tools were shown in the presentations made at the Conference. Problems of development of functional coatings and surfaces and technological control for surface quality of machine parts were considered in the reposts of V.I. Averchenkov, A.V. Totaj (Bryansk), N.S. Sivtsev (Izhevsk), V.S. Antonyuk, G.G. Vlajkov, M.Yu. Kopejkina, V.I. Lavrinenko, B.A. Lyashenko, A.S. Manovitsky, Yu.A. Melnijchuk, N.I. Posvyatenko, E.B. Soroka (Kiev), Yu.A. Kharlamov (Lugansk), L.M. Akulovich, P.A. Vityaz, A.I. Garost, I.A. Ivanov, V.S. Ivashko, M.L. Khejfets (Minsk), V.V. Roshchupkin, A.S. Tyuftaev, G.A. Filippov (Moscow), E.N. Eremin (Omsk), L.G. Vajner (Khabarovsk), O.N. Doronin (Stary Oskol), A.K. Emaletdinov (Ufa), V.M. Bersenev, L.A. Timofeeva, S.V. Sergeev (Kharkov), I.G. Shina (Tashkent) and other representatives of scientific organizations and industrial enterprises.

Developments of Belarusian scientists in area of vacuum spraying of machine parts and cutting tools were presented in the presentation of I.A. Ivanov. Also the investigations showed the peculiarities of coating formation considering the requirements made to the quality of surface of part basis. S.E. Aleksandrov and E.A. Lyamina, scientists of A.Yu. Ishlinsky Institute for Problems in Mechanics of the RAS, presented the results of original investigations directed on application of approach of deformable solid body mechanics for solution of surface engineering tasks.

Large group of presentations was made by the scientists of the Tomsk region, i.e. members of Institute of Strength Physics and Materials Science of RAS SB, Tomsk State University of Architecture and Building, National Research Tomsk Polytechnic University, Seversk Institute of Technology of the National Research Nuclear University MIFI. Results of wide range of investigations dedicated to the issues of development of materials with set functional properties and surface engineering are given in the works. Prof. Yu.N. Saraev showed in his presentation the advantages and directions of further development of electro-technological processes of welding and surfacing based on realization of adaptive algorithms of pulse control of electrical parameters of mode.

Seminar «Welding, surfacing and other renovation technologies on enterprises of mining, machine-building industries and in transport» was traditionally held in the scope of the Conference. The scientists and specialists of industrial enterprises told about their achievements and problems based on real practical examples in a course of seminar. Presentations dedicated to practical experience of arc surfacing, formation of strengthening coatings and modification of surface of machine parts from TM. VELTEK Ltd. (A.A. Golyakevich, L.N. Orlov, V.N. Upyr, A.V. Khilko, Kiev), TM. VELTEK Russia Ltd. (A.A. Kuzubov Jun., Belgorod), «Izovol» group of enterprises (A.A. Kuzubov, Belgorod), Central Research Institute of Structural Materials «Prometey» (M.G. Sharapov, Saint-Petersburg), NPP REMMASH group of companies (V.I. Titarenko, Dnepropetrovsk), Dneprodzerzhinsk MC (O.N. Rokhlin). «Kompozit» Ltd. (V.A. Korotkov, Nizhny Tagil), I.P. Bardin Central Scientific Research Institute of Ferrous Metallurgy (G.A. Fillipov, Moscow) etc. had a great interest.

A review of developments of NPP REMMASH on designing and operation of equipment for surfacing was presented by V.I. Titarenko. Reliable technological equipment, developed by the specialists of REMMASH, is in demand of industrial enterprises of Ukraine and Russia, providing the customers with possibility of efficient application of new developments for surfacing technologies in industry, in particular, of TM. VELTEK production. Russian journals «Uprochn. Tekhnologii i Pokrytiya» (Strengthening technologies and coatings), «Trenie i Smazka v Mashinakh i Mekhanizmakh» (Friction and lubrication in machines and mechanisms), «Naukoyomkie Tekhnologii Mashinostroeniya» (High technologies of machine building) («Mashinostroenie» publishing house, Moscow) and Ukrainian journal «Instrumentalny Svit» (Instrumental world) (Kiev) became the information sponsors of the Conference.

Theses of the presentations, made at the Conference, were included in the published proceedings.

Association of Machine-Building Technologist of Ukraine started preparation of the next 13th International Scientific-and-Technical Conference «Surface engineering and renovation of parts», which will take place in village Gaspra, Yalta, in June 3–7, 2013. We invite the specialists interested in the issues of surface engineering, repair, renovation and strengthening of machine parts to participate in it.

Prof. S.A. Klimenko,
Dr. M.Yu. Kopejkina, AMBTU

Scientific and Technical Conference
«CURRENT PROBLEMS IN METALLURGY AND TECHNOLOGY OF WELDING AND SURFACING OF STEELS AND NON-FERROUS METALS»

To 100 years from the birthday of Prof. D.M. Rabkin, the Honoured Scientist and Technology Engineer, and Prof. I.I. Frumin, Doctor of Technical Sciences

25–26 October 2012

Kiev
E.O. Paton Electric Welding Institute

Organisers of the Conference:
E.O. Paton Electric Welding Institute of the NAS of Ukraine,
and Welding Society of Ukraine

Contacts: (044) 200 54 06, 200 63 57, 200 24 66, 200 82 77
E-mail: office@paton.kiev.ua; tzu@e-mail.ua